

Alma Mater Studiorum – Università di Bologna

DOTTORATO DI RICERCA IN

Chimica

Ciclo XXX

**Settore Concorsuale di afferenza:** 03/A1 CHIMICA ANALITICA

**Settore Scientifico disciplinare:** CHIM/01 CHIMICA ANALITICA

NEW ANALYTICAL TOOLS AND SMARTPHONE-BASED DEVICES  
EXPLOITING CELL-BASED AND BIOLUMINESCENCE DETECTION FOR  
ENVIRONMENTAL AND DIAGNOSTIC APPLICATIONS

**Presentata da:** Maria Maddalena Calabretta

**Coordinatore Dottorato**

**Relatore**

**Chiar.mo Prof. Aldo Roda**

**Prof.ssa Elisa Michelini**

**Esame finale anno 2018**

## **Abstract**

The use of portable light detectors and smart supports and bioinspired materials to confine living cells and use them for field-deployable biosensors has recently attracted much attention. In particular, bioluminescent whole-cell biosensors designed to respond to different analytes or classes of analytes have been successfully implemented in portable and cost-effective analytical devices.

The activity carried out during my PhD was mainly focused on the development of whole-cell bioluminescent (BL) biosensors for multi-analyte detection and their implementation into portable analytical devices for point-of-care and point-of-need applications.

Thanks to the high maturity level of reporter gene technology and the availability of several bioluminescent proteins with improved features, bioluminescence smartphone-based biosensing platforms were developed exploiting highly sensitive luciferases as reporters. A 3D-printed smartphone-integrated cell biosensor based on genetically engineered human cell lines was developed for quantitative assessment of toxicity and (anti)-inflammatory activity with a simple and rapid add-and-measure procedure.

Moreover, since cells in 2D cultures do not often reflect the morphology and functionality of living organisms, thus limiting the predictive value of 2D cell-based assays, we implemented 3D cell-based assays. A non-destructive real-time BL imaging assay of spheroids for longitudinal studies on 3D cell models was first developed exploiting micropatterned 96-well plate format. The assay performance was assessed using the transcriptional regulation of nuclear factor K beta response element in human embryonic kidney cells. The assay can be implemented in any laboratory equipped with basic cell culture facilities and paves the way to the development of new 3D bioluminescent cell-based assays.

<b>CHAPTER 1</b> .....	<b>6</b>
<b>INTRODUCTION</b> .....	<b>6</b>
<b>1.1 BIOLUMINESCENCE</b> .....	<b>7</b>
1.1.1 Bioluminescent systems .....	8
1.1.2 Bioanalytical applications of bioluminescence .....	11
1.1.3 Multiplexing bioluminescence .....	13
<b>1.2 CELL-BASED ASSAYS</b> .....	<b>16</b>
1.2.1 3D cell-based assays .....	18
1.2.2 Whole-cell biosensors .....	20
<b>1.3 3D PRINTING TECHNOLOGIES</b> .....	<b>21</b>
<b>1.4 PORTABLE LIGHT DETECTORS</b> .....	<b>23</b>
1.4.1 Portable light detectors.....	23
1.4.2 Color detectors: CCD vs CMOS .....	24
<b>REFERENCES</b> .....	<b>26</b>
<b>CHAPTER 2</b> .....	<b>33</b>
<b>AIM OF THE THESIS</b> .....	<b>33</b>
<b>CHAPTER 3</b> .....	<b>37</b>
<b>SMARTPHONE-INTERFACED 3D PRINTED TOXICITY BIOSENSOR INTEGRATING BIOLUMINESCENT “SENTINEL CELLS”</b> .....	<b>37</b>
<b>4.1 INTRODUCTION</b> .....	<b>38</b>
<b>4.2 MATERIALS AND METHODS</b> .....	<b>40</b>
4.2.1 Chemicals and reagents.....	40
4.2.2 3D-printed cell minicartridges and smartphone adaptor fabrication.....	41
4.2.3 Android-based application .....	42
4.2.4 Cell culture and transient transfections.....	44
4.2.5 Smartphone-based BL emission characterization of Hek293T cells expressing green-emitting luciferase .....	45
4.2.6 Toxicity assay and analytical performance evaluation .....	45
4.2.7 Real sample analysis.....	46
4.2.8 “Sentinel cells” immobilization .....	47
<b>4.3 RESULTS AND DISCUSSION</b> .....	<b>47</b>
4.3.1 3D printed all-in-one device .....	48
4.3.2 Android-Based Toxicity Application (Tox-App).....	49
4.3.3 “Sentinel cells” assay analytical performance .....	50
4.3.4 Ready-to use cartridges with immobilized “sentinel cells” .....	53
4.3.5 Real samples analysis .....	56

4.4 CONCLUSION .....	57
REFERENCES .....	59
<b>CHAPTER 4 .....</b>	<b>64</b>
<b>EXPLOITING NANOLUC LUCIFERASE FOR SMARTPHONE-BASED BIOLUMINESCENCE CELL BIOSENSOR FOR (ANTI)-INFLAMMATORY ACTIVITY AND TOXICITY.....</b>	<b>64</b>
5.1 INTRODUCTION .....	65
5.2 MATERIALS AND METHODS .....	68
5.2.1 Chemicals and reagents.....	68
5.2.2 3D-printed cartridge and smartphone adaptors .....	69
5.2.3 Evaluation of biosensor inflammatory response with the smartphone .....	70
5.2.4 Smartphone-based real sample analysis .....	71
5.3 RESULTS AND DISCUSSION.....	72
5.3.1 Assay design.....	72
5.3.2 Evaluation of NanoLuc variants expressed in Hek293T cells with smartphone-based detection.....	74
5.3.3 Smartphone-based inflammation assay analytical performance: precision and reproducibility .....	77
5.3.4 Smartphone-based (anti)-inflammatory cell biosensor: analysis of real samples .....	79
5.4 CONCLUSION .....	81
5.5 SUPPLEMENTARY MATERIAL .....	83
ACKNOWLEDGMENTS.....	86
REFERENCES .....	87
<b>CHAPTER 5 .....</b>	<b>93</b>
<b>BIOLUMINESCENCE IMAGING OF SPHEROIDS FOR HIGH-THROUGHPUT LONGITUDINAL STUDIES ON 3D CELL CULTURE MODELS.....</b>	<b>93</b>
6.1 INTRODUCTION .....	94
6.2 MATERIALS AND METHODS .....	95
6.2.1 Materials.....	95
6.2.2 2D cell cultures .....	96
6.2.3 3D cell cultures .....	96
6.2.4 Characterization of 2D and 3D Hek293 cultures expressing PLG2 luciferase .....	96
6.2.5 2D and 3D bioluminescence imaging of Hek293 cells expressing PLG2 luciferase .....	97
6.2.6 Spheroid analysis .....	97
6.2.7 3D bioluminescence imaging assay for inflammatory pathway activation .....	98
6.3 RESULTS AND DISCUSSION.....	98
6.3.1 Characterization of PLG2 luciferase expressed in 3D cell cultures/spheroids.....	98
6.3.2 3D Bioluminescence assay for inflammatory pathway activation .....	103

**6.4 CONCLUSIONS.....105**

**ACKNOWLEDGMENTS.....106**

**REFERENCES .....107**

**CHAPTER 6 ..... 112**

**FUTURE DIRECTIONS..... 112**

**ACKNOWLEDGMENTS ..... 115**

# CHAPTER 1

---

## Introduction

---

*Adapted from: "Field-deployable whole-cell bioluminescent biosensors: so near and yet so far", Elisa Michelini, Luca Cevenini, Maria Maddalena Calabretta, Silvia Spinozzi, Cecilia Camborata, Aldo Roda, Anal Bioanal Chem (2013) 405:6155-6163*

*Adapted from: "Exploiting in vitro and in vivo bioluminescence for the implementation of the three Rs principle (replacement, reduction, and refinement) in drug discovery", Elisa Michelini, Luca Cevenini, Maria Maddalena Calabretta, Aldo Roda, Anal Bioanal Chem (2014) 406:5531-5539*

## 1.1 BIOLUMINESCENCE

Bioluminescence (BL) is a spectacular phenomenon that naturally occurs in several living organisms, from fireflies to bacteria, abyss species, and mushrooms. The light emission derives from different chemical reactions that involve an enzyme, a luciferase, and an organic substrate, general called luciferin. Luciferase catalyses the oxidation of luciferin by molecular oxygen, and its conversion to an excited state of the oxyluciferin molecule, emits visible light that then returns to the ground state [1].

The BL emission intensity depends on the overall quantum yield of the reaction ( $\Phi_{BL}$ ) and can be defined by following the equation:

$$\Phi_{BL} = \Phi_C \Phi_{EX} \Phi_F$$

where  $\Phi_C$  reflects the chemical yield of the reaction,  $\Phi_{EX}$  is the excited state production and  $\Phi_F$  is the emission quantum yield of the excited state.

Compared to conventional chemiluminescent (CL) systems, the peculiar photo-physical property of BL reaction is that the light emission process derives from an enzyme-singlet excited state product complex.

Due to the simple chemistry of BL reactions [2], the non-toxicity of luciferin, the high detectability and the remarkable high quantum yield, which is about one order of magnitude higher than that of CL reactions, many *in vitro* and *in vivo* analytical methods with BL detection have been developed, including gene expression assays, immunoassays, and non-invasive *in vivo* and *in vitro* imaging techniques.

BL-based methods are sensitive and provide good spatial resolution, a wide dynamic range and simple quantitative signal assessment. Indeed, in contrast with fluorescence technique, BL does not require an external excitation light source and in the experimental measurements there are no interference from light scattering and background fluorescence.

Thanks to the possibility of exploiting signal amplification due to the turnover of the luciferase enzymatic reaction, BL systems represent a suitable detection principle for analytical applications where high sensitivity is required for example for detection of low concentrations of target analyte or small sample size [3].

### 1.1.1 Bioluminescent systems

More than 30 different BL systems have been elucidated to date [2], however only 9 natural luciferin structures have been identified.

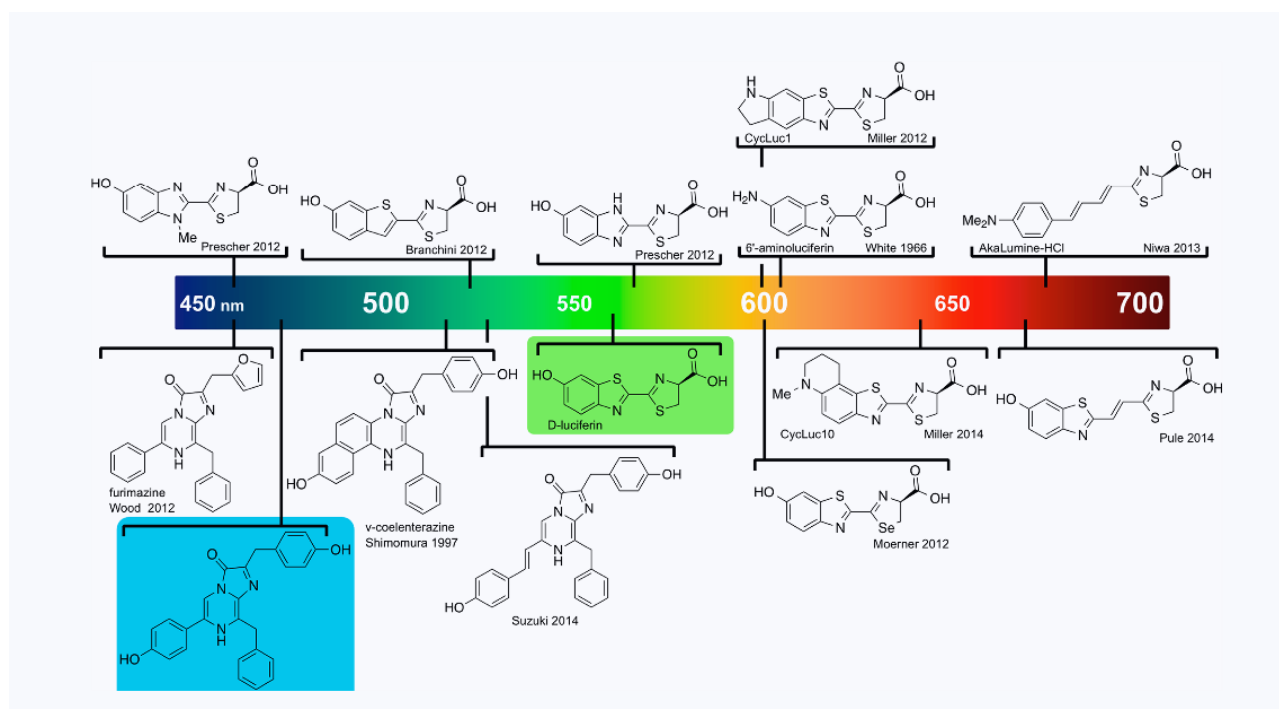


**Figure 1:** “Palette” of luciferin analogues. Native luciferins are highlighted with colored boxes. Brackets denote the wavelength (nanometers) of maximal bioluminescence emission observed upon incubation of the compound with luciferase. While many analogues can provide unique colors of light, most are not efficiently processed by native luciferases.

*Photinus pyralis* (PpyLuc), is the most studied BL protein, with an emission in the yellow-green light ( $\lambda_{em} = 557 \text{ nm}$  at pH 7.8), a glow-type kinetic and a broad emission band. PpyLuc is a 61 kDa monomeric protein that does not require any post-translational modifications. It is suitable for heterologous expression in both

prokaryotic and eukaryotic systems since PpyLuc does not show any toxicity to cells even at high concentrations. PpyLuc bioluminescence shows a remarkable red-shift at lower pH and higher temperatures.

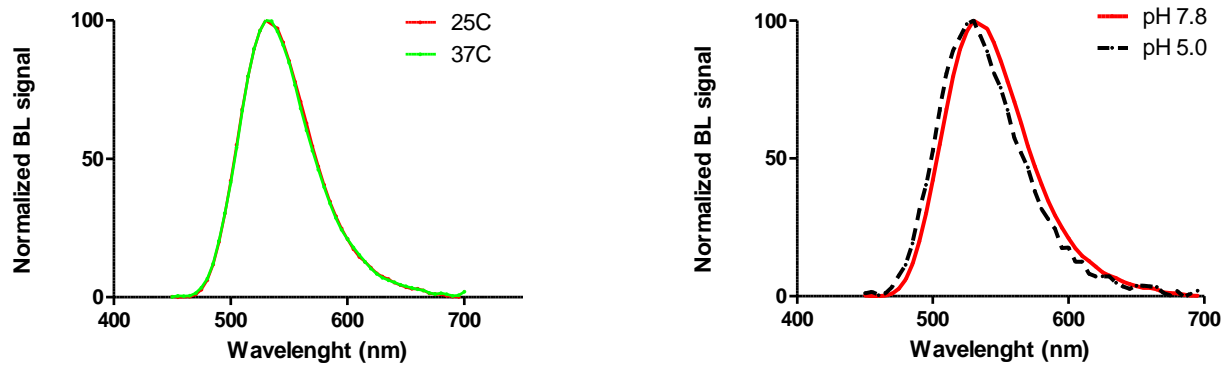


**Figure 2:** Emission spectra of synthetic luciferases obtained incubating the purified protein at 25°C and 37°C (left panel) and at 25°C, pH 7.8 and 5.0 (right panel), respectively.

The luciferase-catalyzed oxidation of luciferin involves the presence of ATP and  $Mg^{2+}$  as co-factors. In particular, as shown in Figure 3, in the first step, D-luciferin in the presence of ATP, is converted into luciferyl adenylate, the central intermediate in the BL reaction. Thanks to the presence of molecular oxygen, around 80% of adenylate is oxidized via a single electron-transfer mechanism [4] into peroxide whose ultimately leads to production of oxyluciferin and emission of a light quantum. Different tautomeric forms of the oxyluciferin in its excited state are possible, but it is thought that the actual emitters inside the luciferase pocket are keto-(-1) or enol-(-1') forms.

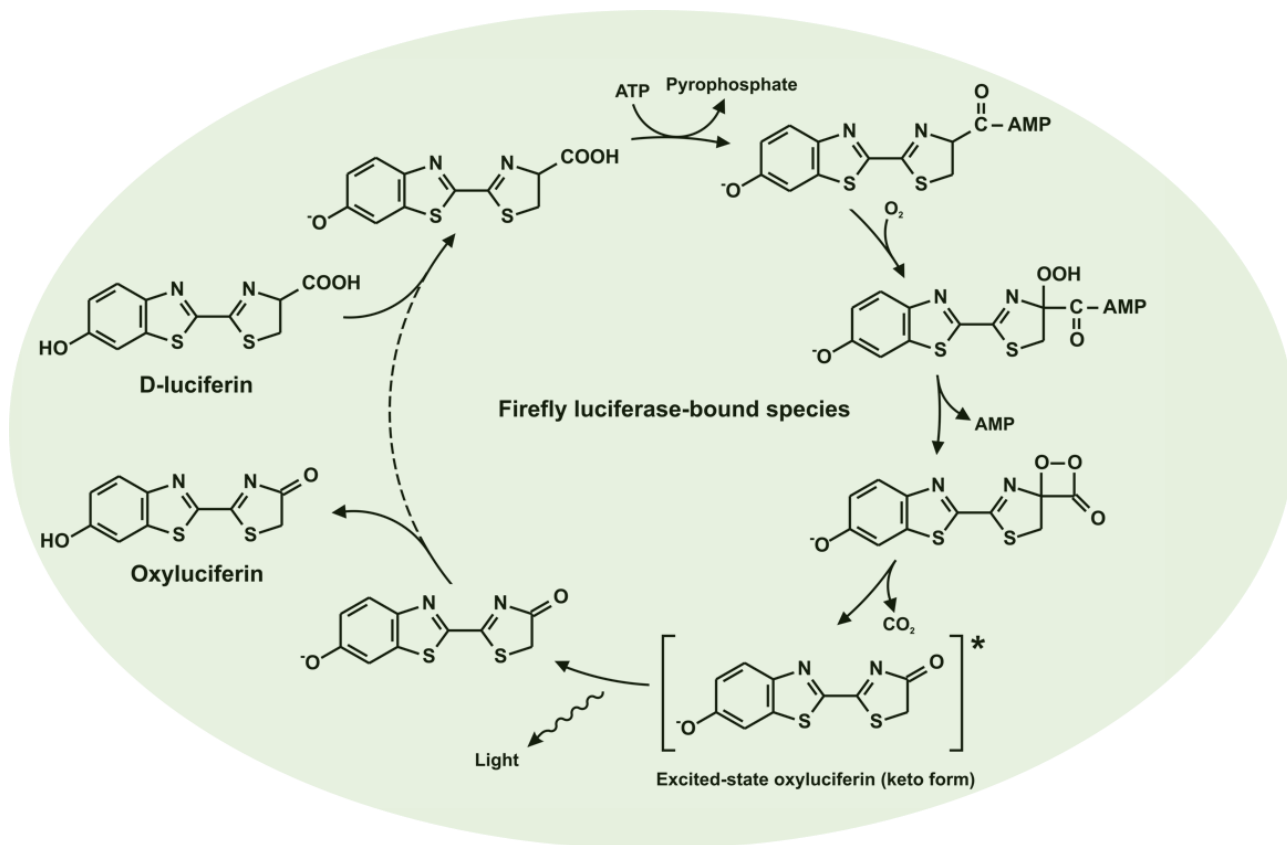


**Figure 3:** The firefly luciferin/luciferase bioluminescence reaction.

As ATP molecules are found in every living organism, the D-luciferin-luciferase reaction is widely employed for ATP detection to identify microbial contaminations and for analysis of seawater and water treatment plants, hygiene monitors in hospitals and cell viability studies [5].

Following *P. pyralis* luciferase, beetle luciferases derived from *Pyrophorus plagiophthalmus* are the second most popular choice [6] thanks to the availability in nature in a wide range colors, from green to red. The possibility to have a wide range of natural and mutant BL reporters with different well-separated emission spectra and improved properties (e.g. thermal stability) is essential for the development of dual-color and multicolour assays [7]. We have also recently developed a dual-luciferase gametocyte assay with immature and mature *Plasmodium falciparum* gametocyte stages expressing red and green-emitting luciferases for anti-malarial drug screening [8]. In particular, this dual color assay

was allowed to quantitatively and simultaneously measure stage-specific drug effects on parasites at different developmental stages with significant reduction of assay time and cost in comparison to state-of-the-art analogous assays.

New luciferases obtained from other species have been recently commercialized showing a good potential; for instance, a synthetic NanoLuc® luciferase designed on the small *Oplophorus* luciferase domain was developed by Hall and colleagues in 2012 [9]. NanoLuc is a 19.1 kDa luciferase enzyme that utilizes a synthetic furimazine substrate (a coelenterazine analogue) to produce high intensity and glow-type luminescence, providing a sensitivity superior than other luciferases (Figure 4). The BL signal intensity is increased by 2.5 million times with respect to the parent luciferase. Thanks to its small size and brightness, NanoLuc has been employed for several applications, for exploring gene regulation and cell signalling, for monitoring protein stability, for the development of novel based BL biosensors and BL imaging.

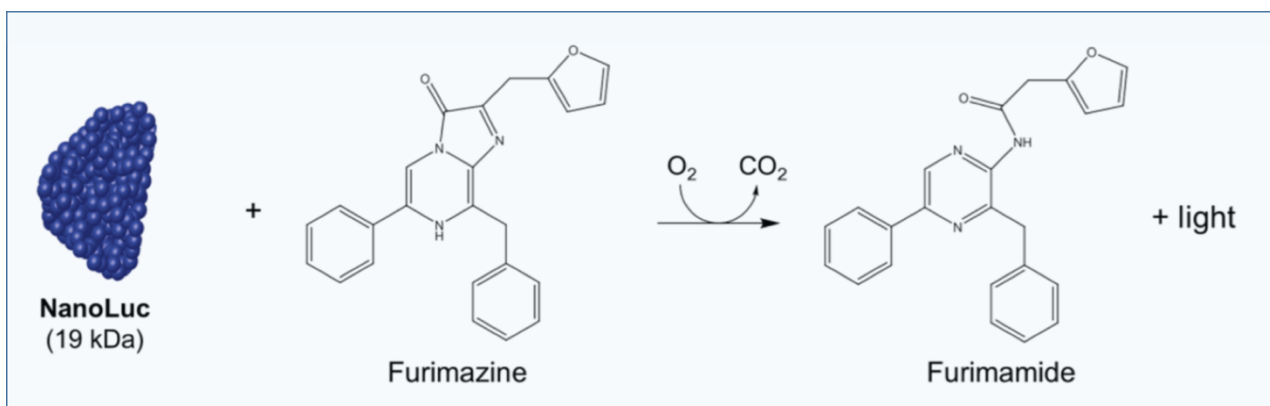


**Figure 4:** Bioluminescence from the NanoLuc system. The synthetic furimazine substrate reacts with NLuc in the presence of molecular oxygen, producing furimamide and luminescence output.

### 1.1.2 Bioanalytical applications of bioluminescence

From an analytical point of view, the light emission produced by a chemical reaction allows quantitative analysis in which, under certain experimental conditions, the light intensity is closely related to the concentration of analyte. In comparison to all

methods based on the interaction of the light with the matter (absorption spectroscopy and fluorimetry), BL has better qualities since the detection of the signal is not influenced either by the drift of the light source and the detector or by interferences due to the light diffusion. For this reason, BL is a suitable method for the detection of analyte molecules in a complex biological matrix.

Different molecular biology tools based on BL reactions have been developed, being suitable for both *in vitro* assays, with purified proteins and cells, and *in vivo* methods, i.e. small animals. The investigation of protein–protein interactions, protein conformational changes, protein phosphorylation, second-messengers expression, and, in general, the study of gene expression and gene regulation *in vitro* and *in vivo* [5,10] are the typical bioanalytical applications of the BL.

Since the luminescence reaction is quantitative, and has an extremely low background, *in vitro* BL imaging is particularly useful for longitudinal studies and quantitative imaging [11]. One of the most frequently used applications of *in vivo* bioluminescence imaging is cell tracking [12]. In this application, luciferase-expressing cancer cells, immune cells, stem cells, or other types of cells can be imaged repeatedly in animal models, providing information about the number and spatial distribution of the cells.

BL proteins can be detected down to very low levels and for this reason they allow an ultrasensitive detection of the target analytes and monitoring of the physiological phenomena under investigation. The recent technical advancement in instrumentation and miniaturization allows to obtain analysis of small-volume samples, which ultimately leads to the development of miniaturized and high-throughput assays.

Ultrasensitive bioassays have been reported, including whole-cell biosensors and miniaturized devices for high-throughput screening (HTS), with applications ranging

from clinical diagnostics to environmental monitoring and drug screening [13].

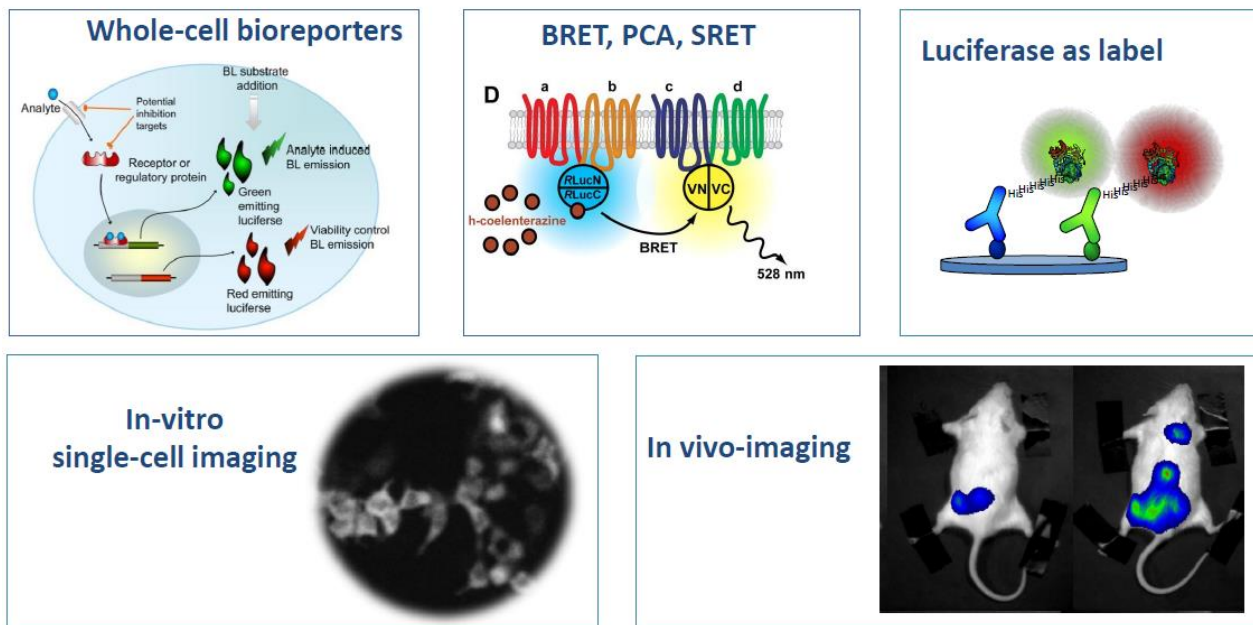


**Figure 5:** Bioanalytical applications of luciferases to *in vitro* and *in vivo* monitor activation of molecular pathways, protein-protein interactions and to quantify target analytes.

### 1.1.3 Multiplexing bioluminescence

Thanks to recent advances in molecular biology, the genes encoding several BL proteins have been cloned and mutated to obtain new BL proteins with improved emission properties. These new probes and labels found widespread use in *in vitro* and *in vivo* assays.

Despite the portfolio of marketed luciferases (Table 1) is smaller than the green fluorescent protein palette, it is worth mentioning that most of such luciferases are available in customized variants that suit different applications. In particular, the incorporation of a protein degradation signal sequence in the luciferase gene confers the luciferase enzyme a shorter half-life [14]. These short-lived luciferases have been widely used in reporter gene assays to monitor transient dynamic changes in gene expression.

**Table 1** Luciferases for which the coding sequence is commercially available for reporter gene applications, calcium detection and *in vivo* imaging

Luciferase	Organism	Length (aa)	Size (kDa)	Substrate	BL $\lambda_{\max}$ (nm)	Company
PpyLuc <sup>a</sup>	<i>Photinus pyralis</i>	550	61	D-luciferin	557	Several companies
GLuc <sup>a</sup>	<i>Gaussia princeps</i>	185	19.9	Coelenterazine	482	Thermo Scientific, Targeting Systems
RLuc <sup>a</sup>	<i>Renilla reniformis</i>	312	36	Coelenterazine	475	Promega, Thermo Scientific, Targeting System
Nanoluc <sup>a</sup>	<i>Oplophorus gracilirostris</i>	171	19.1	Furimazine	465	Promega
Lucia	Derived from marine copepod	210	23	Coelenterazine	NR	InvivoGen
Red-emitting <i>Luciola</i> luciferase	<i>Luciola italica</i>	548	61	D-luciferin	610	Targeting System
CBG99	<i>Pyrophorus plagiophthalmus</i>	542	64	D-luciferin	537	Promega
CBR	<i>Pyrophorus plagiophthalmus</i>	542	64	D-luciferin	613	Promega
<i>Cypridina</i> luciferase	<i>Cypridina noctiluca</i>	555	62	<i>Cypridina</i> luciferin	463	Prolume, Targeting Systems

aa amino acids, BL bioluminescence, NR not reported

<sup>a</sup> Luciferases available in different forms (e.g. intracellular, secreted, and shorter-lived forms)

Bioluminescent reporters with well-separated and different emission spectra are commonly used for the development of dual color and multicolor reporter assays [8,15]. Dual luciferase assay system allows to perform simultaneous monitoring of gene expression, intracellular detection of bioactive compounds, and HTS *in vitro*. Because one of the main drawbacks of dual bioluminescence assays is the effective separation of bioluminescence signals emitted by two reporters, four main strategies can be envisaged (Figure 6): (1) the use of bioluminescent reporters whose emission can be distinguished by emission filters and suitable algorithms (spectral resolution) [16,17]; (2) the use of bioluminescent reporters requiring

different substrates [18]; (3) the use of bioluminescent reporters that are expressed in different cell compartments or are secreted outside the cells (spatial resolution) [19]; (4) the use of bioluminescent reporters that exhibit different emission kinetics, allowing sequential reading (time resolution) [20].

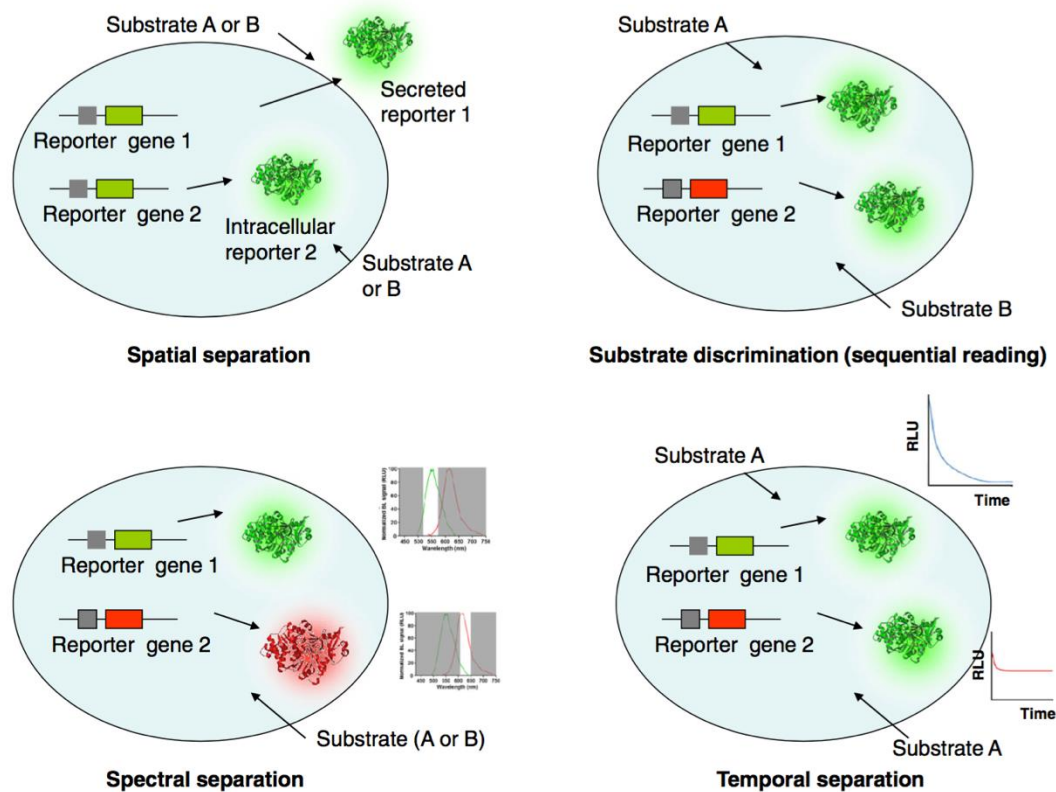


**Figure 6:** Four different strategies for bioluminescence signal separation in dual-reporter assays: the use of bioluminescent reporters that are expressed in different cell compartments or are secreted outside the cells (spatial separation), the use of bioluminescent reporters whose emission can be distinguished by emission filters and suitable algorithms (spectral separation), the use of bioluminescent reporters requiring different substrates and sequential reading (substrate discrimination), and the use of bioluminescent reporters that exhibit different emission kinetics, allowing sequential reading (temporal separation). RLU relative luminescence units.

Thanks to theoretical and experimental studies of color modulation mechanisms, several mutants have been obtained, allowing elucidation of the catalytic mechanism of different luciferases [21-24], and a wide range of luciferases with tuned spectral properties have been reported. Major efforts were directed towards the obtainment of mutants with red-shifted emission for in vivo imaging [25-26]

and, when paired with green-emitting luciferases, for dual color reporter assays [27-28].

A real step forward is needed to develop luciferases that maintain their emission properties in different experimental conditions, such as at different pH and temperature. It is well known that firefly luciferases generally exhibit pH- dependent emission, and very few mutants do not have this drawback. Interestingly, the bioluminescence of luciferases isolated from click beetles and railroad worms [29] is pH-independent, and such enzymes, together with firefly luciferase mutants showing the same property, are thus extremely useful for the development of cell-based assays and *in vivo* models [30].

## **1.2 CELL-BASED ASSAYS**

Bioluminescence-based analytical tools are suitable for high-throughput and high-content screening assays, finding widespread application in several fields related to the drug discovery process. Cell-based bioluminescence assays, because of their peculiar advantages of predictability, possibility of automation, multiplexing, and miniaturization, seem the most appealing tool for high demands of the early stages of drug screening.

Living cells used as sensing systems have proved to be valuable for prediction of the physiological response to drugs, chemicals, and samples in complex matrices, whose toxic effects and specific biological activity can be evaluated in an easy and straightforward manner.

Although many cell-based assays have been described, few can be regarded as true biosensors. According to IUPAC nomenclature, a biosensor is “A device that uses specific biochemical reactions mediated by isolated enzymes, immunosystems, tissues, organelles or whole cells to detect chemical compounds, usually by electrical, thermal, or optical signals” [31]. This definition embraces the concept of a

stand-alone integrated receptor-transducer device able to provide selective (semi)quantitative analytical information. The challenge of on-site analysis, irrespective of whether the application is environmental, food, or clinical, necessarily requires biosensors with high sensitivity, selectivity, robustness, rapidity (possibly approaching real time analysis), ease of operation, possibility of direct analysis of sample in complex matrices without preliminary sample treatment, and, last but not least, cost effectiveness.

Cell-based assays include a variety of assays that measure cell proliferation, toxicity, production of markers, motility, activation of specific signalling pathways and changes in morphology. A large body of evidence suggests that cell-based assays and in vitro assays provide highly valuable information, and are thus able to provide reliable data on toxicity, biological activity, side effects, and metabolism of compounds [32-33]. Reporter gene technology is the main route for identifying leads from large chemical libraries. This approach relies on the use of bioluminescent reporter genes under the transcriptional control of a target gene's regulatory sequences to monitor specific biological pathways. In particular cell-based BL assays are based on cells genetically modified (yeast, bacteria, mammalian cells) containing a BL reporter gene fused to a regulatory DNA sequence (Figure 7). The activation of the regulatory sequence occurs in the presence of a specific analyte or stimulus, that ultimately leads with the production of the BL reporter protein (usually a luciferase), thus enabling correlation of reporter protein expression, measured as light signal, and transcriptional regulation. The availability of a wide portfolio of luciferase reporters that can replace the green fluorescent protein and its variants, multiplexing is no limited to fluorescence detection [34,28].

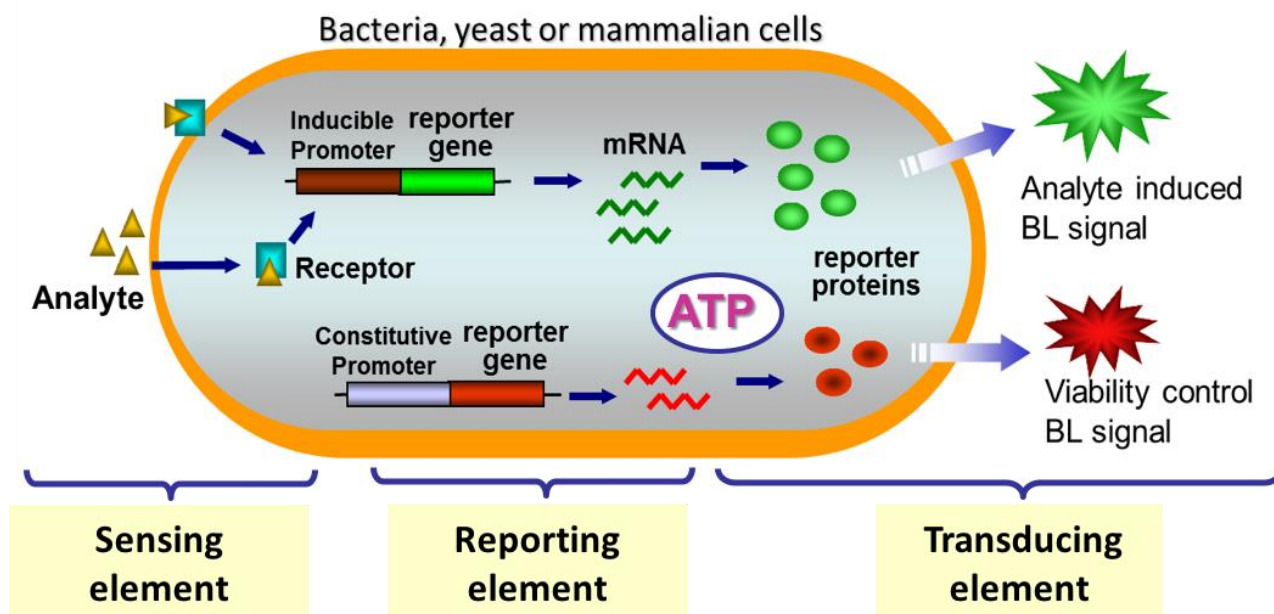


**Figure 7:** Schematic representation of the dual-color bioreporter

### 1.2.1 3D cell-based assays

Cell-based assays based on two-dimensional (2D) represent one of the most appealing and well-established bioanalytical tools for the early stages of the drug discovery process, providing a simple, fast and cost-effective tool to avoid large-scale and cost-intensive animal testing. The standard procedure for drug discovery starts with 2D cell-cultured tests in order to screen active compounds, followed by animal tests and finally to clinical trials. As results, only 10% of these compounds can reach clinical development while the remaining fails during the most expensive clinical trials phase. For this reason, due to their altered response to drugs for unnatural microenvironment, preliminary 2D cell culture tests can provide non-predictive and misleading data for *in vivo* responses [35-37]. Indeed, cells in 2D cultures do not often reflect the morphology and functionality of living organisms, thus limiting the predictivity of 2D cell-based assays. Conversely, thanks to hierarchical structure and cellular heterogeneity, 3D cell models can closely mimic *in vivo* tissue physiology, generating the extracellular matrix and diffusion barriers and restoring cell-to-cell communication. Therefore, compared to the 2D monolayer, 3D

models replicate better intrinsic physiological conditions and *in vivo* cellular responses to external stimuli. As such, 3D-cultured cells are the ideal sensing element in cell-based sensors, providing biologically relevant information and predictive data for *in vivo* tests. It is known that cells in 3D culture environment differ in gene, protein, and cell receptor expression from 2D-monolayer [38-40] and they provide an excellent model as “near-to-*in vivo*” systems. The generation of spheroids is based on the common basic principle of self-assembly [41]. 3D structure spheroids exhibit enhanced cell viability, stable morphology and polarization, increasing proliferative activity and physiological metabolic function [42], which are markedly improved when compared to 2D cell monolayers. However, the open challenge is combining different cell types in co-culture spheroids mimicking the complex natural morphology and physiological tasks of natural tissues.

Many 3D cell-cultures based biosensors can use natural or synthetic hydrogels in order to obtain different 3D cell structures. The wide variety of commercial hydrogels allow the selection of suitable matrices directed for each cell lines and biosensor application. Alternatively, it is possible exploit the intercellular polymeric linker to create 3D cellular aggregates supported by neighboring cells [43], preserving cell viability and exhibiting greater cell function.

3D cell culture-based biosensors can be employed for many biomedical and bioanalytical applications [44], from early detection of illness [45] to environmental monitoring [46].

3D culture systems represent great promise for applications in drug discovery, pharmacological studies, cancer cell biology and tissue engineering, and they should be considered the obligatory step between the traditional 2D monolayer cell culture and animal models.

### **1.2.2 Whole-cell biosensors**

In according to IUPAC nomenclature [31], whole-cell biosensors require the integration of living cell into a device, e.g. by immobilization or encapsulation, in close contact with the transducer, e.g., light detector in optical biosensors. Differently from other biosensing configurations, for example immune and nucleic acid sensors, the use of cells as biorecognition elements enables to obtain informations about the bioavailability of chemicals and their combined effect (e.g. synergistic and/or antagonist and toxicity).

In the past decade there has been increasing demand for in-vitro assays as alternatives to animal testing to investigate the effects of chemicals on biological targets. The European Union (EU) is encouraging the use of in-vitro assays and other approaches to replace animal testing. To this end, several programs and initiatives have been launched by the EU, for example banning of animal testing for cosmetics in 2009 [47] and the European Partnership for Alternative Approaches to Animal Testing (EPAA).

Significant advances have recently been reported both in detection technology and in the genetic engineering of cells, enabling design of cells to respond to different analytes or classes of analyte, with the possibility of performing high-throughput and high-content screening assays on the basis of different transduction principles, even in label-free configurations [48-49]. Several whole-cell biosensors have been applied to different fields, from drug discovery [50] to environmental monitoring [51-53], food control [54], and anti-doping screening [55]. In particular, genetically modified BL biosensors have excellent analytical performance and flexibility of use, being suitable also for integration into field-deployable device [56-57]. By taking advantage of the peculiar features of nanomaterials, hybrid devices with immobilized or micropatterned cells, with great potential applications in biosensing and cell behavior monitoring, have also been obtained [58].

### **1.3 3D PRINTING TECHNOLOGIES**

Three-dimensional (3D) printing is a fabrication process which enables to rapidly produce prototypes, and functional devices [59], such tissue grown scaffolds [60], electronics [61] microfluidics [62] and pneumatics [63]. The earliest printing technique was born in China around the year 200 with a woodblock printing. A block of wood was carved in order to obtain a prototype which was then used to repeatedly form an imprint on a substrate. Starting from this approach, the printing technologies have evolved from the printing press, movable type, lithography, xerography, laser printing to finally 3D printing in which a 3D computer design is converted in a physical pattern through the additive patterning of material using a print head, nozzle, or other mechanisms [64-66].

Stereolithography (SLA) technique was introduced by Charles W-Hull in 1986 (U.S. Patent 4575330) [67]. A laser UV light source is focused on a vat filled of liquid photopolymer resin where layer-by-layer selective polymerization builds 3D structures on a build platform [68-69]. Two different approaches for resin exposure can be used in this technique, free surface or constrained surface [70-71], and two different light sources for printing, laser or digital light projection (DLP). In the free surface approach, the photopolymerization occurs the polymer at the air interface, where the metal build stage is submerged further into the resin-containing vat after the formation of each layer. In the constrained surface approach, the polymerization occurs against the bottom surface of the resin vat, where the metal build stage is suspended upside-down.

One of the most widely rapid 3D prototyping technologies is represented by fused deposition modeling (FDM), introduced for the first time by Scott Crump [72]. FDM 3D printers use thermoplastic materials that are fused and extruded through a nozzle. In order to obtain a 3D structure, the thermoplastic material is deposited layer by layer on the build platform that then cools down and solidifies [70,73-74]. Thanks to

the possibility to print inexpensive and durable [75] biocompatible polymers as acrylonitrile butadiene styrene (ABS), poly(lactic acid) (PLA, a biodegradable polymer), polycarbonate, polyamide and polystyrene, this prototyping method represents an interesting technique for obtaining portable devices [76-77]. In alternative, FDM can be used for printing a wide range of liquid materials, such as metallic solutions, hydrogels, and cell-based solutions thanks to the possibility of extrude liquid precursor through a nozzle without heating.

Another technology for printing polymers, ceramics, metal and biomaterials uses the material jetting 3D printers [78] in which wax-like materials are melted and printed using an inkjet print head onto a mobile build platform. The material, deposited layer by layer, cools and forma solid 3D structure.

Photopolymer jetting, introduced for the first time by Hanan Gothait [79], is another approach for printing support liquid photopolymers onto a mobile build platform. Through UV light, the materials are cured and solidified, allowing layer-by-layer fabrication. Thanks to this technology, many microfluidic devices have been fabricated [80-84].

This 3D printer technology is used for printing any material that is available in powder form and it does not require any support structure. The process is fast, simple and cheap as powder particles are glued together to produce a solid structure and, when repeated, a 3D structure is built up layer-by-layer in the powder bed.

Another process that does not require any support structures is the laser sintering in which laser source and scanning mirrors sinter layer-by-layer plastic powdered material.

Laser melting 3D printing uses a similar concept to laser sintering, but this process builds 3D structures melting and fusing metal powders. Moreover, this approach

requires support structure to anchor the part to the build platform.

Metal powders can be print also with an electron beam melting. In this contest an electron beam is used to melting metal powders, generating lower thermal stress in the structure. Furthermore, the amount of support structures is reduced while the fabrication speed increased.

## **1.4 PORTABLE LIGHT DETECTORS**

To implement cell-based assays into portable formats and turn them into real biosensors with adequate analytical performance the selection of miniaturized light detectors is crucial. Indeed, due to the dim BL signals, to obtain the highest detectability, BL signal measurement requires instrumentation able to collect as much light as possible. Conversely, no specific optics geometry is required as for photoluminescence detection, where an external light source is required.

### **1.4.1 Portable light detectors**

Portable light detectors, such as charge-coupled devices (CCD), complementary metal oxide semiconductors (CMOS), and silicon and organic photodiodes, have a great potential like alternative light sensors due to their compact size and their ability to image and quantify multiple spots simultaneously on the detections area of the sensor. [85-87]. Modern cooled back-side illuminated CCDs create high-quality, low-noise images reaching a quantum efficiency (QE) of up to 90%, read-out noise of  $<5 e^-$ , dark count rates of  $0.001 e^-/s$ , and formats as large as  $4096 \times 4096$  pixels with size down to  $4 \times 4 \mu m$  [88].

Nowadays CMOS sensors represent an interesting alternative, thanks to their small and compact size, low power consumption, camera-on-a-chip integration and lower fabrication costs [89-90]. In comparison to the first generations of CMOS where the majority of the pixel area was dedicated to the support transistors, with a limited photon-sensing area (fill factor), modern back-illuminated CMOS uses the entire

area of each pixel for photon capture. In this configuration CMOS shows higher sensitivity, thus ensuring high signal-to-noise even in low-light conditions.

For measurement of a large number of targets, Sandeau et al [91] reported a large area CMOS bio-pixel array for multiple CL assays directly addressed by single pixels.

In order to obtain reasonable resolution and to prevent light cross-talk between adjacent objects, imaging with charge-transfer sensors needs a simple optics. In optics-free “contact imaging” configurations, the sensor is in contact directly with the surface of the bioassay. Tanaka et al. reported CMOS sensor equipped with RGB color filter array for analyzing single cells assembled directly onto the sensor surface [92]. In order to obtain a thermal insulation between the bioassay components and the cooled CCD sensor, and a coherent photon transfer between the two surfaces, a fiber optic mosaic faceplate or tape was used for contact imaging. Exploiting a thermoelectrically cooled (double Peltier) CCD camera in contact imaging configuration, Roda et al. developed an ultrasensitive portable device for point-of-need CL bioassays [93]. Thanks to this device, Mirasoli et al. developed a miniaturized multiplex biosensor for detecting parvovirus B19 DNA in serum samples [94], showing competitive analytical performance respect to conventional ELISA assay.

#### **1.4.2 Color detectors: CCD vs CMOS**

The possibility to combine several luminescent probes in a single assay with different specific emission wavelengths and bandwidths requires spectral resolved light imaging detection. CCD and CMOS sensors available in monochromatic version present an up to 90% QE across the full visible spectrum but commercially are available also their one-shot color version in which Bayer matrix (a red, green and blue filter patterns) is placed over the pixel array. Thanks to the continuous

improvement in the backside-illuminated CMOS (BSI-CMOS) integrated in smartphone/tablet camera allow advances in image quality, superior functionalities and compact size. Nowadays new developed CMOS sensors with higher pixel numbers (up to 41 MP) have an architecture and multi-lens systems that provide, in low light condition, low noise and high quality image capture. In this configuration smartphone cameras can be used for sensitive chemical luminescence detection allowing the analyte measurements at medium-abundant concentration, as was recently shown for CL-based point of care bioassays [95-96].

Thanks to 3D printing technology, simple and compact 3D-printed low-cost smartphone accessories can be developed for transforming mobile device into a portable mini-luminometer for point-of care testing, exploiting dedicated applications for signal data elaboration, data handling and storage, connectivity, and cloud servicing, for remote sensing.

## REFERENCES

- [1] Kaskova ZM, Tsarkova AS, Yampolsky IV (2016), *Chem. Soc. Rev.*, 2016, 45, 6048
- [2] Shimomura O, (2006) World Scientific Publishing Co. Pte. Ltd, Singapore
- [3] Roda A, Guardigli M, Michelini E, Mirasoli M (2009) *Tracs Trend in Anal Chem*, Volume 28, Issue 3, 307-322
- [4] Branchini BR, Behney CE, Southworth TL, Fontaine DM, Gulick AM, Vinyard DJ and Brudvig GW (2015), *J. Am. Chem. Soc.*, 137, 7592–7595
- [5] Roda A, Pasini P, Mirasoli M, Michelini E, Guardagli M, (2004) *Trends.Biotechnol.* 22, 295-303
- [6] Wood KV, Lam YA and McElroy WD, (1989) *J. Biolumin. Chemilumin.*, (1989), 4, 289–301
- [7] Cevenini L, Camarda G, Michelini E, Siciliano G, Calabretta MM, Bona R, Santha Kumar TR, Cara A, Branchini BR, Fidock DA, Roda A, Alano P., *Analytical chemistry* 86 (17), 8814-8821
- [8] Hall MP, Unch J, Binkowski BF, Valley MP, Butler BL, Wood MG, Otto P, Zimmerman K, Vidugiris G, Machleidt T, Robers MB, Benink HA, Eggers CT, Slater MR, Meisenheimer PL, Klaubert DH, Fan F, Encell LP and Wood KV (2012), *ACS Chem. Biol.*, 7, 1848–1857
- [9] Roda, A., Guardagli, M., Pasini, P., Mirasoli, M. (2003) *Anal. Bioanal. Chem.* 377, 826-33
- [10] L. Cevenini, M. M. Calabretta, A. Lopreside, B. R. Branchini, TL Southworth, E. Michelini, A. Roda, (2017), *Photochemistry and Photobiology* 93 (2), 531-535
- [11] Rehemtulla A, Stegman LD, Cardozo SJ, Gupta S, Hall DE, Contag CH, Ro BD (2000), *Neoplasia* 6, 491-495
- [12] E. Michelini, L. Cevenini, M.M. Calabretta, S. Spinozzi, C. Camborata, A. Roda (2013), *Anal Bioanal Chem* 405:6155-6163
- [13] Leclerc GM, Boockfor FR, Faught Wj, Frawley LS (2000), *Biotechniques* 29:590-591

- [14] Branchini BR, Southworth TL, Khattak NF, Michelini E, Roda A (2005) *Anal Biochem* 345, (1) 140-148
- [15] Cevenini L, Michelini E, D'Elia M, Guardigli M, Roda A (2013), *Anal Bioanal Chem* 405:1035–1045
- [16] Caland F, Miron S, Brie D, Mustin C (2011), I.E. statistical signal processing workshop (SSP), pp 801-804
- [17] Heise K, Oppermann H, Meixensberger J, Gebhardt R, Gaunitz F (2013), *Assay Drug Dev Technol* 11:244–252
- [18] Michelini E, Cevenini L, Mezzanotte L, Ablamsky D, Southworth T, Branchini BR, Roda A (2008), *Photochem Photobiol Sci* 7:212–217
- [19] Hosseinkhani S (2011), *Cell Mol Life Sci* 68:1167–1182
- [20] Woo J, Howell MH, von Arnim AG (2008), *Protein Sci* 17:725–735
- [21] Nakatsu T, Ichiyama S, Hiratake J, Saldanha A, Kobashi N, Sakata K, Kato H (2006), *Nature* 440:372–376
- [22] Navizet I, Liu YJ, Ferré N, Roca-Sanjuán D, Lindh R (2011), *ChemPhysChem* 12:3064–3076
- [23] Vieira J, Pinto da Silva L, Esteves da Silva JC (2012), *J Photochem Photobiol B* 117:33–39
- [24] Branchini BR, Ablamsky DM, Davis AL, Southworth TL, Butler B, Fan F, Jathoul AP, Pule MA (2010), *Anal Biochem* 396:290–297
- [25] Roda A, Mezzanotte L, Aldini R, Michelini E, Cevenini L (2010), *Neurogastroenterol Motil* 22: 1117–e288
- [26] Michelini E, Donati M, Aldini R, Cevenini L, Mezzanotte L, Nardini P, Foschi C, Zvi IB, Cevenini M, Montagnani M, Marangoni A, Roda A, Cevenini R (2012), *Anal Biochem* 430:92–96
- [27] Didiot MC, Serafini S, Pfeifer MJ, King FJ, Parker CN (2011), *J Biomol Screen* 16: 786–793

- [28] Viviani VR, Arnoldi FG, Venkatesh B, Neto AJ, Ogawa FG, Oehlmeyer AT, Ohmiya Y (2006), *J Biochem* 140:467–474
- [29] Wang Y, Akiyama H, Terakado K, Nakatsu T (2013), *Sci Rep* 3:2490
- [30] Contang GH, Bachmann M (2002), 4, *Annu. Rev. Biomed.* 2035-60
- [31] <http://goldbook.iupac.org> Last update: 2014-02-24; version: 2.3.3.
- [32] Cali JJ, Niles A, Valley MP, O'Brien MA, Riss TL, Shultz J (2008), *Expert Opin Drug Metab Toxicol* 4:103–120
- [33] Michelini E, Cevenini L, Mezzanotte L, Coppa A, Roda A (2010), *Anal Bioanal Chem* 398: 227–238
- [34] Nakajima, Y. and Y. Ohmiya (2010), *Expert Opin. Drug Discov.* 5, 835–849.
- [35] Birgersdotter A, Sandberg R, Ernberg I (2005), *Semin Cancer Biol* 15, 405-412]
- [36] Weaver VM, Petersen OW, Wang F, Larabell CA, Briand P, Damsky C, Bissell MJ, (1997), *J cell boil* 137, 231-245
- [37] Bhadriaraju K, Chen CS (2002) *Drug Discov Today* 7, 612-620
- [38] Bahrvand H, Hashemi SM, Kazemi Ashtini S, Farrokhi A (2006) *Int J Dev Biol* 50, 645-652
- [39] Benya PD, Shaffer JD (1982) *Cell* 30, 215-224
- [40] Nelson CM, Bissell MJ (2005), *Semin Cancer Bio*, 15, 342-352
- [41] Whitesides GM, Grzybowski B, (2002) *Science*, 295 pp. 2418-2421
- [42] Antoni D, Burckel H, Josset E, Noel G, (2015) *Int. J. Mol. Sci.*, 16(3), 5517-5527
- [43] Ong S-M, Zhang C, Toh Y-C, Kim SH, Foo HL, Tan CH, Noort DV, Park S, Yu H, (2008), *Biomaterials*, 29, 3237-3244
- [44] Wang J, Wu C, Hu N, Zhou J, Du L, Wang P, (2012) *Biosensors* 2, 127-170

- [45] Ngoepe M, Choonara Y, Tyagi C, Tomar LK, Du Toit LC, Kumar P, Ndesendo VMK, Pillay V (2013), *Sensors* 13, 7680-7713
- [46] Souiri M, Gammoudi I, Mora L, (2012) *J Environ Sci Eng* 2012, 1, 924-935
- [47] Directive 2003/15/EC of the European Parliament and the Council of 27 February amending Directive 76/786/EEC on the approximation of the laws of the member States relating to cosmetic products. *Off J Eur Communities* L66, 26–35
- [48] Raut N, O'Connor G, Pasini P, Daunert S (2012), *Anal Bioanal Chem* 402:3147–3159
- [49] Lagarde F, Jaffrezic-Renault N (2011), *Anal Bioanal Chem* 400:947–964
- [50] Alloush HM, Anderson E, Martin AD, Ruddock MW, Angell JE, Hill PJ, Mehta P, Smith MA, Smith JG, Salisbury VC (2010), *Clin Chem* 56:1862–1870
- [51] Elad T, Belkin S (2012), *Bioeng Bugs* 3:124–128
- [52] Zhang D, He Y, Wang Y, Wang H, Wu L, Aries E, Huang WE (2012), *Microb Biotechnol* 5:87–97
- [53] Jouanneau S, Durand MJ, Thouand G (2012), *Environ Sci Technol* 46, 11979–11987
- [54] Cheli F, Battaglia D, Pinotti L, Baldi A (2012), *J Agric Food Chem* 60, 9529–9542
- [55] Cevenini L, Michelini E, D'Elia M, Guardigli M, Roda A (2013), *Anal Bioanal Chem* 405, 1035–1045
- [56] Charrier T, Chapeau C, Bendria L, Picart P, Daniel P, Thouand G (2011), *Anal Bioanal Chem* 400, 1061–1070
- [57] Roda A, Cevenini L, Michelini E, Branchini BR (2011), *Biosens Bioelectron* 26, 3647–3653
- [58] Ben-Yoav H, Melamed S, Freeman A, Shacham-Diamand Y, Belkin S (2011), *Crit Rev Biotechnol* 31, 337–353
- [59] P. Marks, M. Campbell, J. Aron and H. Lipson, *New Sci.*, 2011, 2823, 17–20  
Search PubMed

- [60] J. N. Hanson Shepherd, S. T. Parker, R. F. Shepherd, M. U. Gillette, J. A. Lewis and R. G. Nuzzo, *Adv. Funct. Mater.*, 2011, 21, 47–54 CrossRef CAS
- [61] B. Y. Ahn, E. B. Duoss, M. J. Motala, X. Guo, S.-I. Park, Y. Xiong, J. Yoon, R. G. Nuzzo, J. A. Rogers and J. A. Lewis, *Science*, 2009, 323, 1590–1593 CrossRef CAS
- [62] D. Therriault, S. R. White and J. A. Lewis, *Nat. Mater.*, 2003, 2, 265–271 CrossRef CAS
- [63] F. Ilievski, A. D. Mazzeo, R. F. Shepherd, X. Chen and G. M. Whitesides, *Angew. Chem., Int. Ed.*, 2011, 50, 1890–.
- [64] Gross BC, Erkal JL, Lockwood SY, Chen C, Spence DM (2014), *Anal. Chem.* 86, 3240–53
- [65] Shallan AI, Smejkal P, Corban M, Guijt RM, Creadmore MC (2014), *Anal. Chem.* 86 3124–30
- [66] Knowlton S, Onal S, Yu C H, Zhao J J and Tasoglu S 2015 Bioprinting for cancer research *Trends Biotechnol.* 33 504–13
- [67] C. Hull, *Mod. Cast.* 1988, 78, 38; Google Patents, US Patent No. 4,575,330
- [68] T. Nakamoto, K. Yamaguchi, P. A. Abraha, K. Mishima, J.; *Micromech. Microeng.* 1996, 6, 240;
- [69] Bertsch A, Bernhard P, Vogt C, Renaud P, (200) *Rapid Prototyping J.*, 6, 259
- [70] Waldbaur A, Rapp H, Lange K, Rapp BE (2011), *Anal. Methods* 3, 2681-716
- [71] Huang Y-M, Jeng J-Y and Jiang C-P (2003), *J. Mater.Process. Technol.* 140, 191-6
- [72] Crump SS (1992) *Google Patents*. US Patent No. 5,121,32
- [73] Pham D and Gault R (1998) *Int. J. Mach. Tools. Manuf* 38 1257-87
- [74] Sood AK, Ohdar R and Mahapatra S (2009) Improving dimensional accuracy of fused deposition modelling processed part using grey Taguchi method *Mater. Des.* 30, 4243-5
- [75] Au A K, Huynh W, Horowitz LF, Folch A (2016), *Angew. Chem. Int. Ed. Engl.* 55 2-22

- [76] Cevenini L, Calabretta MM, Lopreside A, Tarantino G, Tassoni A, Ferri M, Roda A, Michelini E (2016), *Anal and bioanal Chem*, 408 (30), 8859-8868
- [77] Cevenini L, Calabretta MM, Tarantino G, Michelini E, Roda A *Sensors and Actuators B: Chemical* (2016) 225, 249-257
- [78] Calvert P (2001) Inkjet printing for materials and devices *Chem. Mater.* 13,3299-305
- [79] Gothait H Apparatus and method for three-dimensional model printing (2001) Google Patents
- [80] Erkal JL, Selimovic A, Gross BC, Lockwood SY, Walton EL, McNamara S, Martin RS, Spence DM (2014), *Lab Chip* 14 2023–32
- [81] Begolo S, Zhukov D, Selck DA, Li L, Ismagilov RF (2014), *Lab Chip* 14, 4616–28
- [82] Causier A, Carret G, Boutin C, Berthelot T, Berthault P (2015), *Lab Chip* 15 2049–54
- [83] Bonyár A, Sántha H, Ring B, Verga M, Kovacs JG, Harsányi G (2010), *Procedia Eng.* 5 291–4
- [84] Anderson KB, Lockwood SY, Martin RS, Spence DM (2013), *Anal. Chem.* 85 5622–6
- [85] Lengger S, Otto J, Elsasser D, Shneider O, Tiehm A, Fleischer J, Niessner R, Seidel M (2014), *Anal. Bioanal. Chem* 406,3323-3334
- [86] Zangheri M, Di Nardo F, Anfossi L, Giovannoli C, Baggiani C, Roda A, Mirasoli M (2015), *Analyst* 140, 358-365
- [87] Zhou Z, Xu LR, Wu SZ, Su B (2014) *Analyst* 139, 4934-4939
- [88] Roda A, Mirasoli M, Michelini E, Di Fusco M, Zangheri M, Cevenini L Roda B, Simon P (2016) *Biosensors and Bioelectronics* 76, 164-179
- [89] Singh RR, Lench L, Guenther A, Genov R, (2011) *IEEE J. Solid-state circuits* 47, 282-2833

- [90] Rodrigues, ERGO, LAPA, R.A.S. (2010), Anal Bioanal. Chem. 397,381-388
- [91] Sandeau L, Vuillaume C, Contié S, Grinerval E, Belloni F, Rigneault H, Owens RM, Brennan Fournet M (2015), Lab Chip 15, 877-881
- [92] Tanaka T, Saeki T, Sunaga Y, Matsunaga T (2010), Biosens And Bioelectron 26,1460-1465
- [93] Roda A, Mirasoli M, Dolci LS, Buragina A, Bonvicini F, Simoni P, Guardigli M (2011) Anal. Chem. 83, 3178-3185
- [94] Mirasoli M, Bonvicini F, Dolci LS, Zangheri M, Gallinella G, Roda A (2013), Anal Bioanal Chem 398, 227-238
- [95] Roda A, Guardigli M, Calabria D, Calabretta MM, Cevenini L, Michelini E (2014), Analyst 139, 6494-6501
- [96] Roda A, Michelini E, Cevenini L, Calabria D, Calabretta MM, Simoni P (2014) Anal Chem 86, 7299-7304

## CHAPTER 2

---

### ***Aim of the thesis***

---

The activity carried out during my PhD was mainly focused on the development of portable whole-cell bioluminescent (BL) biosensors for multianalyte detection and their implementation into portable analytical devices for point-of-care and point-of-need applications. In particular, through reporter gene technology, cells (bacteria, yeast and mammalian cell lines) have been genetically engineered with a bioluminescent reporter protein (e.g., luciferases from different organisms), whose expression is under the regulation of a specific promoter and/or regulatory sequence activated by a target analyte or a class of analytes. After addition of a suitable BL substrate (e.g., D-luciferin, coelenterazine, furimazine) the luciferase catalyzes a reaction that produces light and the BL is directly proportional to the activation of a molecular target or to the bioavailable fraction of an analyte. Using living cells as sensing systems it is possible to develop cell-based assays and whole-cell biosensors to monitor physiological response to drugs, for detecting analytes for environmental and food monitoring and for the evaluation of specific biological activity and toxic effects. Indeed, the high detectability of the bioluminescent signal and the possibility to combine luciferases with different BL emission properties provides new analytical tools suitable for the development of cell-based bioluminescent assays in multiplex formats. Moreover, since BL signal is produced by a chemical reaction and it does not require an external light source, BL detection is suitable for the development of portable miniaturized devices. The assays were validated and characterized in terms of analytical performance and applied to different fields, from environmental monitoring to clinical diagnostics. Such devices were fabricated using a dual-extrusion 3D printer, using thermoplastic material (ABS) and bioluminescent whole-cell biosensors have been obtained by genetically engineered cells that respond to different analytes.

In Chapter 3, a smartphone-based bioluminescence (BL) whole-cell biosensor is reported for acute toxicity evaluation. The developed whole-cell biosensor integrates bioluminescent living cells (HEK293T) constitutively expressing green

thermostable luciferase mutant and a smartphone equipped with custom-designed accessories produced employing a low-cost desktop 3D printer. The add-on assembly comprises two parts: a smartphone adaptor, containing a plano-convex lens aligned with the camera and a slot for inserting the cartridge hosting pre-loaded cells and reagents. The developed device demonstrated the feasibility to accurately detect and quantify the BL signals of genetically engineered human cell line expressing green-emitting luciferase with a limit of detection (LOD) of  $5 \times 10^3$  cells. The toxicity test showed performance comparable to that obtained using portable cooled CCD camera, confirming the suitability of this approach. Moreover, an android app was also developed to provide a user-friendly built-in data analysis. Real samples were analysed, including ubiquitous products used in everyday life. The results showed good correlation with those obtained with laboratory instrumentation and commercially available toxicity assays, thus supporting potential applications of the proposed device for portable real-life needs.

In Chapter 4, a bioluminescence smartphone-based cell biosensor exploiting NanoLuc luciferase as sensitive reporter to assess the (anti)-inflammatory activity of a sample and its acute toxicity evaluation was developed. In particular, this biosensor was employed for quantitative assessment of (anti)-inflammatory activity and toxicity of a sample and its preliminary application for testing extracts of white grape pomace was evaluated. NanoLuc (Nluc) and its destabilized BL reporter (NlucP) were investigated to identify the most suitable intracellular BL reporter for smartphone-based detection in order to obtain cell biosensors with adequate analytical performance, especially in terms of sensitivity and short assay time. Human embryonic kidney cell lines (Hek293T) were genetically engineered to express NanoLuc luciferase either under the regulation of NF $\kappa$ B response element or a constitutive cytomegalovirus (CMV) promoter. Results confirmed the suitability of the smartphone biosensing platform for analysis of untreated complex biological matrices.

Chapter 5 reports a non-destructive real-time BL imaging assay of spheroids for longitudinal and high-throughput studies on 3D cell models. 3D cell-culture models often promote levels of cell differentiation and tissue organization not possible in conventional 2D culture systems providing excellent *in vitro* models suitable to mimic *in vivo* tissue physiology. To this end, a high-throughput assay for tumor necrosis factor  $\alpha$  (TNF  $\alpha$ ) detection in a 96 well- micro-patterned microplate using a transcriptional biosensor system relying on BL 3D spheroids is reported. Three day-old HEK293 spheroids, transfected with a reporter construct in which the PLG2 luciferase is placed under the control of the NFkB response element, were incubated with different concentrations of TNF  $\alpha$ . Dose-response curves for TNF $\alpha$  were obtained with both monolayer cultures and spheroids, obtaining EC50 values of  $2.6 \pm 0.4$  and  $3.5 \pm 0.5$  ng/ml, respectively. Compared with the 2D format, a higher NFkB basal activation ( $4.1 \pm 0.3$  fold) was found in 3D spheroids. This result is consistent with *in vivo* data, thus corroborating the hypothesis that spheroids provide a more physiological condition than 2D cell-based biosensors.

## CHAPTER 3

---

# **Smartphone-interfaced 3D printed toxicity biosensor integrating bioluminescent “sentinel cells”**

---

*Reproduced from: “Smartphone-interfaced 3D printed toxicity biosensor integrating bioluminescent “sentinel cells”*

*Luca Cevenini, Maria Maddalena Calabretta, Giuseppe Tarantino, Elisa Michelini, Aldo Roda*

*Sensors and Actuators B: Chemical (2016) 225, 249-257*

## 4.1 INTRODUCTION

The availability of toxicity sensors suitable for rapid field testing is highly valuable also considering the recent global security threats. The routine monitoring of water, food and the environment for chemical and biological threat agents is often hampered by the fact that most of the available techniques, such as those based on high performance liquid chromatography-tandem mass spectrometry, require clean samples and sophisticated equipment, and are thus unsuitable for real-time, cost-effective and on-field testing [1]. Additionally, threats may derive from different sources, therefore conventional analytical methods able to detect one or few analytes are inappropriate [2]. Both enzymatic and microbial biosensors have been developed to detect general toxicity or environmental pollutants including heavy metals, endocrine disruptors, explosives [3-8]. The Microtox® toxicity test, based on the use of bioluminescent bacteria *Vibrio fischeri*, has been considered as the official standard for acute toxicity assay in several countries such as Germany (DIN 38412-1990) and USA (ASTM method D5660-1995) [9]. This test relies on the use of bioluminescent bacteria where the light emission of bacteria after being challenged by a sample is compared to light output of a control sample. The difference between two light outputs is ascribed to the toxic effect of sample. Moreover whole-cell biosensors present the important feature of assessing not the total concentration of a given analyte in a sample but rather its bioavailability, i.e., the fraction of analyte which is able to permeate in the cell membrane and once entered into the cell interact with specific molecular targets. Such systems provide quantitative information about biological effects of a sample such is the case of biosensors for mercury and organic mercury (methylmercury) in water samples [10,11]. All chemical and biological threat agents share the ability to damage in some ways living cells, which can be therefore employed as “living sentinels”. We previously demonstrated the possibility to integrate microbial cells (including *Escherichia coli*, *Saccharomyces cerevisiae* and *Magnetospirillum gryphiswaldense*) into portable

analytical devices relying on the use of charge-coupled device (CCD) detectors [12,13]. The use of mammalian cells, which actually mirror what happens in-vivo, would provide a more reliable mean to assess cytotoxicity to humans, as previously demonstrated in proof-of-concept toxicity biosensor devices exploiting eukaryotic cells-lines [14,15]. Recently an automated bench-top mammalian cell-based toxicity sensor was reported incorporating fluidic biochips with endothelial cells and Electric Impedance Sensing (EIS) detection [14]. Such systems, being able to assess the cellular cytotoxic responses, were successfully applied to toxicity test screening and to early warning real-time biomonitor [16]. Despite adequate analytical performance of these biosensors, they still require additional instrumentation and cell culture facilities. Also portable prototype devices require detectors and laptop control computer for data elaboration. In this view, the implementation of an analytical platform requiring only disposable ready-to-use cartridges containing the sensing cells and a smartphone for light detection is extremely appealing. The possibility to run tests that are routinely performed by trained personnel in laboratories with benchtop instrumentation such as microscopes and spectrophotometers with smartphone-interfaced devices offers tremendous potential in those situations in which a rapid and reliable response is needed, for example self-monitoring of chronic pathologies, and for early detection of toxicity and pollutants in water, food and the environment. In contrast to conventional biosensors and point-of-care (POC) systems that require external components like detectors and power supplies, smartphones offer the unique opportunity to have an all-in-one device that integrates a digital camera with portability and wireless data transfer [17]. Ozcan pioneered the concept of cellphone-based devices [18] and applied it to several types of bioassays including lateral flow immunoassay and enzymatic assays for the detection of biomarkers in biological fluids and other bioanalytical applications [19]. Several examples can be cited from the literature, most of them relying on colorimetric or fluorescent assays [20-23]. Interestingly,

data connectivity and geotagging capabilities of smartphones can also be exploited for distributed sensing, as demonstrated by Wei et al who developed a smartphone-based mercury(II) ion sensor platform with ppb sensitivity [24]. We previously demonstrated the feasibility of implementing enzyme-based assays with bioluminescence detection into smartphones and we fabricated cartridges with facile and low-cost 3D printing technology [25,26].

Nonetheless, to the best of our knowledge, the exploitation of bioluminescent cells as sensing elements in a smartphone-based platform has not been explored yet.

Here we report a portable toxicity sensor incorporating bioluminescent cells into a smartphone-based device. We fabricated 3D printed cartridges to integrate an array of bioluminescent cells into ready-to-use cartridges and demonstrated the feasibility to accurately detect and quantify the BL signals. We used human embryonic kidney cells (Hek293T) constitutively expressing a green-emitting luciferase as “sentinel cells” and an Android app was developed to provide a user-friendly environment. Additionally, we obtained a smartphone accessory including pre-loaded cartridges with immobilized cells, reagents’ reservoirs and droppers to provide a ready-to-use device. The analytical performance of the smartphone-biosensor was evaluated with model and real samples.

## **4.2 MATERIALS AND METHODS**

### **4.2.1 Chemicals and reagents**

Human embryonic kidney Hek293T cells were from ATCC (American Type Culture Collection [ATCC], Manassas, VA, USA) and materials used for culturing of cells were from Carlo Erba Reagents (Cornaredo, Milano, Italy). The enzymes required for cloning were from Fermentas (Vilnius, Lithuania). The kits for plasmid extraction and

purification and beetle D-luciferin potassium salt were from Promega (Madison, WI, USA). All other chemicals were purchased from Sigma (St. Louis, MO, USA).

The mammalian expression plasmid pCDNA-PpyGRTS expressing the *P.pyralis* luciferase green thermostable mutant was obtained from vector pGEX-PpyGRTS [27], kindly provided by Prof. Bruce Branchini (Connecticut College, New London, CT), by standard molecular cloning procedures.

#### **4.2.2 3D-printed cell minicartridges and smartphone adaptor fabrication**

Minicartridges and smartphone adaptors were fabricated using a desktop 3D printer Makerbot Replicator 2X (Makerbot, Boston MA, USA) using thermoplastic acrylonitrile butadiene styrene (ABS) polymer. Two cartridges were designed in this work: the first one was created for calibration purposes using black and white ABS and contains an array of 16 well of 50  $\mu$ L each (3.5 mm x 3.5 mm x 4.5 mm). The second cartridge (Fig.1(b)), printed with white ABS, contains 4 wells (volume of about 150  $\mu$ L each, size 4.5 mm x 4.5 mm x 7.5 mm) and two reservoirs, one for BL reagent and one for control. The cartridge also includes a sliding-lid created with dual-extrusion of black and transparent ABS. The adaptor, which provides a dark box, was designed to fit the Samsung Galaxy Note II smartphone. The open-source Tinkercad browser-based 3D design platform (Autodesk, Inc) was used to create 3D models. MakerWare v.2.4 software was used to set up printing options.

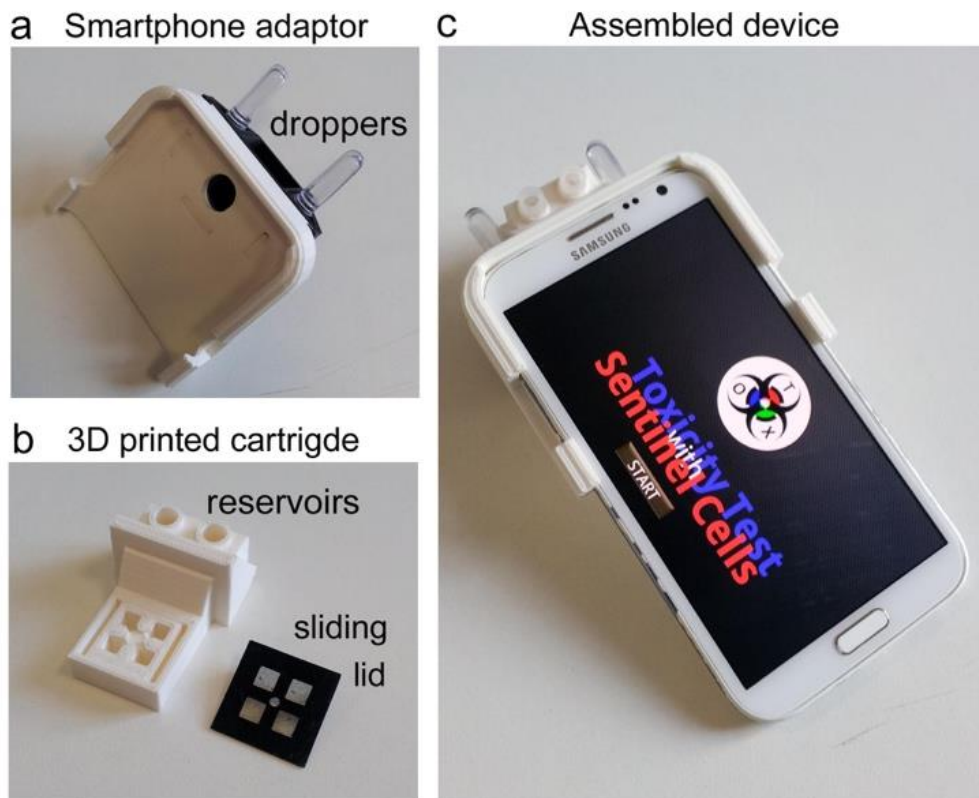


**Fig. 1.** (a) 3D printed smartphone adaptor designed for the Samsung Galaxy Note II with a black ABS dark box, comprising slots for droppers. (b) 3D printed cartridge, composed of a white ABS piece comprising 4 wells and BL substrate reservoirs and a black sliding lid with transparent ABS windows. (c) The assembled smartphone-based device with running the specifically designed application for BL signal acquisition and analysis.

#### 4.2.3 Android-based application

We developed a custom application (Tox-App) running on Android using Python (<https://www.python.org/>) and Kivy Open source Python library (<http://kivy.org/#home>) to convert the camera images into a quantitative and user-friendly output. The Tox-App functions as follows (see Fig. 2):

(a-b) the user selects the TOX icon and then to the “start” button to run the application on the smartphone;

(c) in the home page several tabs can be selected; the user can choose among reading the “Procedure”, analyzing a sample with the “test sample” button, or opening previous data using “Select image”. The “Info” box provide information about App developer “Unibo, Laboratory of Analytical and Bioanalytical Chemistry”;

d) in the “Procedure” box the user can read the instructions to perform the assay and some images provide a quick view of the steps;

(e) the “Begin” button allows to proceed to the “Checklist” box where preset timers guide the user through the steps following the correct incubation time (30min) before image acquisition. At the end of the countdown the “Acquire” button activates the cellphone camera and the BL image is taken;

(f) by clicking “Analyze” the BL image is rapidly processed on the smartphone within few seconds;

(g) the result is displayed as percentage of “Cell viability” together with a warning message (“Safe”, “Harmful” or “Highly toxic”). Both BL raw image and results can be saved for downstream applications such as sending the results to a central laboratory or cloud computing.



**Fig. 2.** (a) Screenshots of Tox-App running on an Android smartphone are shown. By clicking the “start” button (b) the application runs and several tabs can be selected (c). The “Procedure” box (d) provide to the user the instructions to perform the assay, then the Begin button allow to proceed to the “Checklist” box (e) where preset timers guide the user through the correct incubation times before BL image acquisition. The instructions can be also eluded by selecting “Test sample” in the home page, which jumps the user directly to the checklist. At the end of the countdown the smartphone camera is activated and the user can simply touch the “Acquire” button to capture the BL image of both the test and control wells. (f) The acquired images are rapidly analyzed on the smartphone and the sample toxicity result is displayed as “Cell viability” value and a warning message (Safe, Harmful, Highly toxic). BL image and results can be also saved for downstream application (i.e. sending results to a central laboratory).

#### 4.2.4 Cell culture and transient transfections

HEK293T cells were routinely grown in Dulbecco Modified Essential Medium (DMEM high glucose 4,5g/L, GE Healthcare) supplemented with 10% fetal bovine serum, L-

Glutamine 2mM, 50 U/ $\mu$ L penicillin, and 50  $\mu$ g/mL streptomycin. FuGENE HD transfection reagent (Promega) was used for transient transfections according to the manufacturer instructions. One day before transfection cells were plated on 24 well plate at a density of  $8 \times 10^4$  cells/well and transfected with pCDNA-PpyGRTS expression vector using the FuGENE<sup>®</sup>HD:DNA ratio of 3:1 according to the manufacturer's instructions and incubated at 37°C with 5% CO<sub>2</sub> for 24h.

#### **4.2.5 Smartphone-based BL emission characterization of Hek293T cells expressing green-emitting luciferase**

Luminescence measurements of engineered HEK293T cells were performed in duplicate into the 16-well cartridge and with a Varioskan Flash multimode reader (Thermo Fisher Scientific, Waltham, MA, USA) for comparison. Briefly, 24h post transfection the cells were collected and resuspended in DMEM at  $2 \times 10^6$  cell/mL and used for kinetic measurements and calculation of minimum number of detectable cells. Kinetic measurements were performed with Varioskan luminometer in 384-well plate, using 50  $\mu$ L of cell suspension, for 5 min with 200ms integration time, after automatic injection of 50  $\mu$ L of D-luciferin solution, 1mM pH 5.5 in citrate buffer 0.1 M. A volume of 30  $\mu$ L of serial dilutions of cells were pipetted into the multiwell cartridge and imaged with the smartphone after addition of 20  $\mu$ L of D-luciferin 1mM solution. Images were taken at 0.9 MP with 5s integration time using Camera FV-5 Lite app (FGAE, Stuttgart, Germany) and analyzed using ImageJ software (National Institutes of Health, Bethesda, MD). The minimum number of detectable cells was calculated as the number of cells providing a BL signal corresponding to the blank signal plus three times its standard deviation. Blank signal was obtained by measuring same number of non-transfected cells.

#### **4.2.6 Toxicity assay and analytical performance evaluation**

Smartphone-based toxicity assays were performed using the 4-wells minicartridges. Briefly, 24h post transfection the cells were collected, resuspended in Dulbecco's

Modified Eagle Medium (DMEM), counted and transferred to the minicartridges at  $5 \times 10^4$  cells/well (50  $\mu\text{L}$ ). Each ready-to-use cartridge was prepared by assembling the sliding lid and dispensing 200  $\mu\text{L}$  of BL reagent (1mM D-luciferin solution) in the reagent's reservoir and 200  $\mu\text{L}$  of PBS in the other reservoir. Dimethyl sulfoxide (DMSO) was used as model toxic compound and DMSO dilutions ranging from 0.25 to 100% v/v were prepared in MilliQ water. A volume of 30  $\mu\text{L}$  was dispensed in duplicate to the test wells while 30  $\mu\text{L}$  of PBS was added to control wells. Following the Tox-App procedure, after 30 min incubation at room temperature, 50  $\mu\text{L}$  of BL substrate was added to each well and BL images were taken and analyzed as previously described. All measurements were performed in duplicate and repeated with 6 different cartridges.

The same experiments were also performed using the disposable droppers provided within the device: first one drop (about 30  $\mu\text{L}$ ) of PBS was added to control wells followed by sample addition using the same dropper, then the whole volume (200  $\mu\text{L}$ ) of BL reagent was drawn from the reservoir with the other dropper and dispensed to all the four wells simultaneously through the central injection hole.

Toxicity assays for DMSO were also performed using the Cell-TiterGlo assay (Promega) in 384 well plate with the Varioskan luminometer. All experiments were performed in triplicate and repeated at least three times.

#### **4.2.7 Real sample analysis**

To test the feasibility of the proposed smartphone-based toxicity biosensor we first assessed the toxicity of real-life samples, including tap water, moisturizers, stain removers, mineral and synthetic oils, bio-degreaser, floor and toilet cleaner and an alcohol based aftershave. Samples were tested in duplicate using either the Cell-TiterGlo assay (Promega) in 384 well plate (50  $\mu\text{L}$  of cells, 30  $\mu\text{L}$  sample and 50  $\mu\text{L}$  Cell-TiterGlo reagent) with the Varioskan Flash luminometer and with the

smartphone biosensor as previously described. All measurements were performed in duplicate and repeated at least 3 times with three different cartridges.

#### **4.2.8 “Sentinel cells” immobilization**

To evaluate the feasibility of obtaining actual ready-to-use cartridges with pre-loaded “sentinel cells” we performed preliminary cell immobilization experiments. Cell suspensions were prepared in DMEM as described before at  $2 \times 10^6$  cell/mL and mixed with 2% agarose solution (cooled down to about 40°C) at 1:1 ratio. Cell-agarose mixtures were then transferred (50  $\mu$ L/well) into 4-wells 3D-printed cartridges and stored at 4°C for 6 days. A cartridge was used each day to evaluate biosensor response using 5% v/v DMSO (final concentration) as moderate toxic sample. Briefly, each cartridge was equilibrated at room temperature (23°C) for 15 min, then 30  $\mu$ L of DMSO solution and 30  $\mu$ L of PBS were dispensed in duplicate in sample and control wells, respectively, and incubated for 30 min at room temperature. After addition of 1mM D-luciferin solution (50  $\mu$ L), BL images were taken and analysed as previously described and the biosentinel response of control wells at day 0 (freshly immobilized cells) was set as 100%. All measurements were repeated with 3 different cartridges.

### **4.3 RESULTS AND DISCUSSION**

Main goal of the present work was the development of a low-cost smartphone-based device with ability to easily and quantitatively assess toxicity of a sample. To develop a smartphone-interfaced biosensor we addressed two main shortcomings, related to both “hardware” and “software”, that decrease marketability and real-life uses of several smartphone-based biosensing platforms, i.e., the need for external material, equipment, and/or specialized manpower (e.g., to perform precise pipetting of microvolume solutions) and easy readout [6, 28-30].

To overcome such limitations and provide a stand-alone device we included i) a custom-developed Tox-App to provide the end-user an immediate and quantitative

result about toxicity of tested sample, ii) an all-in-one cartridge holding all reagents (BL reagent and control sample) and sampling material (droppers). Another non-negligible advantage is the low cost production of the portable and compact device, which was completely fabricated by 3D printing, and the use of bioluminescent cells as power-free living biosentinels.

#### **4.3.1 3D printed all-in-one device**

We designed a smartphone holder suitable to i) integrate a minicartridge of pre-loaded cells, ii) create a dark box, iii) integrate reagents' reservoir and disposable droppers for easy sampling, iv) allow for light acquisition thanks to transparent windows in the cartridge's lid. Facile and low-cost 3D printing technology was selected to include these features in a compact accessory and rapidly generate a number of prototypes [31]. 3D models were rapidly generated with a printing time of about 30 min for either the minicartridge and the cellphone adaptor. Computer aided design program was used to generate 3D models, then converted to stereo lithography (.stl) file format and elaborated with a slicer software. The 3D objects were then printed layer-by-layer from the bottom up by heating and extruding thermoplastic ABS filaments.

The smartphone adaptor was designed to fit a Samsung Galaxy Note II (Fig. 1(c)) and was fabricated in three pieces to simplify the interchangeability between smartphones with central camera. In this way the black "dark box", which also comprises two slits for the droppers, can be reused with different smartphone covers and the 3D printed cartridges are almost universal (Fig.1(a)).

The ready to use, disposable cell-cartridges were designed as an all-in-one frame which provide duplicates for both control and test wells and two reservoirs for the BL substrate and PBS buffer (Fig. 1(b)). Since for BL signal acquisition the precise focal distance is not required (about 8 cm for this smartphone model), the depths of the cartridge array and the dark box were selected to allow the simultaneous

imaging of the wells while maintaining a compact size (device height 3 cm). The upper portion of the well array is specifically “carved” to allow an almost equal distribution of the BL substrate, injected through a central hole in the lid, to all the 4 wells simultaneously. A black sliding lid with transparent windows was created to protect the cells and avoid crosstalk between wells while allowing to acquire the BL signals with only a 5% reduction of transmitted light with respect to those obtained without the lid.

#### **4.3.2 Android-Based Toxicity Application (Tox-App)**

In mobile-based sensing devices, smartphones are frequently used for data acquisition or visualization. In such configurations smartphone-based sensing exploits available apps for image storing and/or for sending results (eg., raw images) to labs for data handling and interpretation with pc image analysis software packages such as the open source ImageJ (<http://imagej.nih.gov/ij>). This leads to an increase in time-to-results and unsuitability for locations with scarce or no internet access, which is a common condition in developing countries or remote areas. Conversely, we developed an Android App for to provide i) user instructions and assay timing, ii) image capture, iii) automatic analysis and results.

The main script of the application uses Python Imaging Library exploiting its image processing and graphics capabilities. Since samples and controls’ positions are fixed, the first step of our algorithm is the creation of four matrices of 150x150 pixels matching the cartridge wells. Each pixel in our matrices is represented by three numbers corresponding to its RGB values, then the mean RGB of each matrix is calculated and an additional average is computed between the two matrices of sample and control wells, respectively. The "Cell viability" value of the sample, discriminating between three different situations arbitrarily set as “Safe” (100-80%), “Harmful” (79-30%) and “Highly toxic” (<30%), is computed as percentage of BL signal normalized with respect to control set as 100%.

Major advantage of Tox-App, in comparison to previously reported apps is its data handling capability. In fact, similar apps often rely on a server that elaborates data and sends back results [32]. Although this data transfer occurs almost in real time (within two min) it cannot be used in those areas where connectivity is poor or limited. Contrarily, the Tox-App (Fig. 2) provides immediate and quantitative results about sample toxicity in terms of cell viability and with a user-friendly warning message that classifies sample toxicity accordingly as safe, harmful or highly toxic.

#### **4.3.3 “Sentinel cells” assay analytical performance**

In an effort to obtain a biosensor able to provide a response relevant to human physiology, we selected human embryonic kidney cell lines which are considered a good model for toxicity studies [33]. Additionally, these cells are easy to grow and can be transfected with high efficiency, thus being a good candidate for the integration into the biosensor. We selected as reporter protein the green emitting *P. pyralis* thermostable mutant PpyGRTS, which was previously described [27]. This human codon optimized luciferase is rapidly produced and accumulates in mammalian cell, even at 37°C, thus providing a sensitive reporter BL cell-line. In addition, its BL emission spectra (with maximum at 549nm and an half bandwidth of 70nm) nearly overlaps the spectral transmittance of the green filter of the Bayer matrix in the smartphone CMOS sensor, allowing a better sensitivity and reduced noise in the green channel.

To explore the suitability of using the integrated CMOS sensors of a smartphone to image the BL signals emitted by cells, we preliminary evaluated the minimum number of detectable Hek293T cells expressing luciferase PpyGRTS. To this end a 4x4 mini cartridge (Fig. 3(a)) was fabricated as described in Materials and Methods section. Cell dilutions were imaged with the smartphone and compared to BL signals obtained with the reference Varioskan Flash luminometer (Fig. 3(b)) using 384

microwell plates. The cell number leading to a signal corresponding to that of the blank plus three standard deviations, was  $(6.5 \pm 0.2) \times 10^3$  cells for the smartphone device and about 10 cells for the Varioskan Flash. Measurements performed with the luminometer provided a minimum number of detectable cells three decades lower than those obtained with the smartphone. These results prompted us to use an average number of  $5 \times 10^4$  cells per well to provide acceptable BL signal intensity in control wells.

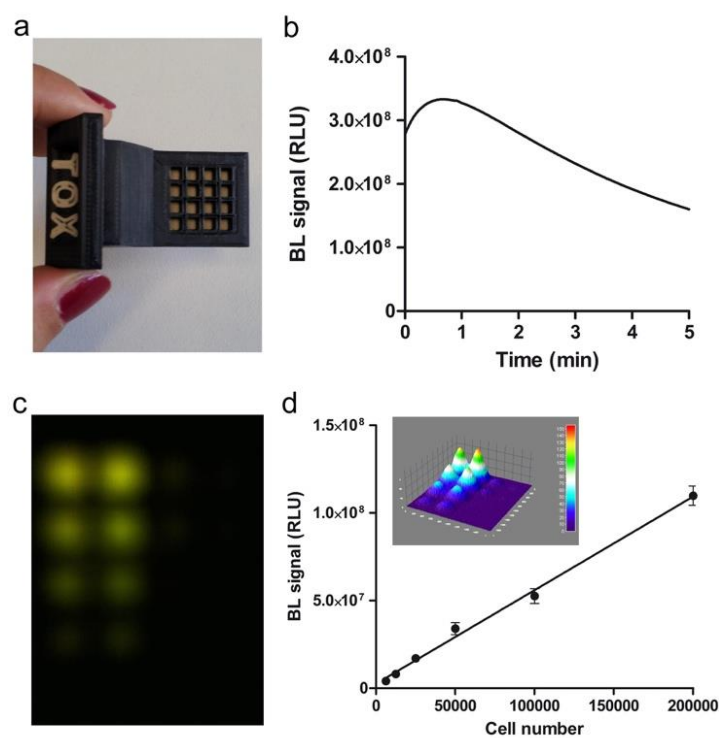


**Fig. 3.** (a) Picture of the 3D printed multi-well cartridge used for determination of minimum number of detectable cells. The minicartridge (dimensions: 36 mm x 50 mm x 24 mm) was fabricated with dual-extrusion of black and white ABS, contains 16 wells of about 3.5 mm x 3.5 mm x 4.5 mm each. (b) BL emission kinetic of transfected Hek293T cells obtained with Varioskan luminometer after addition of D-luciferin solution. (c) BL image of serial dilution of cells, seeded in duplicate in the multiwell cartridge, obtained with the smartphone after addition of D-luciferin solution. Images were taken at 0.9 MP with 5s integration time using Camera FV5-lite App. (d) Elaboration of BL image with ImageJ software to quantify the BL signal of each well and to calculate the minimum number of detectable “sentinel cells”. Inset: interactive 3D surface plot of BL image of panel c.

The analytical performance of the toxicity assay with “sentinel cells” was evaluated by testing different concentrations of toxic simulated samples. We first used DMSO, chosen as model toxic compound for its well-known toxic effect [34]. A toxicity curve for DMSO in the range from 0.1 to 40% v/v was obtained with the smartphone (Fig. 4(b)). An IC<sub>50</sub> of  $8.9 \pm 0.7$  % v/v was calculated vs an IC<sub>50</sub> of  $5.7 \pm 0.5$  % v/v obtained with the commercial Cell-TiterGlo kit (data not shown). A within-run coefficient of variation of 9% and 12% was obtained by using 6 different cartridges at 1% and 10% v/v DMSO concentrations, respectively. Since the final device integrates droppers for reagents and sample addition without the need of additional instrumentation (e.g., laboratory micropipettes) we compared results obtained with the all-in-one-device assay format (with integrated droppers) with those obtained with same assay but precise manual dispensing using conventional laboratory micropipettes. As expected a higher, but still acceptable for on-site analysis, CV% (15%) was obtained with the provided droppers compared to 10% obtained using laboratory pipettes.

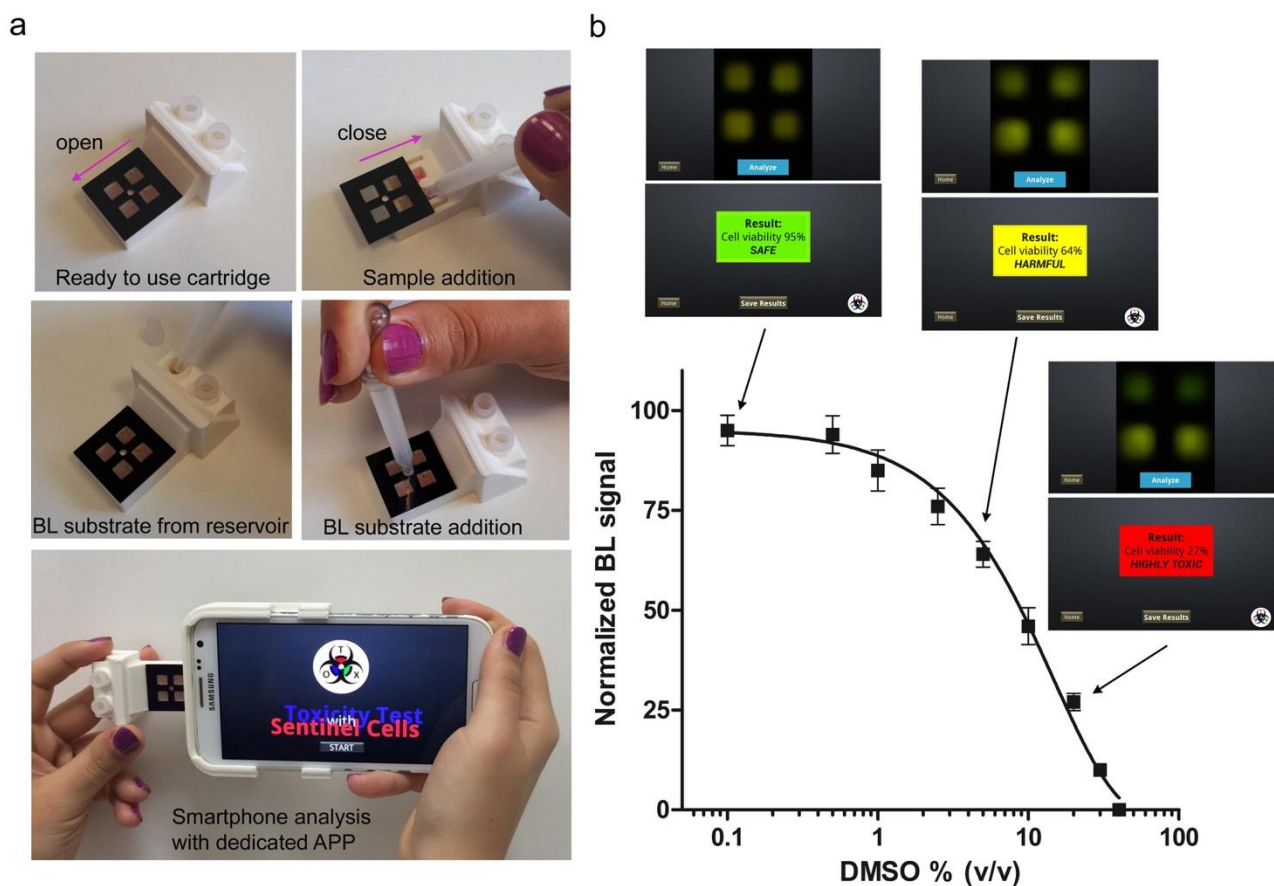


**Fig. 4.** (a) Pictures describing the easy steps required to perform a toxicity test: open the ready to use cartridge by sliding the lid and add one drop of sample to each test well, then close the lid and add the BL substrate from the reservoir with the other dropper. Insert the cartridge into the adaptor and acquire the BL image. The running Tox-App guide the user through the steps and process the images providing user-friendly results. (b) DMSO toxicity curve obtained with the smartphone and screenshots of BL image and relative result of selected DMSO concentrations of 0.1, 5 and 20% corresponding to the three warning levels of the Tox-App, set as “Safe” (100-80%), “Harmful” (79-30) and “Highly toxic” (<30%).

#### 4.3.4 Ready-to use cartridges with immobilized “sentinel cells”

We evaluated the feasibility of immobilizing the “sentinel cells” to obtain actually ready-to-use cartridges that can be stored for short periods of time, until needed. To this end several 3D-printed 4-well cartridges containing agarose-immobilized cells were prepared, stored at 4°C and daily used to assess the “sentinel cells” response using 5% DMSO as model sample. Preliminary results (Fig. 5(a)) clearly indicate that the cells rapidly lose the capability to act as “living sentinels”. This could be due to

the lack of optimal culture conditions (i.e. temperature, humidity, CO<sub>2</sub> and pH) which negatively affect cell metabolism and the intracellular machinery involved in the luciferase production. Noteworthy, each cartridge contains two control wells whose mean BL signal is used by the Tox-App to normalize the mean BL signal of sample wells and calculate the cell viability value of sample wells, accordingly and normalize the analytical signals accordingly. This correction allows to extend the storage time of cartridges with immobilized cells. In fact, since the loss of responsiveness due to cartridge storage equally affects both control and sample wells, an internal correction is obtained. As shown in Fig. 5(a) this auto-correction can be exploited up to day 3 in which, although control signal drops to 20% and sample signal to 14%, the Tox-App provides as output a cell viability of 65% which is consistent to 67% (both classified as “Harmful”) obtained with freshly prepared cells. After more than 3 days of a 4-day storage the BL signal of control well decreases more than 95% and the Tox-App does not was unable to process the raw data, providing a “Test failed: unable to measure control wells” message.

The short time stability of sentinel cells in the present configuration surely limits the supply of cartridges in decentralized laboratories, even so ready-to-use cartridges might be prepared in specialized manufacturing sites and transported or delivered within 2-3 days at quite remote distance within 2-3 days where the analysis is required, including small labs, hospitals and on the field. Indeed the smartphone-based toxicity biosensor could also represent an alternative to expensive luminometers in small laboratories.

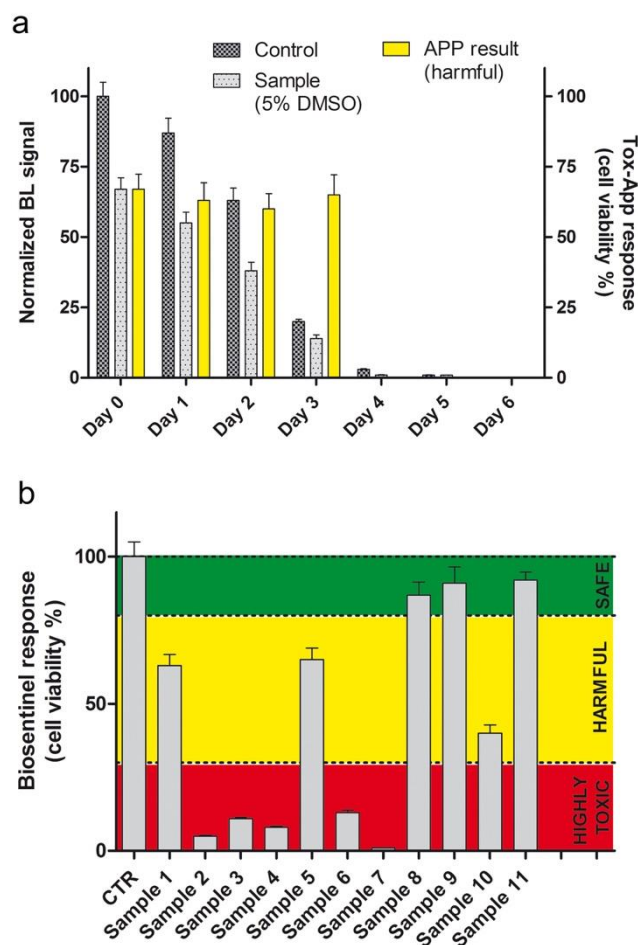


**Fig. 5.** (a) Immobilized “sentinel cells” responsiveness. Cartridges with pre-loaded “sentinel cells” immobilized in agarose-containing medium were prepared and stored at 4°C for 6 days. A cartridge was used each day to evaluate biosensor response using 5% v/v DMSO as moderate toxic sample. The biosentinel response of control wells at day 0 (freshly immobilized cells) was set as 100%. The results obtained with the Tox-App (in terms of cell viability %) are also shown. After day 3 data were not processed due to excessive cell-death even in control wells. (b) Real sample analysis. The toxicity of several “everyday life” products was assessed using the smartphone biosensor; samples included: (1) 10% Ethanol, (2) floor cleaner (3) toilet cleaner, (4) bio-degreaser, (5) mineral oil, (6) aftershave, (7) washing additive, (8) moisturizer, (9) liquid hand soap, (10) skin toner, (11) tap water. All measurements were repeated with three different cartridges.

Further work will be focused to increase the stability of immobilized mammalian cell lines stored at unconventional conditions with respect to standard culture settings (usually 37°C, 5% CO<sub>2</sub>, 95% relative humidity). We are working to optimize a previously developed matrix combining natural and synthetic polymers able to keep

immobilized microbial bioreporters (*E. coli* and *S. cerevisiae*) alive and responsive for up to 1 month. [13]. The potential of hypothermic storage of mammalian cells has been recently outlined by Xu et al. who employed a cell-membrane-mimetic polymer hydrogel to keep mouse cells alive for more than 1 week at 4 °C and 4 days at 25 °C [35]. Even more promising is the possibility to obtain spheroids and exploit the long term metabolic arrest induced by air-drying. A 6-week long-term viability (at least 6 weeks) during storage in air, at room temperature of Hek293 cells was obtained by Jack et al. using partially dried 3-D multicellular spheroids [36]. Such approaches could represent a significant step forward towards the development of robust cell-based biosensors and for their facile transport and storage.

#### **4.3.5 Real samples analysis**

To investigate the suitability of using the developed smartphone toxicity platform for actual applications we analysed real-life samples such as tap water, detergents and other products commonly handled in everyday life. Results are shown in Fig. 5(b), in which the output of the Tox-App quickly highlights sample toxicity: 3 samples were classified as safe, 3 as harmful, and 5 as highly toxic. The samples were analysed both with the smartphone-based biosensor and with a commercial toxicity assay for mammalian cells (CellTiterGlo® assay) that quantitates ATP, considered as an indicator of metabolically active cells. As previously described, the Tox-App provides both quantitative results in terms of cell viability and includes a qualitative readout for immediate understanding of potential health threats. Albeit most of the viability values correlate well with CellTiterGlo®, there are some discrepancies that could be ascribed to the diverse configuration of the two assays. In fact, in the smartphone-based assay the luciferase is expressed inside the cells and, by using a permeable D-luciferin solution, the BL reaction only relies on intracellular ATP of metabolically active cells. Conversely, in the commercial kit the luciferase and BL substrate are added together with a lysing reagent to release ATP from the cells, but also extracellular ATP that has been released from dead cells or

even due to plate contamination take part to the reaction, thus contributing to the light output. Nevertheless, the smartphone-interfaced whole-cell biosensor proved suitable for user-friendly, rapid and affordable toxicity testing.

#### **4.4 CONCLUSION**

We hereby report the first bioanalytical application of a smartphone to detect the BL signal of genetically engineered bioluminescent living cells. We developed an integrated smartphone-based toxicity biosensor, relying on BL “sentinel cells” into 3D printed cartridges. The developed device, which includes all chemical reagents and droppers for sample and BL substrate addition, together with the custom designed Tox-App, provides a standalone platform for user-friendly quantitative toxicity testing. The 3D-printed smartphone adaptors could be easily designed and produced at low-cost for any kind of mobile device, resulting in a very versatile approach.

Future work will be focused on the immobilization of mammalian cells into suitable biocompatible matrices to improve cell viability during cell storage [37-38] or on the use of alternative eukaryotic cell-lines which are less demanding in terms of culturing condition (e.g. trout cell lines, [15]). In addition, as direct 3D printing of living cells is an emerging approach for regenerative medicine and in vitro drug-screening and toxicology applications, the use of “bio-inks” [39] could be also applied to enable a direct and robust deposition of “sentinel cells” into 3D-printed devices for the development of integrated biosensors.

Conscious that huge efforts will be required to extend the lifespan of the integrated cells and to improve their responsiveness to reduce the time-to-response signal, the author believe that it could find significant application as rapid alerting tool. Such validated biosensor could represent a turnkey solution for rapid, sensitive, portable

toxicity sensor, currently not available in the market, suitable for detecting the presence of harmful pollutants in civil and military water supplies, for terrorism surveillance, and for detection of health threats in drinking water in developing countries.

## REFERENCES

- [1] O.A. Sadik, A.K. Wanekaya, S. Andreescu. Advances in analytical technologies for environmental protection and public safety. *J. Environ. Monit.* 6 (2004) 513-522.
- [2] H.T. Chau, K. Kadokami, H.T. Duong, L. Kong, T.T. Nguyen, T.Q. Nguyen, Y. Ito. Occurrence of 1153 organic micropollutants in the aquatic environment of Vietnam *Environ. Sci. Pollut. Res. Int.* in press doi:10. 1007/s11356-015-5060-z
- [3] S. Yagur-Kroll, E. Schreuder, C.J. Ingham, R. Heideman, R. Rosen, S. Belkin. A miniature porous aluminum oxide-based flow-cell for online water quality monitoring using bacterial sensor cells. *Biosens. Bioelectron.* 64 (2015) 625-632.
- [4] A. Date, P. Pasini, S. Daunert. Construction of spores for portable bacterial whole-cell biosensing systems. *Anal. Chem.* 79 (2007) 9391-9397.
- [5] S. Yagur-Kroll, L. Lalush, R. Rosen, N. Bachar, Y. Moskovitz, S. Belkin. *Escherichia coli* bioreporters for the detection of 2,4-dinitrotoluene and 2,4,6-trinitrotoluene. *Appl. Microbiol. Biotechnol.* 98 (2014) 885-895.
- [6] H.J. Shin. Genetically engineered microbial biosensors for in situ monitoring of environmental pollution. *Appl. Microbiol. Biotechnol.* 89 (2011) 867-877.
- [7] S. Esteban, M. Gorga, M. Petrovic, S. González-Alonso, D. Barceló, Y. Valcárcel. Analysis and occurrence of endocrine-disrupting compounds and estrogenic activity in the surface waters of Central Spain. *Sci. Total Environ.* 466-467 (2014) 939-951.
- [8] A.K. Wanekaya, W. Chen, A. Mulchandani. Recent biosensing developments in environmental security. *J. Environ. Monit.* 10 (2008) 703-712.
- [9] M. Álvarez-Guerra, A. Irabien, A. Design of ionic liquids: an ecotoxicity (*Vibrio fischeri*) discrimination approach. *Green Chem.* 13 (2011) 1507-1516.

- [10] A. Rantala, M. Utriainen, N. Kaushik, M. Virta, A.L. Välimaa, M. Karp. Luminescent bacteria-based sensing method for methylmercury specific determination. *Anal. Bioanal. Chem.* 400 (2011) 1041-1049.
- [11] K. Martín-Betancor, I. Rodea-Palomares, M.A. Muñoz-Martín, F. Leganés, F. Fernández-Piñas. Construction of a self-luminescent cyanobacterial bioreporter that detects a broad range of bioavailable heavy metals in aquatic environments. *Front. Microbiol.* 6 (2015) 186
- [12] A. Roda, L. Cevenini, S. Borg, E. Michelini, M.M. Calabretta, D. Schüler. Bioengineered bioluminescent magnetotactic bacteria as a powerful tool for chip-based whole-cell biosensors. *Lab Chip.* 13 (2013) 4881-4889.
- [13] A. Roda, L. Cevenini, E. Michelini, B.R. Branchini. A portable bioluminescence engineered cell-based biosensor for on-site applications. *Biosens. Bioelectron.* 26 (2011) 3647-3653.
- [14] T.M. Curtis, M.W. Widder, L.M. Brennan, S.J. Schwager, W.H. van der Schalie, J. Fey, N. Salazar. A portable cell-based impedance sensor for toxicity testing of drinking water. *Lab Chip* 9 (2009) 2176-2183.
- [15] L.M. Brennan, M.W. Widder, L.E. Lee, W.H. van der Schalie, Long-term storage and impedance-based water toxicity testing capabilities of fluidic biochips seeded with RTgill-W1 cells. *Toxicol. In Vitro.* 26 (2012) 736-745.
- [16] U. Green, J.H. Kremer, M. Zillmer, C. Moldaenke. Detection of chemical threat agents in drinking water by an early warning real-time biomonitor. *Environ. Toxicol.* 18 (2003) 368-374
- [17] A. Ozcan, Mobile phones democratize and cultivate next-generation imaging, diagnostics and measurement tools. *Lab Chip* 14 (2014) 3187-3194.

- [18] D. Tseng, O. Mudanyali, C. Oztoprak, S.O. Isikman, I. Sencan, O. Yaglidere, A. Ozcan. Lensfree microscopy on a cellphone. *Lab Chip* 10 (2010) 1787-1792.
- [19] S.K. Vashist, O. Mudanyali, E.M. Schneider, R. Zengerle, A. Ozcan. Cellphone-based devices for bioanalytical sciences. *Anal. Bioanal. Chem.* 406 (2014) 3263-3277.
- [20] X. Liu, T.Y. Lin, P.B. Lillehoj. Smartphones for cell and biomolecular detection. *Ann. Biomed. Eng.* 42 (2014) 2205-2217.
- [21] K. Ming, J. Kim, M.J. Biondi, A. Syed, K. Chen, A. Lam, M. Ostrowski, A. Rebbapragada, J.J. Feld, W.C. Chan. An integrated quantum dot barcode smartphone optical device for wireless multiplexed diagnosis of infected patients. *ACS Nano* 9 (2015) 3060-3074.
- [22] D.N. Breslauer, R.N. Maamari, N.A. Switz, W.A. Lam, D.A Fletcher. Mobile phone based clinical microscopy for global health applications. *PLoS One.* 4 ( 2009). e6320
- [23] S.K. Ludwig C. Tokarski, S.N. Lang, L.A. van Ginkel, H. Zhu, A. Ozcan, M.W. Nielen. Calling biomarkers in milk using a protein microarray on your smartphone. *PLoS One* 10 (2015) e0134360.
- [24] Q. Wei, R. Nagi, K. Sadeghi, S. Feng, E. Yan, S.J. Ki, R. Caire, D. Tseng, A. Ozcan. Detection and spatial mapping of mercury contamination in water samples using a smart-phone. *ACS Nano* 8 (2014) 1121-1129.
- [25] A. Roda, M. Guardigli, D. Calabria, M.M. Calabretta, L. Cevenini, E. Michelini. A 3D-printed device for a smartphone-based chemiluminescence biosensor for lactate in oral fluid and sweat. *Analyst* 139 (2014) 6494-6501.
- [26] A. Roda, E. Michelini, L. Cevenini, D. Calabria, M.M. Calabretta, P. Simoni. Integrating biochemiluminescence detection on smartphones: mobile chemistry platform for point-of-need analysis. *Anal. Chem.* 86 (2014) 7299-7304.

- [27] B.R. Branchini, D.M. Ablamsky, M.H. Murtiashaw, L. Uzasci, H. Fraga, T.L. Southworth. Thermostable red and green light-producing firefly luciferase mutants for bioluminescent reporter applications. *Anal. Biochem.* 361 (2007) 253-262.
- [28] J.H. Lee, R.J. Mitchell, B.C. Kim, D.C. Cullen, M.B. Gu. A cell array biosensor for environmental toxicity analysis. *Biosens. Bioelectron.* 21 (2005) 500-507.
- [29] E.K. Bolton, G.S. Sayler, D.E. Nivens, J.M. Rochelle, S. Ripp, M.L. Simpson. Integrated CMOS photodetectors and signal processing for very low-level chemical sensing with the bioluminescent bioreporter integrated circuit. *Sens. Actuators B Chem.* 85 (2002) 179-185.
- [30] A. Roda, B. Roda, L. Cevenini, E. Michelini, L. Mezzanotte, P. Reschiglian, K. Hakkila, M. Virta. Analytical strategies for improving the robustness and reproducibility of bioluminescent microbial bioreporters. *Anal. Bioanal. Chem.* 401 (2011) 201-211.
- [31] D. Tseng, O. Mudanyali, C. Oztoprak, S.O. Isikman, I. Sencan, O. Yaglidere, A. Ozcan. Research highlights: printing the future of microfabrication. *Lab Chip* 10 (2010) 1787-1792.
- [32] B. Berg, B. Cortazar, D. Tseng, H. Ozkan, S. Feng, Q. Wei, R.Y. Chan, J. Burbano, Q. Farooqui, M. Lewinski, D. Di Carlo, O.B. Garner, A. Ozcan. Cellphone-Based Hand-Held Microplate Reader for Point-of-Care Testing of Enzyme-Linked Immunosorbent Assays. *ACS Nano* 9 (2015) 7857-7866.
- [33] D. Li, Q. Huang, M. Lu, L. Zhang, Z. Yang, M. Zong, L. Tao. The organophosphate insecticide chlorpyrifos confers its genotoxic effects by inducing DNA damage and cell apoptosis. *Chemosphere.* 135 (2015) 387-393.
- [34] D.V. Banthorpe, D.M. Lamont. Potential toxicity of solutions of dimethyl sulphoxide. *Nature* 215 (1967) 1296-1297.

- [35] Y. Xu, K. Mawatari, T. Konno, T. Kitamori, K. Ishihara. Spontaneous Packaging and Hypothermic Storage of Mammalian Cells with a Cell-Membrane-Mimetic Polymer Hydrogel in a Microchip. *ACS Appl Mater Interfaces* 7 (2015) 23089-23097.
- [36] G.D. Jack, J.F. Garst, M.C. Cabrera, A.M. DeSantis, S.M. Slaughter, J. Jervis, A.I. Brooks, M. Potts, R.F. Helm. Long term metabolic arrest and recovery of HEK293 spheroids involves NF-kappaB signaling and sustained JNK activation. *J Cell Physiol.* 206 (2006) 526-536.
- [37] E. Michelini, A. Roda. Staying alive: new perspectives on cell immobilization for biosensing purposes. *Anal Bioanal Chem* 402 (2012) 1785-1797.
- [38] O.I. Berthuy, L.J. Blum, C.A. Marquette. Cells on chip for multiplex screening. *Biosens Bioelectron.* In press doi: 10.1016/j.bios.2015.04.024.
- [39] CJ Ferris, K.G. Gilmore, G.G. Wallace, M. In het Panhuis. Biofabrication: an overview of the approaches used for printing of living cells. *Appl. Microbiol. Biotechnol.* 97 ( 2013) 4243-4258.

## CHAPTER 4

---

### **Exploiting NanoLuc luciferase for smartphone-based bioluminescence cell biosensor for (anti)-inflammatory activity and toxicity Introduction**

---

*Reproduced from: "Exploiting NanoLuc luciferase for smartphone-based bioluminescence cell biosensor for (anti)-inflammatory activity and toxicity"*

*Luca Cevenini, Maria Maddalena Calabretta, Antonia Lopreside, Giuseppe Tarantino, Annalisa Tassoni, Maura Ferri, Aldo Roda, Elisa Michelini*

*Analytical and Bioanalytical Chemistry 2016, 408 (30), 8859-8868*

*Reproduced by permission of Springer (License number 425027008415)*

## 5.1 INTRODUCTION

According to a recent estimate (May 2015) of the International Telecommunication Union there are more than seven billion mobile cellular subscriptions worldwide, corresponding to 97% of the world population [1]. Although this percentage is biased by the fact that there is more than one mobile subscription per person in developed nations, it is clear that this ubiquitous distribution provides an unprecedented opportunity to provide people new affordable tools to address “mobile” needs, including recreational and self-diagnosis applications, e.g., electrocardiographic monitoring during physical exercise and glucose self-monitoring [2-4], as well as public safety and environmental monitoring [5].

The disruptive potential of technologies enabling on-site environmental detection and medical diagnostics in resource-limited settings was already clear several years ago, as demonstrated by the huge number of portable biosensors and devices reported in scientific literature [6-8]. In the last five years we witnessed an exponential growth in the number of proof-of-concept smartphone biosensors [9] in which the smartphone integrated detector showed sufficient sensitivity to replace portable light detectors such as CCD and photodiodes for detecting medium-high concentrations of analyte [10]. For example, a comparison between a BI-CMOS sensor with 8-megapixel (8MP) camera of an Iphone 5S and a cooled MZ-2PRO CCD camera was reported. By analyzing standard solutions of  $H_2O_2$  by CL reaction, the cooled camera was able to detect a concentration of  $H_2O_2$  three decades lower than the BI-CMOS detector [11,12].

The smartphone-integrated CMOS has been exploited as optical detector for several biosensing configurations relying on fluorescence, absorbance, reflectance, surface plasmon resonance, electrochemiluminescence, and bio-chemiluminescence [13-16]. Applications of this approach span from diagnostics of simplex virus type 2 (HSV-2) with an integrated LAMP assay [17] to multiplexed homogeneous assays of

proteolytic activity exploiting quantum dots [18] and immunodetection of *Escherichia coli* and *Salmonella* [19].

Another promising initiative is Google's Project Ara, relying on an Android-powered modular smartphone concept in which the user can select his own modules with custom specification, e.g., just as if they were Lego pieces [20].

The feasibility of integrating genetically engineered cells into a smartphone-based 3D-printed device to obtain a cheap and user-friendly toxicity biosensor has been previously demonstrated [21]. Cell biosensors offer the peculiar feature of providing quantitative information about the actual biological activity of analytes present in a sample. Indeed, living cells respond either to analytes that bind to specific membrane receptors activating signaling cascades as well as to the fraction of analyte able to enter into the cell and interact with intracellular molecular targets. In this view, in comparison to bacterial bioreporters [22-24], the use of mammalian cell lines is particularly attractive since they represent a better model of human physiology, providing more predictive biological information [25,26].

Bioluminescent cell biosensors are obtained by introducing into the cell a synthetic DNA construct in which the expression of a luciferase is under the control of a promoter, which can be constitutive or regulated by response elements activated by specific receptors upon binding with target analytes [27-28].

One of the main advantages of cell biosensors based on reporter gene technology is related to the internal amplification of the cell response, i.e. the activation of the promoter leads to the production of several luciferase proteins, allowing highly sensitive detection. In addition the availability of semi-synthetic luciferases with improved emission properties and emitting at different wavelengths, are continuously expanding the portfolio of BL reporter that can be exploited to develop cell biosensor even in multiplexed format [29-32].

Nevertheless, when compared to cell lines constitutively expressing high levels of luciferase used as viability reporter, it is expected that cell biosensors with inducible response will result in lower expression of the reporter protein (e.g., at low-level promoter activity). Therefore, especially if the smartphone camera is used as detector, a more powerful luciferase might be required to obtain a sensitive detection. These considerations prompted us to exploit the NanoLuc luciferase, a small luciferase (less than 20 kDa) originally obtained from a deep sea shrimp [33], which is claimed to have higher specific activity than conventional firefly luciferase (>100fold). NanoLuc has been used for several bioanalytical applications ranging from reporter gene assays [34-35], to protein-protein interaction [36], immunoassay [37] and BL imaging [38]. The feasibility of using NanoLuc for smartphone based applications has been very recently demonstrated by Arts and colleagues, who reported a cell-free bioluminescence resonance energy transfer (BRET) for antibody detection [39]. This work is based on purified fusion proteins containing NanoLuc as BL donor and mNeonGreen fluorescent protein as acceptor and the presence of target antibody results in a color change from green-blue to blue which is detected with the smartphone camera and elaborated with a custom developed app.

Here we report the development of cell biosensors based on NanoLuc luciferase as BL reporter and their integration in a smartphone-based device, to assess the (anti)-inflammatory activity of a sample as well as its toxicity.

As first proof of concept we decided to focus on inflammatory pathway, mediated by Nuclear Factor kappa B (NFkB) transcription factor, which has a pivotal role in mammalian cells regulating the expression of several genes involved in inflammation and innate immunity and also acts as crucial player in many steps of cancer initiation and progression. Since several chronic diseases and intense physical exercise states are characterized by elevated oxidative stress and inflammatory biomarkers, a current market trend is to provide anti-inflammatory and antioxidant

dietary supplements and functional foods to improve performance during athletic training or wellness. Several nutritional supplements were identified to suppress NFkB pathway, including omega-3 fatty acids [40], glucosamine sulfate [41], and squalene [42] among others, thus a simple device to rapidly assess the (anti)-inflammatory potential and the toxicity of a given sample could be useful.

To this end human embryonic kidney (Hek293T) cell lines were genetically engineered to express the NanoLuc luciferase either under the regulation of NFkB response element or a constitutive cytomegalovirus (CMV) promoter. Two different NanoLuc variants, namely the unfused NanoLuc (Nluc) and its destabilized version NanoLuc-PEST (NlucP), were tested to identify the most suitable intracellular BL reporter for smartphone-based detection.

A 3D-printed smartphone adaptor designed to fit the Nokia Lumia 1020 and 4x4 wells cell cartridges were fabricated using black acryl nitrile butadiene styrene (ABS) to provide a user-friendly apparatus. The analytical performance of the smartphone-based cell biosensor was evaluated with the inflammatory cytokine tumor necrosis factor (TNF $\alpha$ ) and white grape pomace extracts were analyzed as proof-of-concept real samples analysis.

## **5.2 MATERIALS AND METHODS**

### **5.2.1 Chemicals and reagents**

Human embryonic kidney Hek293T cells were from ATCC (American Type Culture Collection [ATCC], Manassas, VA, USA) and cell culture reagents were from Carlo Erba Reagents (Cornaredo, Milano, Italy). Tumor necrosis factor- $\alpha$  (TNF $\alpha$ ) was purchased from Sigma (St. Louis, MO, USA). The restriction enzymes required for cloning were from Fermentas (Vilnius, Lithuania). The mammalian expression plasmid pNL1.1[Nluc], pNL1.2[NlucP] and pGL4.32[luc2P/NF-kB-RE/Hygro], plasmid

extraction kit FuGENE HD transfection reagent and NanoGlo substrate were from Promega (Madison, WI, USA). NanoLuc luciferase variants Nluc and NlucP were cloned into either pCDNA vector and pGL4.32 backbone to replace Luc2P luciferase, yielding pCMV\_Nluc, pCMV\_NlucP, pNFkB \_Nluc and pNFkB \_NlucP respectively. Briefly, the CMV promoter (883bp) was extracted from pCDNA3 backbone using BglIII and HindIII restriction enzymes, while the 170bp fragment containing five copies of an NF-kB response element and minimal CMV promoter was cut from pGL4.32[luc2P/NF-kB-RE/Hygro] using KpnI and NcoI. These fragments were purified after 1% agarose gel electrophoresis and ligated into pNL1.1[Nluc] and pNL1.2[NlucP] backbones (previously cut with corresponding restriction enzymes) obtaining pCMV\_Nluc, pCMV\_NlucP, pNFkB\_Nluc and pNFkB\_NlucP reporter vectors. The selection of correct clones was confirmed by restriction map analysis and sequencing.

Ethanol extracts from white grape pomace (a mix of *Vitis vinifera* L., cv. Trebbiano and Verdicchio, by Cantine Moncaro wineries, Jesi, Ancona, Italy) were obtained as previously reported [43]. Grape pomace was washed with water in defined conditions (2 hours at 30°C for Sample 1; 6 hours at 30°C for Sample 2; 2 hours at 37°C for Sample 3) and then extracted overnight at 24°C in 95% (v/v) ethanol.

### **5.2.2 3D-printed cartridge and smartphone adaptors**

A cartridge of 40x40mm, 5 mm high, containing an array of 16 square wells (5mm wide and 5mm deep each) was created with a desktop 3D printer (Makerbot Replicator 2X) using black ABS. Smartphone adaptors were designed to fit a Nokia Lumia 1020 and printed using black ABS (FormFutura, Nijmegen, NL) at 300µm layer resolution.

## Smartphone-based BL emission characterization of Hek293T cells expressing NanoLuc luciferase

HEK293T cells were grown in Dulbecco Modified Essential Medium (DMEM high glucose 4.5g/L, GE Healthcare) supplemented with 10% fetal bovine serum, L-Glutamine 2mM, 50 U/ $\mu$ L penicillin, and 50  $\mu$ g/mL streptomycin. Cells were plated on 24 well plate at a density of  $1 \times 10^5$  cells/well and transfected with 0.5 $\mu$ g pCMV\_Nluc or 0.5 $\mu$ g pCMV\_NlucP expression vector according to the manufacturer's instructions, using a FuGENE HD:DNA ratio of 3:1 and incubated at 37°C with 5% CO<sub>2</sub>. At 24h post transfection the cells were collected and resuspended in DMEM at  $2 \times 10^6$  cell/mL and BL emission spectra (450-750 nm) and kinetic measurements (5 min with 200ms integration time) were performed with Varioskan luminometer (Thermo Fisher Scientific, Waltham, MA, USA) using 50  $\mu$ L of cell suspension in 96-well plate, after automatic injection of 50  $\mu$ L of NanoGlo substrate.

To evaluate the minimum number of detectable cells, serial dilutions of cells (50  $\mu$ L) were pipetted into the multiwell cartridge and imaged with the smartphone after addition of 50  $\mu$ L of NanoGlo. Images were taken with 4s integration time and different sensitivity settings (from ISO100 to ISO4000) using Nokia Pro Cam App and analyzed using ImageJ software (National Institutes of Health, Bethesda, MD). The minimum number of detectable cells was calculated as the number of cells providing a BL signal corresponding to the blank signal (culture medium only) plus three times its standard deviation. All measurements were performed in duplicate and repeated at least three times with different cell cartridges.

### **5.2.3 Evaluation of biosensor inflammatory response with the smartphone**

Biosensor response for TNF $\alpha$  was evaluated using Hek293T cells, transiently transfected with 0.5 $\mu$ g pNFkB\_Nluc or 0.5 $\mu$ g pNFkB\_NlucP in 24 well plates as previously described. 24h post transfection a 40 $\mu$ L-volume of resuspended cells was

transferred ( $5 \times 10^4$  cells/well) into the 3D printed cell array and incubated in duplicate with 10  $\mu$ L of TNF $\alpha$  dilutions (0.1-20 ng/mL). Same volume of culture medium was used as control. After 2h incubation at room temperature or at 37°C and 5% CO<sub>2</sub>, a 50  $\mu$ L-volume of NanoGlo substrate was added to each well and image was acquired with the smartphone (4s, ISO 800) equipped with the 3D printed black-box accessory. Images were analysed with ImageJ software and data plotted using GraphPad Prism v.5 (GraphPad Software, Inc. La Jolla, CA). All measurements were performed in duplicate and repeated at least three times with different cell cartridges.

#### **5.2.4 Smartphone-based real sample analysis**

(Anti)-inflammatory activity and toxicity of ethanol grape extracts was performed using a cell-cartridge prepared as follows. A 40  $\mu$ L-volume of Hek293T-pNF $\kappa$ B\_NlucP resuspended in medium containing 2 ng/mL TNF $\alpha$  was seeded in duplicate in four rows (left side of the cartridge). In parallel, a 40  $\mu$ L-volume of Hek293T-pCMV\_NlucP cells was seeded in duplicate in the right side of the same cartridge. A 10  $\mu$ L-volume of ethanol was added to both TNF $\alpha$  “reference” wells and viability control “CTR” wells. A 10  $\mu$ L-volume of each sample was added into each row, then the cartridge was incubated and analyzed as previously described. Statistical analysis was performed by using one-way Anova and  $p < 0.05$  was accepted as significant. Activation of NF $\kappa$ B with 2 ng/mL TNF $\alpha$  was used to calculate fold induction of treated cells vs “reference” cells.

## 5.3 RESULTS AND DISCUSSION

### 5.3.1 Assay design

Thanks to the high maturity level of reporter gene technology [44] and the availability of several bioluminescent proteins with improved features, a cell-biosensing smartphone platform was developed exploiting the highly sensitive NanoLuc luciferase as reporter. The possibility to use a smartphone camera to detect BL emitted from living cells or enzymatic reactions was previously reported [4]. In particular, mammalian cell lines were transfected with a firefly luciferase and used them as “sentinel cells” [21] as a rapid tool to detect general toxicity of samples. Nevertheless, the integration into smartphone-based platform of bioluminescent cells able to respond to specific target analytes or to specific stimuli, such as inflammatory or oxidant effects, surely represents an interesting evolution of smartphone-based cell-biosensors.

To evaluate the feasibility of this approach Hek293T cells were engineered with a reporter construct in which the NanoLuc luciferase is placed under the control of NF $\kappa$ B (Nuclear Factor  $\kappa$ B) response element; in such configuration, the binding of TNF $\alpha$  to its specific receptor (TNFR) activates the intracellular inflammatory pathway which leads to the expression of NanoLuc luciferase (Fig. 1a). Upon addition of substrate furimazine, BL emission is acquired with a light sensor, such as a smartphone camera.

In order to obtain cell biosensors with adequate analytical performance, especially in terms of sensitivity and short assay time, two NanoLuc luciferase variants were selected, i.e., Nluc and its destabilized version (NlucP), having the same coding sequence fused to a protein destabilization (PEST) sequence (Fig. 1b), as BL reporter. This enzyme is claimed to be about 150-fold brighter than firefly luciferase, producing a glow-type emission using the coelenterazine analogue furimazine (Fig. 1c).

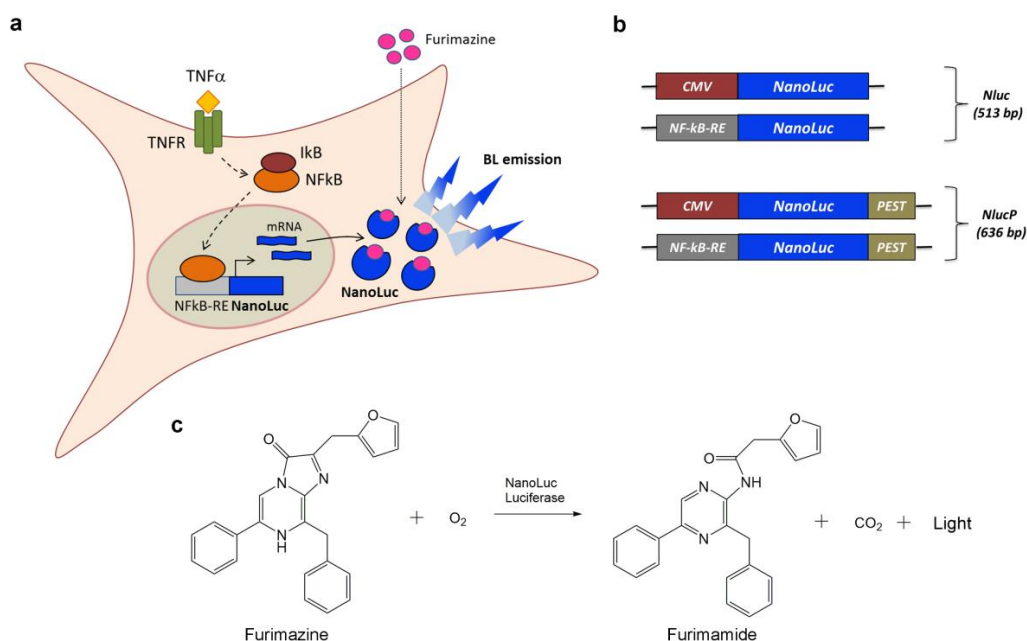


**Fig. 1:** a) Schematic representation of the cell biosensor developed for the evaluation of (anti)-inflammatory activity. Hek293T cells were transiently transfected with a vector containing five copies of NF-κB response element (NFκB-RE) and the NanoLuc luciferase as reporter. The binding of TNF $\alpha$  to the TNFR receptor activates the intracellular signalling pathway which leads to the expression of NanoLuc luciferase. Light emission was obtained after addition of the substrate furimazine. b) Schematic representation of the genetic constructs developed in this work and used to transfect Hek293T cells. NanoLuc luciferase variants Nluc and NlucP (destabilized reporter with a C-terminal PEST sequence that lead to a more rapid intracellular degradation) were cloned under the control of either a constitutive CMV promoter (for cytotoxicity biosensor) and the NFκB response element (for inflammation biosensor). c) Diagram of chemical reaction catalyzed by NanoLuc luciferase using the coelenterazine analog furimazine (2-furanylmethyl-deoxy-coelenterazine) as substrate

In addition, the small size (19 kDa) and the absence of post-translational modifications and disulphide bonds, enable rapid synthesis and folding of the reporter upon induction, thus reducing total assay time.

The smartphone Nokia Lumia 1020 was selected since it is equipped with a very powerful 41 MP camera and it is a widely distributed mobile device. Thanks to 6-lens optics configuration and the possibility to control the shutter speed up to 4s, this device is suitable for low-light imaging applications. A 3D printed adaptor (Fig.

2a) and cell-cartridges (Fig. 2b) comprising 16 wells (100 $\mu$ L volume each) were fabricated with black ABS to provide a dark-box and avoid crosstalk between adjacent wells. The whole accessory device weights only 70g and maintains a compact dimension (65x65mm, 60mm height) for easy implementation with the smartphone (Fig. 2c).

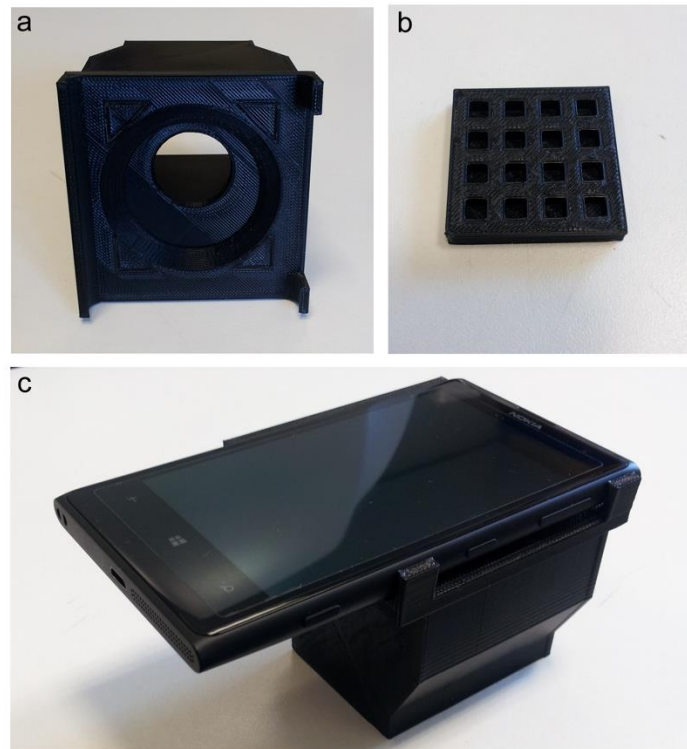


**Fig. 2:** a) 3D printed smartphone accessory designed to fit a Nokia Lumia 1020, providing a dark box for acquisition of bioluminescent emission. The accessory weights only 70g and maintains a compact dimension (65x65mm, 60mm height). b) Multiwell cartridge printed with black ABS containing 16 wells of 5x5mm (100 $\mu$ L volume each) and c) assembled self-standing smartphone-based device

### 5.3.2 Evaluation of NanoLuc variants expressed in Hek293T cells with smartphone-based detection

To evaluate Nluc and NlucP suitability as reporter proteins for smartphone-based BL detection, their coding sequences were preliminary cloned into a mammalian expression vector under the regulation of a constitutive CMV promoter (Fig. 1b). As expected, both NanoLuc variants showed the same BL emission spectra with a

maximum peak at 450nm and half-bandwidth of 75 nm (Fig. 3a). This emission largely overlaps with the relative response of the blue filter of smartphone CMOS sensor allowing a sensitive BL signal acquisition (data not shown). Emission kinetics of same number of transfected cells reveal that cells expressing Nluc provide a BL signal about 10-fold higher than NlucP, the latter providing a more stable BL signal which allows a more reliable image acquisition (Fig. 3b).

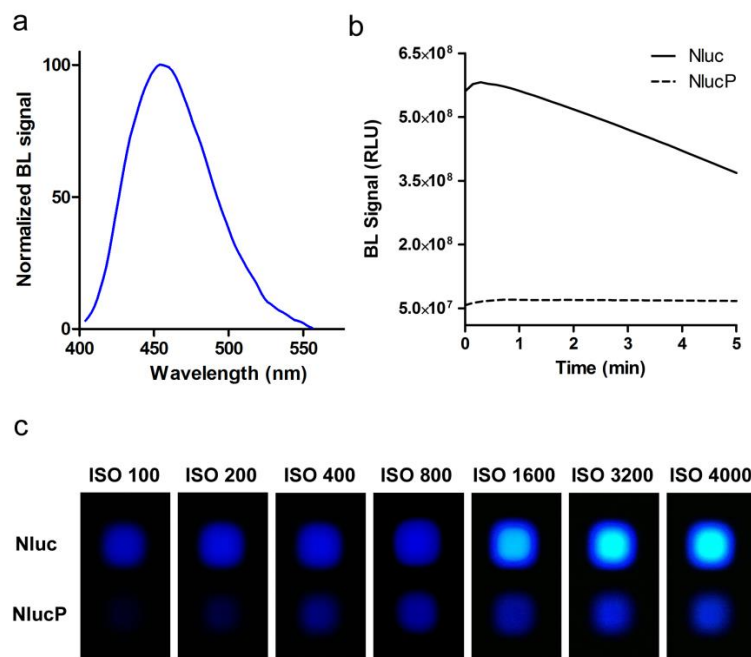


**Fig. 3** a) Bioluminescent emission spectra obtained with Hek293T cells expressing the Nluc luciferase. The normalized emission spectra of NlucP is overlapping (data not shown). b) Emission kinetics of Nluc and NlucP expressed in mammalian cells using NanoGlo substrate. c) Images of same number of cells expressing Nluc and NlucP, obtained with the smartphone (Lumia 1020) at different ISO settings (4s acquisition time) (See Materials and Methods for experimental details)

BL images of  $5.0 \times 10^4$  Hek293T cells expressing Nluc or NlucP obtained with the smartphone, using an exposure time of 4s, at different ISO settings are shown in Fig. 3c. Due to the higher accumulation in the cells, Nluc emission is clearly detectable even at low sensitivity (ISO 100) but also produces unwanted aberrant images at higher ISO. On the contrary, NlucP emission requires higher ISO setting to be effectively detected with the smartphone-camera. According to these results, we selected to use 4 s acquisition time and ISO 800 settings, which allow to detect BL

signal of both luciferases, avoiding color shift and artifacts that could affect quantitative analysis.

RGB measurements of BL images revealed that the blue channel accounts for the 98.3% of emitted light, while signals on the red and green channels are negligible, contributing only for 0.4 and 1.3%, respectively. The fact that Nluc emission in the red and green channels is lower than 1.3% could permit its use in combination with a red or green-emitting luciferase to develop multiplex biosensors.

BL images of serial dilutions of Hek293T cells expressing Nluc and NlucP are shown in Fig. S2, resulting in a LOD of  $150\pm 30$  and  $950\pm 50$  cells, respectively. Despite an higher amount of cells will be used for the assay, this low limit of detection corroborates the hypothesis that NanoLuc should provide a detectable signal even at low induction levels and with shorter incubation time.

Time course expression of Nluc and NlucP under the control of NFkB response element, show that Nluc signal at high concentrations of TNF $\alpha$  is visible even at 30 min whereas with NlucP longer incubation time is required for sensitive detection (Fig S3). However, we noticed that using Nluc also non-induced cells (control) emit a BL signal that increases with prolonged incubation time (1.2 times the background after 30 min and 2.6 and 4.5 times at 1h and 2h respectively); this is probably due to a basal activity of NFkB response element and/or crosstalk between signalling pathways. This basal activation is not observed using NlucP, since weak basal expression is counterbalanced by its rapid degradation thus avoiding intracellular accumulation with non-specific induction. Nevertheless, BL emission of NlucP is clearly visible within just 2 hours upon induction, even at low concentration, providing fold response values similar to those obtained with Nluc (i.e.  $5.3\pm 0.8$  and  $4.7\pm 0.3$  at 2.5 ng/mL TNF $\alpha$ , for Nluc and NlucP respectively).

We also evaluated the capability of both NanoLuc variants for cell-viability assessment using DMSO as model toxic compound (data not shown). Differently from firefly-luciferases, the luminescent reaction catalysed by NanoLuc is ATP-independent (Fig. 1c) and the high stability of Nluc, makes it unsuitable for such purpose, while the destabilized version NlucP, shows a remarkable decrease at increasing DMSO concentration, within the 2h assay time.

Taken together, these results imply that both variants are suitable for smartphone-based detection. Nevertheless NlucP represents the ideal reporter for the development of smartphone-interfaced cell-biosensors, since a low number of cells can be used in combination with shorter incubation time with analyte, providing adequate analytical performance.

### **5.3.3 Smartphone-based inflammation assay analytical performance: precision and reproducibility**

NanoLuc luciferase variants Nluc or NlucP were cloned under the control of five copies of an NFkB response element (NFkB-RE). BL images obtained with cells transfected with pNFkB\_Nluc or pNFkB\_NlucP, incubated with TNF $\alpha$  dilutions in the cell-cartridge, are shown in Fig. 4a and Fig. 4c, respectively. The assay in optimized conditions consists of incubation of 10  $\mu$ L of TNF $\alpha$  dilutions (concentration range from 0.05-20 ng/mL) per each cartridge well containing  $5 \times 10^4$  cells (40 $\mu$ L volume) for 2h at room temperature. Cell cartridge is then imaged with Nokia Lumia equipped with the 3D-printed accessory, for 4s at ISO 800 after addition of 50  $\mu$ L NanoGlo substrate and gentle resuspension to obtain an efficient and homogeneous cell lysis. Dose-response curves obtained by quantifying BL emission with ImageJ are shown in Fig. 4b and Fig. 4d.

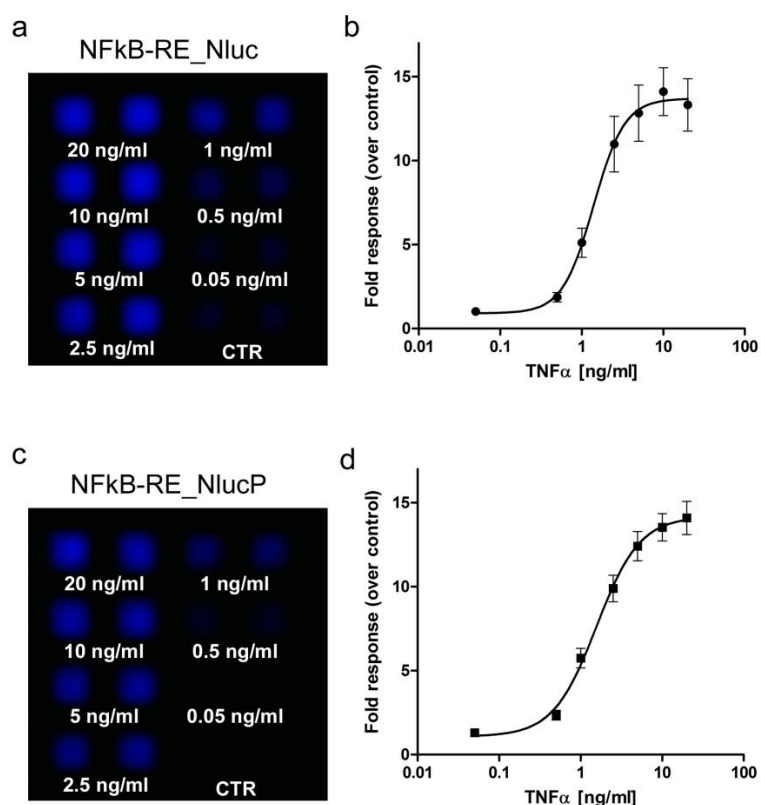


**Fig. 4:** a) Image obtained with Hek293T cells transfected with NFκB-RE\_Nluc reporter vector and incubated with indicated concentrations of TNFα. b) Dose-response curve obtained by using three cartridges elaborated with ImageJ and plotted as fold response with respect to control (non-induced cells). c) Image and d) dose-response curve obtained with Hek293T cells incubated with indicated concentrations of TNFα, using the destabilized NlucP as reporter under the control of NFκB-response element

Dose-response curves in optimized conditions showed the same LOD of  $0.4 \pm 0.1$  ng/mL for both obtained Nluc and NlucP and an EC50 of  $1.3 \pm 0.4$  ng/mL and  $1.7 \pm 0.2$  ng/mL, respectively.

Results obtained by incubating the cartridges in the incubator were not significantly different from those obtained at room temperature, with a LOD of  $0.5 \pm 0.1$  ng/mL for Nluc, probably due to the short incubation time (2h) that does not enable cells to dramatically change their metabolism and, as a consequence, response to analytes is within intrinsic biological variability.

The concordance of results obtained with both luciferase variants confirms their suitability as sensitive reporters to be implemented in smartphone-based detection. The response was reproducible with an intra-assay variability of 7% for NlucP and 15% for Nluc and an inter-assay variability of 10% and 18%, respectively. Additionally, the possibility to use NlucP even for cell-viability assessment, makes this variant more advisable for smartphone-interfaced toxicity biosensing.

These values agree with those we obtained with benchtop measurements relying on NFkB reporter gene bioassays using Hek293T cells transfected with pGL4.32[luc2P/NF-kB-RE/Hygro] vector, but requiring longer incubation times (5h) and expensive instrumentation. The assay provided a LOD of  $0.10 \pm 0.05$  ng/mL and  $EC_{50} = 1.6 \pm 0.2$  ng/mL for TNF $\alpha$ , (See supplementary material, FigS4).

#### **5.3.4 Smartphone-based (anti)-inflammatory cell biosensor: analysis of real samples**

In the perspective of using our smartphone-based assay for rapid and cost-effective characterization of bioactivity of unknown samples, we propose a cell-cartridge arrangement, comprising both cell biosensors for inflammatory and general toxicity activity detection, i.e., Hek293T\_NFkB\_NlucP and Hek293T\_CMV\_NlucP cells (Fig. 5a), in which up to three samples or the same sample at different concentrations can be tested simultaneously. Each cartridge also contains reference wells incubated with 2 ng/mL TNF $\alpha$  and viability control wells (CTR). We selected to induce sample-wells with 2 ng/mL TNF $\alpha$ , a concentration near the  $EC_{50}$ , in order to evaluate both anti- and pro-inflammatory activity of samples, with high sensitivity.

White grape pomace ethanol extracts, which are known to contain several bioactive compounds such as catechin, epicatechin, quercetin and gallic acid [45], were tested. BL image obtained with the smartphone (Fig. 5a) provides a direct visual estimation of sample bioactivity and cytotoxicity.

Quantitative analysis revealed that sample no.1 has both inflammatory activity (normalized BL signal  $145 \pm 5\%$ ) and cytotoxicity (normalized BL signal  $50 \pm 3\%$ ), Sample no. 2 has no significant effect on the cells, while sample no.3 shows a remarkable anti-inflammatory activity (normalized BL signal  $25 \pm 4\%$ ), probably due to suppression of cytokines-induced I $\kappa$ B degradation [46], although multiple mechanisms that could affect NF $\kappa$ B pathway at different levels of the signaling cascade cannot be excluded. No cytotoxicity was observed (Fig. 5b).

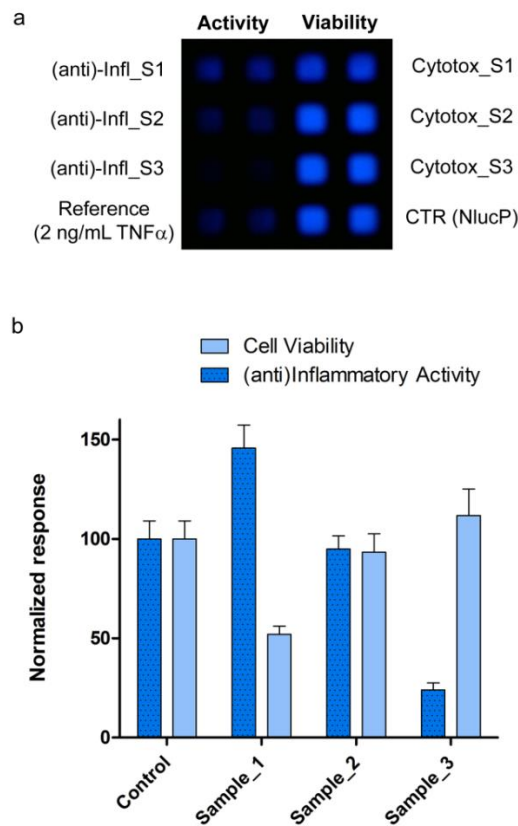


**Fig. 5:** a) Image and b) graphical elaboration of real sample analysis using a cell-cartridge comprising either Hek293T-NF $\kappa$ B\_NlucP cells (in duplicate on the left side) and Hek293T-CMV\_NlucP cells (in duplicate on the right side). Control sample for inflammatory activity was obtained by incubating cells with 2ng/mL TNF $\alpha$  while control for toxicity was obtained by incubating cells with a solution of 20% EtOH. Both BL signals of control wells were set at 100 to normalize results and enable both evaluation of anti and pro-inflammatory activity. As a proof of concept, three white grape extracts were analyzed: sample no. 1 shows both inflammatory activity and cytotoxicity, sample no. 2 has no effect on the cells and sample no. 3 shows a remarkable anti-inflammatory activity and no cytotoxicity. All measurements were performed in duplicate and repeated at least with three different cell cartridges.

In an effort of obtaining a ready-to use cartridge we previously evaluated the feasibility of immobilizing cells and store them for few days, for example to mimic transport of the cartridge from the production laboratory to where the analysis is needed (e.g., small company, private consumer). The possibility of keeping the cell biosensors viable for 2–3 days has been demonstrated. This storage is consistent with transport or delivery of the cell cartridges where the analysis is required [21]. Future work will be directed to optimize the shelf-life of cell cartridges, i.e. direct growth of cell-biosensor on 3D-scaffold inside the 3D-printed cartridges.

For actual implementation of cell biosensors into portable smartphone-based devices two main challenges can be identified, i.e., the identification of innovative strategies for cell immobilization to keep biosensors alive and responsive for long periods of time, and the improvement of light emitted by the cells to enable detection with integrated CMOS, which are obviously less sensitive than benchtop detectors. The major goal of this work was to address the detectability issue by careful selection of reporter gene, optimization and standardization of assay conditions, and light acquisition parameters to provide researchers of the field new directions and tools.

## **5.4 CONCLUSION**

In this work we report the development of a bioluminescence smartphone-based cell biosensor exploiting NanoLuc luciferase as sensitive reporter for quantitative assessment of (anti)-inflammatory activity and toxicity of a sample and its preliminary application for testing extracts of white grape pomace. Such smartphone-based biosensing platform could meet the needs of small medium enterprises not fully equipped with analytical laboratories and expensive equipment required for first-level safety and efficacy tests and could be deployed as rapid screening tool for R&D activities of SME looking for new bioactive products. The proposed approach thus offers a valuable pre-screening tool to select the best

promising samples, e.g., pure molecules, active ingredients, food byproducts, vegetal extracts, to undergo more specific and accurate analysis by external authorized laboratories. This first pre-screening is not trivial, since it could in principle reduce the number of samples to be sent to outsource analysis and, by providing real-time results, it could enable a continuous in house management and tuning of procedures and protocols to obtain the most active products.

## 5.5 SUPPLEMENTARY MATERIAL

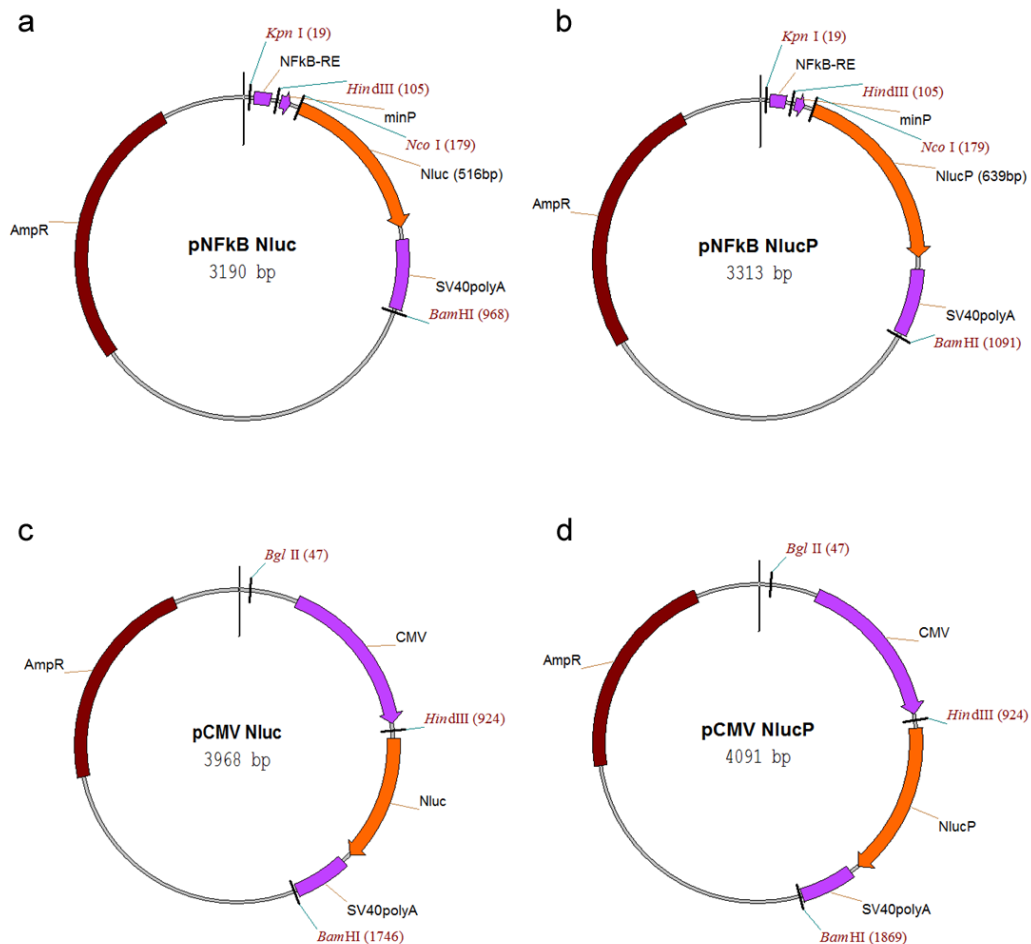


**Fig.S1** Schematic maps (Vector NTI) of final vectors created in this work and used to transfect Hek293T cells. The NFkB-RE driven Nanoluc plasmids pNFkB\_Nluc (a) and pNFkB\_NlucP (b) were obtained by cloning the 170bp fragment containing five copies of an NF-kB response element and a minimal CMV promoter from pGL4.32[luc2P/NF-kB-RE/Hygro] using KpnI and NcoI, into pNL1.1[Nluc] and pNL1.2[NlucP] backbone, respectively. The constitutive expression vectors pCMV\_Nluc (c) and pCMV\_NlucP (d) were created by cloning the full CMV promoter (883bp) from pCDNA3 backbone, into pNL1.1[Nluc] and pNL1.2[NlucP] backbone, respectively, using BglII and HindIII restriction enzymes. The selection of correct clones was confirmed by restriction map analysis and DNA sequencing.

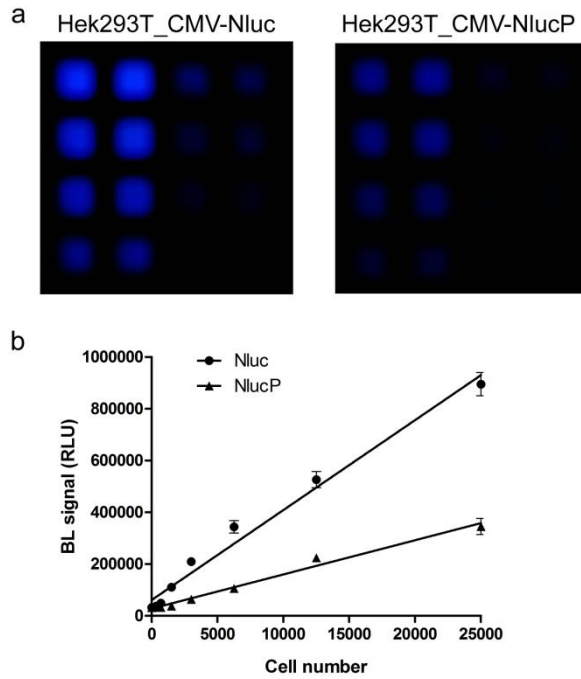


**Fig.S2 a)** Images obtained with serial dilution of Hek293T cells (in duplicate from top left: 24000, 12000, 6000, 3000, 1500, 750, 375, 0) constitutively expressing Nanoluc luciferase variants Nluc or NlucP (destabilized). **b)** Elaboration of BL images with ImageJ software to quantify the signal of each well and to calculate the minimum number of detectable cells.

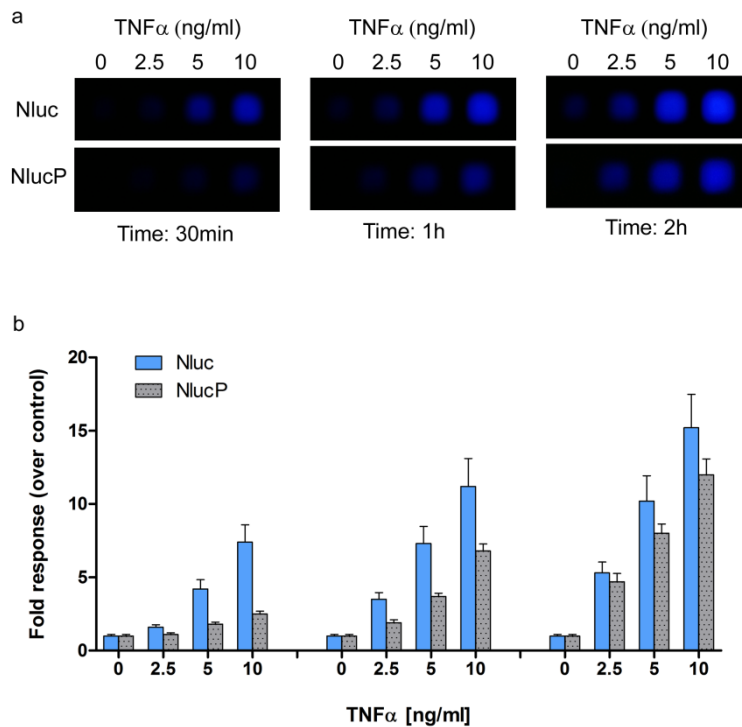


**Fig.S3 a)** Time course images of Hek293T cells expressing Nluc or NlucP luciferase variants under the control of NF- $\kappa$ B response element, obtained with indicated concentration of TNF $\alpha$ , at different incubation time and **b)** corresponding fold responses obtained using ImageJ software for the quantification of BL signals.

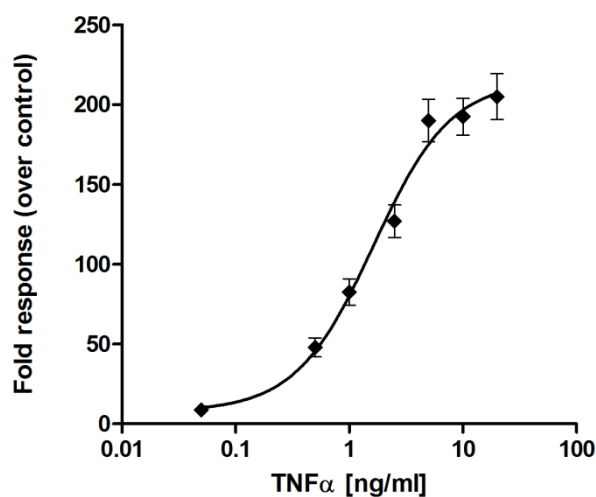


**Fig.S4** Dose response curve for TNF $\alpha$  (EC50=1.6 $\pm$ 0.2 ng/mL; LOD=0.10 $\pm$ 0.05 ng/mL) obtained with a traditional cell-based assay using a benchtop luminometer, according to the protocol provided by Promega. Briefly, Hek293T cells (2x10<sup>4</sup> cells/well) were transfected with 0.1 $\mu$ g pGL4.32[luc2P/NF-kB-RE/Hygro] vector into 96-well plates and incubated for 24h in a humidified 37°C, 5% CO<sub>2</sub> incubator. Then, culture media was replaced with 100 $\mu$ l of DMEM containing indicated TNF $\alpha$  dilutions (induction solution) or DMEM alone (control solution) and the plate was incubated for 5h in the tissue culture incubator. Luciferase activity was determined using the Varioskan Flash multimode reader (300ms integration time) after addition of 100 $\mu$ l BrightGlo substrate. All experiment were performed in duplicate and repeated at least three times. Fold response was calculated as ratio between average relative light units of induced cells over control cells, and plotted using GraphPad Prism software.

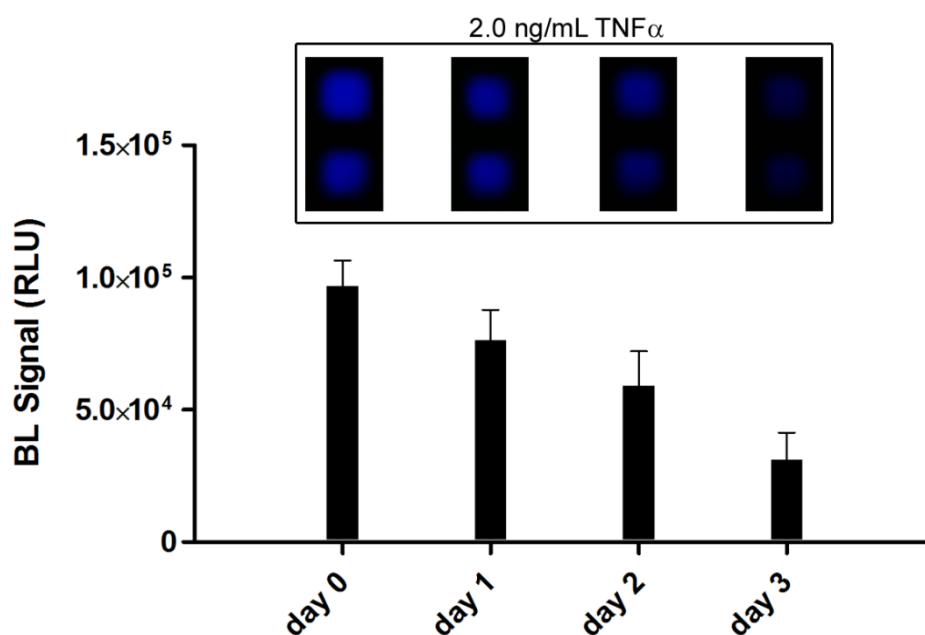


**Fig.S5** BL signals and corresponding images (inset) obtained with Hek293T\_NF-kB\_NlucP cells incubated at room temperature (25°C) for indicated time before performing the assay. A cartridge was used each day to evaluate the cell response using 2 ng/mL TNF $\alpha$  (selected reference concentration) for 2h at room temperature and images were acquired for 4s at ISO 4000. BL signal intensity decreases with increasing “storage” time with respect to those obtained at day 0 (freshly prepared cells). After only 48h (day 2) about 40% drop in bioluminescence and an increased variability (CV%=25%) was observed, affecting the analytical performance of the assay. These results indicate that a small cell incubator for storage and transport of the cartridges at controlled conditions (37°C, 5% CO<sub>2</sub>) would be required to obtain a robust portable analytical platform for on-field analysis.

## ACKNOWLEDGMENTS

The grape pomace samples were obtained in the frame of a project supported by Sadam Engineering (Sadam Eridania Spa group, Bologna, Italy) to Annalisa Tassoni. This research was sponsored in part by the NATO Science for Peace and Security Programme under Grant No.985042.

## REFERENCES

- [1] <http://www.itu.int/en/ITU-D/Statistics/Pages/facts/default.aspx>
- [2] Spethmann S, Prescher S, Dreger H, Nettle H, Baumann G, Knebel F, Koehler F. Electrocardiographic monitoring during marathon running: a proof of feasibility for a new telemedical approach. *Eur J Prev Cardiol.* 2014;21:32-7.
- [3] Garabedian LF, Ross-Degnan D, Wharam JF. Mobile Phone and Smartphone Technologies for Diabetes Care and Self-Management. *Curr Diab Rep.* 2015;15:109.
- [4] Roda A, Guardigli M, Calabria D, Calabretta MM, Cevenini L, Michelini E. A 3D-printed device for a smartphone-based chemiluminescence biosensor for lactate in oral fluid and sweat. *Analyst.* 2014;139:6494-501.
- [5] Zhang D, Jiang J, Chen J, Zhang Q, Lu Y, Yao Y, Li S, Logan Liu G, Liu Q. Smartphone-based portable biosensing system using impedance measurement with printed electrodes for 2,4,6-trinitrotoluene (TNT) detection. *Biosens Bioelectron.* 2015;70:81-8.
- [6] Yin K, Zhang W, Chen L. Pyoverdine secreted by *Pseudomonas aeruginosa* as a biological recognition element for the fluorescent detection of furazolidone. *Biosens Bioelectron.* 2014; 51:90-6.
- [7] Bawei Li, Longwen Fu, Wei Zhang, Weiwei Feng, Lingxin Chen. Portable paper-based device for quantitative colorimetric assays relying on light reflectance principle. *Electrophoresis.* 2014; 35: 1152-9.
- [8] Turner AP. Biosensors: sense and sensibility. *Chem Soc Rev.* 2013; 42:3184-96.
- [9] Comina G, Suska A, Filippini D. Towards autonomous lab-on-a-chip devices for cell phone biosensing. *Biosens Bioelectron.* 2016;77:1153-67.

- [10] Mirasoli M, Nascetti A, Caputo D, Zangheri M, Scipinotti R, Cevenini L, de Cesare G, Roda A. Multiwell cartridge with integrated array of amorphous silicon photosensors for chemiluminescence detection: development, characterization and comparison with cooled-CCD luminograph. *Anal Bioanal Chem.* 2014;406:5645-56.
- [11] Roda A, Cevenini L, Borg S, Michelini E, Calabretta MM, Schüler D. Bioengineered bioluminescent magnetotactic bacteria as a powerful tool for chip-based whole-cell biosensors. *Lab Chip.* 2013;13:4881-9.
- [12] Roda A, Cevenini L, Michelini E, Branchini BR. A portable bioluminescence engineered cell-based biosensor for on-site applications. *Biosens Bioelectron.* 2011;26:3647-53.
- [13] Zhang D, Liu Q. Biosensors and bioelectronics on smartphone for portable biochemical detection. *Biosens Bioelectron.* 2016;75:273-84.
- [14] Roda A, Mirasoli M, Michelini E, Di Fusco M, Zangheri M, Cevenini L, Roda B, Simoni P. Progress in chemical luminescence-based biosensors: A critical review. *Biosens Bioelectron.* 2016;76:164-79.
- [15] Liu X, Lin TY, Lillehoj PB. Smartphones for cell and biomolecular detection. *Ann Biomed Eng.* 2014;42:2205-17.
- [16] Vashist SK, Mudanyali O, Schneider EM, Zengerle R, Ozcan A. Cellphone-based devices for bioanalytical sciences. *Anal Bioanal Chem.* 2014;406:3263-77.
- [17] Liao SC, Peng J, Mauk MG, Awasthi S, Song J, Friedman H, Bau HH, Liu C. Smart Cup: A Minimally-Instrumented, Smartphone-Based Point-of-Care Molecular Diagnostic Device. *Sens Actuators B Chem.* 2016;229:232-38.
- [18] Petryayeva E, Algar WR. Multiplexed homogeneous assays of proteolytic activity using a smartphone and quantum dots. *Anal Chem.* 2014;86:3195-202.

- [19] Nicolini AM, Fronczek CF, Yoon JY. Droplet-based immunoassay on a 'sticky' nanofibrous surface for multiplexed and dual detection of bacteria using smartphones. *Biosens Bioelectron.* 2015;67:560-9.
- [20] [www.projectara.com/](http://www.projectara.com/)
- [21] Cevenini L, Calabretta MM, Tarantino G, Michelini E, Roda A. Smartphone-interfaced 3D printed toxicity biosensor integrating bioluminescent "sentinel cells". *Sens. Actuators B: Chem.* 2016; 225:249-57.
- [22] Charrier T, Durand MJ, Jouanneau S, Dion M, Perneti M, Poncelet D, Thouand G. A multi-channel bioluminescent bacterial biosensor for the on-line detection of metals and toxicity. Part I: design and optimization of bioluminescent bacterial strains. *Anal Bioanal Chem.* 2011;400:1051-60.
- [23] Bazin I, Seo HB, Suehs CM, Ramuz M, De Waard M, Gu MB. Profiling the biological effects of wastewater samples via bioluminescent bacterial biosensors combined with estrogenic assays. *Environ Sci Pollut Res Int.* 2016; DOI 10.1007/s11356-016-6050-5.
- [24] Elad T, Seo HB, Belkin S, Gu MB. High-throughput prescreening of pharmaceuticals using a genome-wide bacterial bioreporter array. *Biosens Bioelectron.* 2015;68:699-704.
- [25] Michelini E, Cevenini L, Calabretta MM, Calabria D, Roda A. Exploiting in vitro and in vivo bioluminescence for the implementation of the three Rs principle (replacement, reduction, and refinement) in drug discovery. *Anal Bioanal Chem.* 2014;406:5531-9.
- [26] Class B, Thorne N, Aguisanda F, Southall N, McKew JC, Zheng W. High-throughput viability assay using an autonomously bioluminescent cell line with a bacterial Lux reporter. *J Lab Autom.* 2015;20:164-74.

- [27] Raut N, O'Connor G, Pasini P, Daunert S. Engineered cells as biosensing systems in biomedical analysis. *Anal Bioanal Chem.* 2012;402:3147-59.
- [28] Michelini E, Cevenini L, Mezzanotte L, Leskinen P, Virta M, Karp M, Roda A. A sensitive recombinant cell-based bioluminescent assay for detection of androgen-like compounds. *Nat Protoc.* 2008;3:1895-902.
- [29] Branchini BR, Southworth TL, Fontaine DM, Kohrt D, Talukder M, Michelini E, Cevenini L, Roda A, Grossel MJ. An enhanced chimeric firefly luciferase-inspired enzyme for ATP detection and bioluminescence reporter and imaging applications. *Anal Biochem.* 2015;484:148-53.
- [30] Branchini BR, Southworth TL, Fontaine DM, Davis AL, Behney CE, Murtiashaw MH. A *Photinus pyralis* and *Luciola italica* chimeric firefly luciferase produces enhanced bioluminescence. *Biochemistry.* 2014;53:6287-9.
- [31] Yasunaga M, Murotomi K, Abe H, Yamazaki T, Nishii S, Ohbayashi T, Oshimura M, Noguchi T, Niwa K, Ohmiya Y, Nakajima Y. Highly sensitive luciferase reporter assay using a potent destabilization sequence of calpain 3. *J Biotechnol.* 2015;194:115-23.
- [32] Ohmiya Y. Simultaneous multicolor luciferase reporter assays for monitoring of multiple genes expressions. *Comb Chem High Throughput Screen.* 2015;18:937-45.
- [33] Hall MP, Unch J, Binkowski BF, Valley MP, Butler BL, Wood MG, Otto P, Zimmerman K, Vidugiris G, Machleidt T, Robers MB, Benink HA, Eggers CT, Slater MR, Meisenheimer PL, Klaubert DH, Fan F, Encell LP, Wood KV. Engineered luciferase reporter from a deep sea shrimp utilizing a novel imidazopyrazinone substrate. *ACS Chem Biol.* 2012;7:1848-57.

- [34] Masser AE, Kandasamy G, Kaimal JM, Andréasson C. Luciferase NanoLuc as a reporter for gene expression and protein levels in *Saccharomyces cerevisiae*. *Yeast*. 2016;33:191-200.
- [35] De Niz M, Stanway RR, Wacker R, Keller D, Heussler VT. An ultrasensitive NanoLuc-based luminescence system for monitoring *Plasmodium berghei* throughout its life cycle. *Malar J*. 2016;15:232.
- [36] Dixon AS, Schwinn MK, Hall MP, Zimmerman K, Otto P, Lubben TH, Butler BL, Binkowski BF, Machleidt T, Kirkland TA, Wood MG, Eggers CT, Encell LP, Wood KV. NanoLuc Complementation Reporter Optimized for Accurate Measurement of Protein Interactions in Cells. *ACS Chem Biol*. 2016;11:400-8.
- [37] Boute N, Lowe P, Berger S, Malissard M, Robert A, Tesar M. NanoLuc Luciferase - A Multifunctional Tool for High Throughput Antibody Screening. *Front Pharmacol*. 2016;7:27.
- [38] England CG, Ehlerding EB, Cai W. NanoLuc: A Small Luciferase Is Brightening Up the Field of Bioluminescence. *Bioconjug Chem*. 2016;27:1175-87.
- [39] Arts R, den Hartog I, Zijlema SE, Thijssen V, van der Beelen SH, Merks M. Detection of Antibodies in Blood Plasma Using Bioluminescent Sensor Proteins and a Smartphone. *Anal Chem*. 2016;88:4525-32.
- [40] Fahrman JF, Ballester OF, Ballester G, Witte TR, Salazar AJ, Kordusky B, Cowen KG, Ion G, Primerano DA, Boskovic G, Denvir J, Hardman WE. Inhibition of nuclear factor kappa B activation in early-stage chronic lymphocytic leukemia by omega-3 fatty acids. *Cancer Invest*. 2013;31:24-38.
- [41] Bak YK, Lampe JW, Sung MK Effects of dietary supplementation of glucosamine sulfate on intestinal inflammation in a mouse model of experimental colitis. *J Gastroenterol Hepatol*. 2014;29:957-63.

- [42] Sánchez-Fidalgo S, Villegas I, Rosillo MÁ, Aparicio-Soto M, de la Lastra CA. Dietary squalene supplementation improves DSS-induced acute colitis by downregulating p38 MAPK and NFκB signaling pathways. *Mol Nutr Food Res*. 2015;59:284-92.
- [43] Ferri M, Bin S, Vallini V, Fava F, Michelini E, Roda A, Minnucci G, Bucchi G, Tassoni A. Recovery of polyphenols from red grape pomace and assessment of their antioxidant and anti-cholesterol activities. *N Biotechnol*. 2016;33:338-44.
- [44] Cevenini L, Calabretta MM, Calabria D, Roda A, Michelini E. Luciferase Genes as Reporter Reactions: How to Use Them in Molecular Biology? *Adv Biochem Eng Biotechnol*. 2016;154:3-17.
- [45] Jara-Palacios MJ, Hernanz D, Cifuentes-Gomez T, Escudero-Gilete ML, Heredia FJ, Spencer JP. Assessment of white grape pomace from winemaking as source of bioactive compounds, and its antiproliferative activity. *Food Chem*. 2015;183:78-82.
- [46] Nunes C, Ferreira E, Freitas V, Almeida L, Barbosa RM, Laranjinha. Intestinal anti-inflammatory activity of red wine extract: unveiling the mechanisms in colonic epithelial cells. *J.Food Funct*. 2013;4:373-383.

## CHAPTER 5

---

### **Bioluminescence imaging of spheroids for high-throughput longitudinal studies on 3D cell culture models**

---

*Reproduced from: "Bioluminescence imaging of spheroids for high-throughput longitudinal studies on 3D cell culture models"*

*Luca Cevenini<sup>‡</sup>, Maria Maddalena Calabretta<sup>‡</sup>, Antonia Lopreside, Bruce R. Branchini, Tara L. Southworth, Elisa Michelinì, Aldo Roda*

*Photochemistry and Photobiology (2017), 93 (2), 531-535*

*Reproduced by permission of Wiley Online Library: 4250270236662*

## 6.1 INTRODUCTION

Cell-based assays represent an invaluable tool for the early stages of the drug discovery process [1]. Thanks to their easy adaptability to high-throughput and high-content screenings (HTS and HCS), cell models can identify bioactive molecules interacting with molecular targets well in advance of pre-clinical studies. In particular, owing to their high sensitivity and high dynamic range, cell-based assays relying on bioluminescent (BL) reporter proteins are highly favored in HTS when compared with well-established fluorescence-based assays [2]. In BL assays, a reporter protein, such as a luciferase, is expressed under the regulation of a target promoter sequence or enhancer elements, thus enabling correlation of reporter protein expression, measured as light signal, and transcriptional regulation [3].

Moreover, thanks to the availability of a palette of luciferase reporters that can nowadays compete with green fluorescent protein (GFP) and its variants, multiplexing is no limited to fluorescence detection [4,5]. Multiplexed BL assays can be performed both *in vitro* and *in vivo*, i.e., in small animal non-invasive imaging [6]. Different luciferases have been obtained by cloning the genes from new organisms, by mutagenesis of the genes, and by combining the N-domain and C-domains of luciferases from different species [7-10]. This availability enabled the development of high-content assays and orthogonal assays, the latter relying on the use of two unrelated luciferases for monitoring the same target. This strategy was successfully applied to improve the robustness and reliability of large HTS [11,12].

Therefore BL cell-based assays based on two-dimensional (2D) monolayer cell culture models represent well-established reliable tools that improved the first steps of drug-screening, in compliance with the 3Rs (Replacement, Reduction, Refinement) principle [13-15]. However, cells in 2D cultures often do not reflect the morphology and functionality of their native three-dimensional (3D) phenotypes; thus, the relevance of information obtained by the 2D assay is reduced [16]. The

more in vitro models represent tissue-specific functionality and, possibly, in vivo physiology, the better the prediction of the potential impact of a drug candidate before it enters animal and clinical trials. Therefore, the cell microenvironment has to mimic in vivo physiological conditions including spatial and temporal dimensions and dynamics, physical interactions, such as cell-cell contact, and the cell-extracellular matrix [17-19]. Several technologies are currently available to produce such microtissues with good control of the dimensions and that exhibit tissue-like phenotypes including porous scaffolds and polymers, hydrogels, and ultra-low attachment cell culture plates [20-23]. These methods take advantage of the natural self-assembly tendency that is typical of several cell types. When cells are grown as spheroids they are able to generate their extracellular matrix and communicate with other cells as in their native environment [24].

Several 3D cell-based assays have been reported, although most of them rely on viability and morphology endpoints with fluorescent readouts [18, 24-25]. The transition from BL 2D cell-based assays to 3D is not trivial since most current BL assays were designed and optimized for monolayer or suspension cultures. To the best of our knowledge, BL non-lysing approaches have not yet been reported for imaging of live spheroids. Here, we report a non-invasive real time imaging assay of 3D cell cultures for longitudinal and high-throughput studies that can be easily implemented for screening of drugs and new molecules of interest.

## **6.2 MATERIALS AND METHODS**

### **6.2.1 Materials**

The Human Embryonic Kidney HEK293 cell line was obtained from ATCC (American Type Culture Collection [ATCC], Manassas, VA, USA). Dulbecco's modified Eagle's medium high glucose (DMEM), fetal bovine serum (FBS), L-Glutamine, penicillin and streptomycin were from Carlo Erba Reagents (Cornaredo, Milano, Italy). The

restriction enzymes required for cloning were from Fermentas (Vilnius, Lithuania). Tumor necrosis factor- $\alpha$  (TNF $\alpha$ ) was from Sigma-Aldrich (St. Louis, MO, USA) and plasmid extraction kit, FuGENE HD transfection reagent and D-luciferin were from Promega (Madison, WI, USA). The PLG2 luciferase gene, previously obtained and described [10] was cloned into the pCDNA3 vector and pGL4.32[luc2P/NF- $\kappa$ B-RE/Hygro] backbone to replace Luc2P luciferase, yielding vectors named pCMV\_PLG2 and pNF $\kappa$ B\_PLG2.

### **6.2.2 2D cell cultures**

Hek293 cells were grown in DMEM supplemented with 10% (v/v) FBS, 2 mM L-glutamine, 50 U/mL penicillin and 50  $\mu$ g/mL streptomycin. Cells were plated in black, clear bottom 96-well plates at a density of  $2 \times 10^4$  cells per well, with 100  $\mu$ l of complete growth medium.

### **6.2.3 3D cell cultures**

Hek293 spheroids were obtained using 96 well micro-space round bottom cell culture plates with a non-adherent surface generously provided by Elplasia<sup>TM</sup>, Kuraray, Japan. Before cell seeding, 100  $\mu$ L of complete culture medium was added to each well followed by 200  $\mu$ L of cell suspension ( $2 \times 10^4$  cells per well). The plate was then incubated at 37°C with 5% CO<sub>2</sub>. Spheroids growth was monitored every 24 h for a period of 4 days.

### **6.2.4 Characterization of 2D and 3D Hek293 cultures expressing PLG2 luciferase**

The day after seeding, cells grown in 2D and 3D format were transfected with 0.10  $\mu$ g of pCMV\_PLG2 according to the manufacturer's instructions, using a FUGENE HD:DNA ratio of 3:1 and incubated at 37°C with 5% CO<sub>2</sub>. At 24 h post transfection, BL emission spectra (450-750 nm) and kinetic measurements (10 min with 200 ms integration time) were obtained in 96-well plates with a Varioskan Flash luminometer (Thermo Fisher Scientific, Waltham, MA, USA) after automatic

injection of 100  $\mu\text{L}$  of 1 mM D-Luciferin citrate solution pH 5.0. All experiments were performed in triplicate and repeated at least three times.

### **6.2.5 2D and 3D bioluminescence imaging of Hek293 cells expressing PLG2 luciferase**

Cells grown for 24 h in 2D and 3D microplates were transfected with 0.10  $\mu\text{g}$  of pCMV\_PLG2 using a FUGENE HD:DNA ratio of 3:1 and incubated for 24 h at 37°C with 5%  $\text{CO}_2$ . BL imaging was performed using an inverted microscope (Olympus CK40) connected to an electron multiplying charge coupled device (EM-CCD) camera (ImagEM-X2, Hamamatsu). Images of 2D and 3D cell cultures were acquired using 10X (Olympus A10PL) and 4X (SPlan4SL) objectives with an integration time of 30 sec, at a gain level set to 500, after the addition of 100  $\mu\text{L}$  of 1 mM D-luciferin substrate in citrate buffer pH 5.0. Overlay images were obtained using HCLImage software (v 4.1.2.0). All experiments were performed in triplicate and repeated at least three times.

### **6.2.6 Spheroid analysis**

Brightfield images of Hek293 spheroids were analyzed using ImageJ version 1.51d software to calculate the projected area (A) and perimeter (P) of each spheroid [26]. A sphericity factor, named  $\phi$ , was then calculated as follows:

$$\phi = \frac{\pi \times \sqrt{\frac{4A}{\pi}}}{P} \quad (1)$$

### **6.2.7 3D bioluminescence imaging assay for inflammatory pathway activation**

A 3D assay for inflammatory activity was developed by employing 3-day old Hek293 spheroids. Briefly, Hek293 cells were plated in 96-well micro-space round bottom cell culture plates (Elplasia) at a concentration of  $2 \times 10^4$  cells/well in a total volume of 100  $\mu$ L of medium. After 72 h, cells were transfected with 0.10  $\mu$ g of plasmid pNFkB\_PLG2 per well using a FUGENE HD:DNA ratio of 3:1. At 48 h post transfection, medium was changed and cells were treated in triplicate with 50  $\mu$ L of TNF $\alpha$  solutions in culture medium (0.1-20 ng/mL) or with 50  $\mu$ L of culture medium as a control. After 4 h incubation at 37°C, 100  $\mu$ L of 1 mM D-luciferin substrate in citrate buffer pH 5.0 [27] was added to each well. Images were acquired with the ImagEMX2 EMCCD camera with an integration time of 30 sec, gain 500, using 4X objectives. Bioluminescence images were quantified using ImageJ software; a region of interest (ROI) was manually designed around each spheroid and its BL intensity was calculated with respect to the projected area (corrected BL emission). The mean of corrected BL emissions obtained from 20 spheroids was used for the dose-response curve generated using GraphPad Prism software. All measurements were performed in triplicate and repeated at least three times.

## **6.3 RESULTS AND DISCUSSION**

### **6.3.1 Characterization of PLG2 luciferase expressed in 3D cell cultures/spheroids**

A new enhanced chimeric luciferase mutant, named PLG2, was selected as a reporter protein for engineering spheroids. PLG2 is characterized by improved spectral and physical properties, i.e., enhanced activity compared with the *Photinus pyralis* wild-type luciferase (PpyWT) (about 35%), absence of red-shifting of bioluminescence at low pH ( $\sim$ 6.5), and improved thermostability (24 h vs. 20 min at 37 °C). Stability to pH and temperature is a desirable feature for BL reporters to be

used within cells or living animals, where 37°C and low pH conditions, e.g., as consequence of cell metabolism, are commonly found. This luciferase has a  $K_m$  value of  $52 \pm 6 \mu\text{M}$  for D-luciferin, which is about 3-fold higher than the value of PpyWT, and a  $K_m$  value for Mg-ATP very similar to PpyWT ( $79 \pm 5 \mu\text{M}$  vs  $86 \pm 7 \mu\text{M}$ , respectively). For evaluating the potential application of PLG2 luciferase in spheroid-based assays, two main issues were considered: the possibility to perform bioluminescence measurements in non-lysing conditions, to enable repetitive measurements for longitudinal studies, and likely biodistribution issues that are not encountered with monolayer or suspension cultures. To this end, we first characterized PLG2 expression in spheroids to evaluate emission spectra, kinetics and highlight possible problems that could circumvent BL detection in 3D cultures, such as substrate and oxygen availability issues at the core of spheroids. As expected, the emission spectra did not change when compared with those obtained with Hek293 monolayer cultures (Fig.1a) and spectra with a maximum emission at 556 nm and bandwidth at half-maximal intensity of 68 nm were obtained.

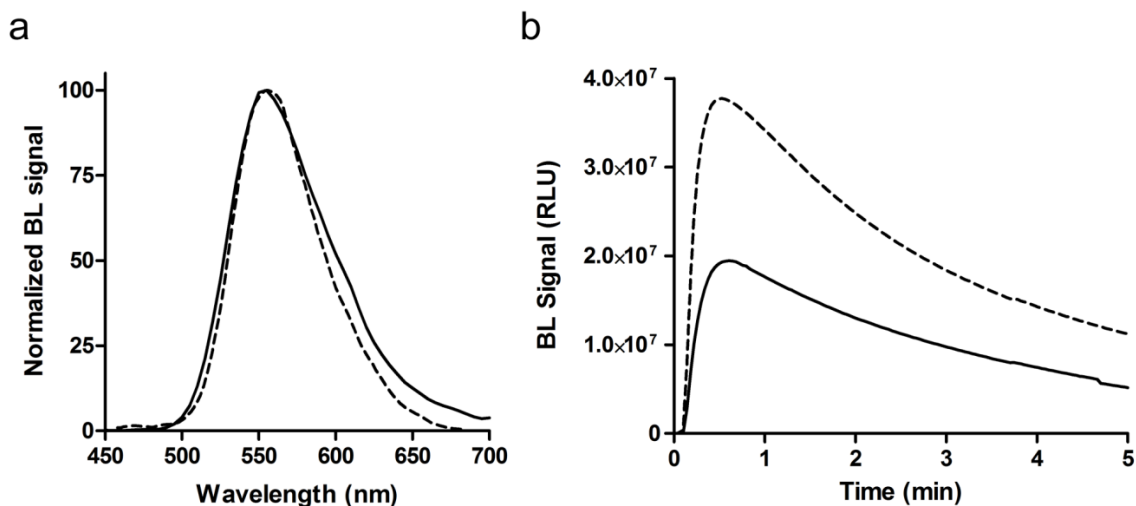


**Figure1.** (a) Normalized emission spectra of PLG2 luciferase expressed in spheroids (solid line) and in 2D monolayer cell cultures (dotted line). Spectra were obtained in non-lysing conditions using D-luciferin as the substrate, as described in the Materials and Methods. (b) Comparison of BL intensities and kinetic profiles obtained with Hek293 cells ( $2 \times 10^4$  per well) expressing PLG2 luciferase and cultured to form spheroids (solid line) or Hek293 cells ( $2 \times 10^4$  per well) grown in 2D monolayer cell cultures (dotted line) in 96 well plates.

Those values are consistent with those previously reported [10] in monolayer cultures. Bioluminescence emission kinetics were measured by adding a non-lysing formulation of D-luciferin previously optimized for live cell imaging [28]. Cells grown either in 2D and 3D culture format showed a glow-type emission with a peak 35s after substrate addition and the BL signal decreased by half after 5 min (Fig.1b). Thus, the emission kinetics obtained with 3D cell culture are suitable for BL imaging. An optimal acquisition time window was identified between 25 and 55s, when the mean BL signal is  $97 \pm 3\%$  of maximum emission. However, despite the same number of cells were seeded in 3D and 2D format, BL intensities per well obtained with spheroids are approximately half of those obtained with 2D cultures. This may be partially explained by the inability of D-luciferin solution to penetrate spheroids in depth, thus only external cell layers contribute to BL emission. More studies will be required to address this point. Moreover, photon losses and scattering effects of PLG2 green emission must be considered. This aspect will be further investigated using a microscope equipped with optical emission filters and a combination of red- and green-emitting luciferases respectively expressed in the core region and in surface layers, to quantitatively assess and optimize the substrate concentration and distribution within the spheroids.

The typical output from BL imaging of Hek293 cells ( $2.0 \times 10^4$  cells/well) cultured on conventional 96-well plates and transfected to constitutively express PLG2 is shown in Fig. 2a-c. Cells grew as a monolayer and were imaged before confluency using a 20X objective to identify individual cells (about 800 cells with an average dimension of  $20 \pm 5 \mu\text{m}$ ). Pseudocolor overlay was then used to quantify single cell emission corrected by the size of each cell. BL imaging also allows direct visualization of the transfection efficiency and to evaluate the metabolic activity of the cells. Indeed, despite that all cells are transfected with a plasmid for the constitutive expression of the same PLG2 luciferase, BL intensities might be quite different due to the

metabolic state of individual cells, which can affect the rate of protein expression and degradation, ATP content, etc.).

Bioluminescence imaging of spheroids was performed using clear bottom 96-well micro-space culture plates, where the bottom of each well contains micro patterned cone-shaped holes (about 130 micro-spaces) treated with poly(2-hydroxyethyl methacrylate) to create a low-adhesion surface. Cells grown in such plates are forced to interact with each other forming multicellular aggregates within few hours, evolving into spheroids of homogeneous morphology during incubation for several days. The dimension and compactness of the spheroids can be defined by selecting the initial cell number and incubation time in the 3D culture plate. A seeding cell density of  $4 \times 10^4$  cells was found to be suitable for efficient formation of spheroids with an average diameter of  $210 \pm 25 \mu\text{m}$  by day 3 (Fig.2d). The obtained spheroid size is suitable to avoid necrosis in the core and to maintain the functionality of the cells within the aggregate [29]. The sphericity factor ( $\Phi$ ) of 30 spheroids on day 3 was calculated according to equation [1] obtaining an average value of  $0.943 \pm 0.007$ . This is close to the icosahedron value (0.939) and indicates that the aggregates are quite uniform and of nearly spherical shape.

Since PLG2 luciferase requires oxygen for BL emission, one issue is related to oxygen availability at the core of spheroid. According to a previous report [30], if we consider a partial pressure of 150 mm Hg for oxygen at 37°C, the outer layer of each spheroid, considered to have a depth of 10–20  $\mu\text{m}$ , approximately reaches complete saturation (90%), and no oxygen limitations are observed with spheroids with an average diameter of 100  $\mu\text{m}$ . A spheroid with a diameter of 150  $\mu\text{m}$  contains less than 2% of cells within a hypoxic core, and 98% of cells composing the spheroids have sufficient oxygen for BL reactions. The BL imaging of Hek293 spheroids expressing PLG2 luciferase (Fig.2e-f) with a 4X objective allows simultaneous recording of the BL emission from at least 20 spheroids in each field. Then, ROIs are

manually selected around each spheroid to quantify the BL emission and corresponding surface area, to correct the signal from each spheroid according to its dimension.

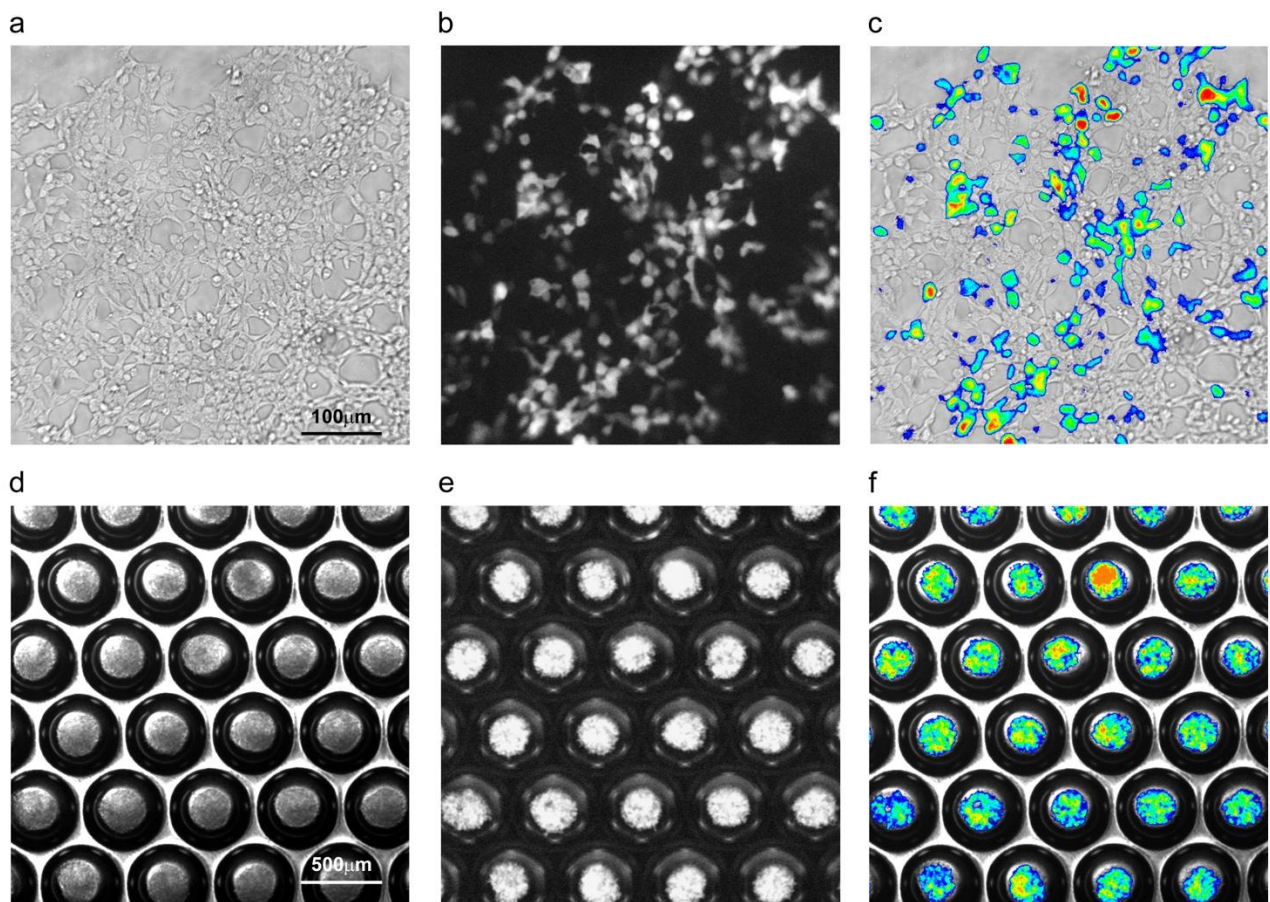


**Figure 2.** Brightfield, bioluminescence and pseudocolor overlay images of Hek293 cells expressing PLG2 luciferase, grown in 2D (a,b,c) or in 3D microplate format (d,e,f).

In contrast with confocal fluorescence microscopy, BL emission cannot currently be scanned in z-axis to make a 3D reconstruction of emitted light. In the present configuration, i.e. using micro molded plates to create spheroids and an inverted microscope, it is only possible to focus on a few cells on the bottom surface of the spheroids, while BL emission originates in the upper portion of the aggregate. This results in more blurred images compared with the 2D format. Nevertheless, since the aim is to determine the global distribution and biological effect of a given

treatment/target in a more in-vivo like format, BL imaging of spheroids can represent a convenient, easy to use approach.

### 6.3.2 3D Bioluminescence assay for inflammatory pathway activation

To evaluate the feasibility of using 3D bioluminescence imaging of Hek293 spheroids for upgrading 2D drug screening, we first developed a 3D assay for inflammatory activity. Three day-old Hek293 spheroids, transfected with a reporter construct in which the PLG2 luciferase is placed under the control of the NFkB (Nuclear Factor kB) response element, were incubated with different concentrations of TNF $\alpha$  (concentration range 0.1-10 ng/mL) for 5 h. The binding of TNF $\alpha$  to its specific endogenous receptor (TNFR) activates the intracellular inflammatory pathway, leading to PLG2 expression.

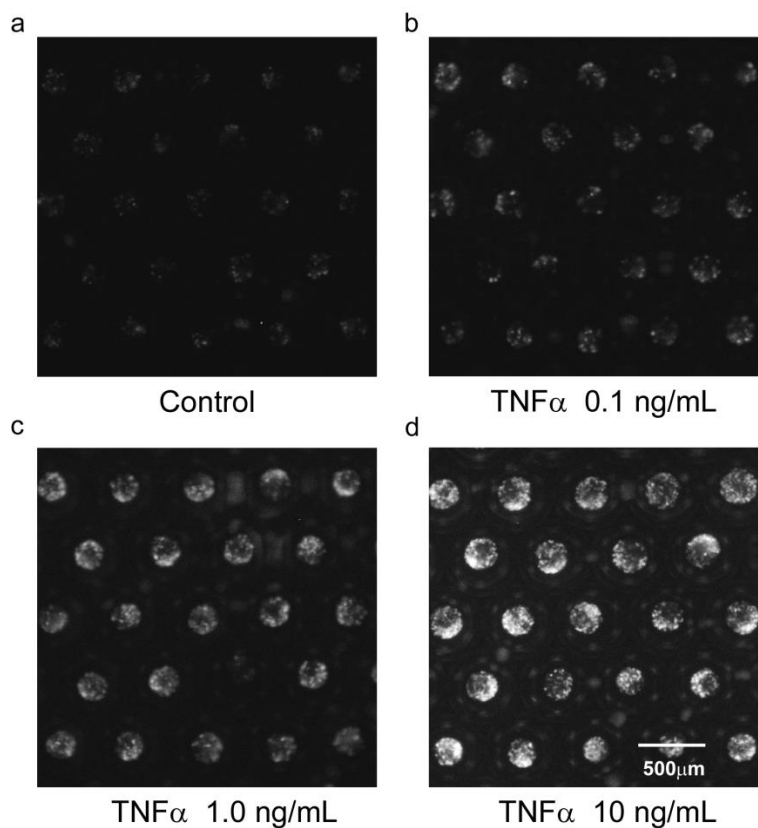


**Figure 3.** 3D bioluminescent assay for inflammatory pathway activation. Bioluminescence imaging of Hek293 spheroids (4X objective, 30 s acquisition) transfected with 0.10  $\mu$ g of reporter plasmid pNFkB\_PLG2 and treated, 48 h post-transfection with medium only as a control (a) or 0.1, 1.0 or 10 ng/mL TNF $\alpha$  solutions (b,c,d). Magnification bar is 500  $\mu$ m.

Hek293 spheroids of uniform size and shape (Fig.3a-d) had BL emission that increased with TNF $\alpha$  concentration in a dose dependent matter. Noticeably, the BL emission from individual spheroids was not homogeneous. This distribution is actually expected since cells have been transfected directly in 3D; thus, the cell response is affected by the diffusion of the transfection complex within the aggregates. We choose to transfect 1 day-old already formed aggregates (mean dimension  $120 \pm 15 \mu\text{m}$ , estimated 350 cells/spheroid) to simulate the delivery of the nano complex (i.e. plasmid DNA/ FugeneHD cationic polymer) and visualize its biodistribution and cell response after treatment, based on PLG2 expression. To evaluate the response of all the cells composing the spheroid, the establishment of stable cell lines will be required.

Dose-response curves for TNF $\alpha$  were obtained with both monolayer cultures and spheroids, obtaining EC50 values of  $2.6 \pm 0.4$  and  $3.5 \pm 0.5$  ng/ml, respectively (Fig.4). Compared with the 2D format, a higher NF $\kappa$ B basal activation ( $4.1 \pm 0.3$  fold) was found in 3D spheroids. This is consistent with results obtained by Jack et al., who reported the presence of an intra-spheroid cytokine signaling that propagated inside the aggregate inducing NF $\kappa$ B and JNK pathways [31].

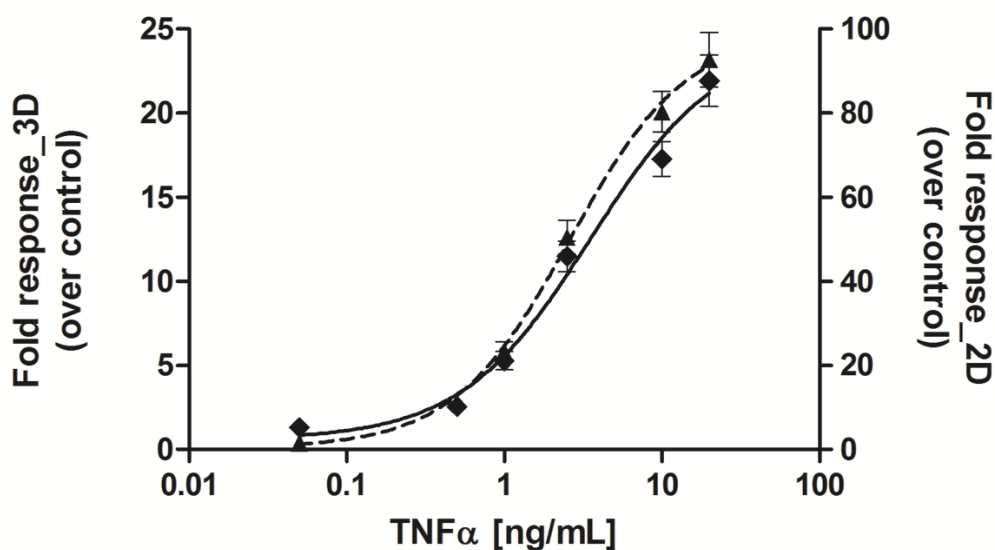


**Figure 4.** Dose-response curves obtained in 2D (dotted line) or 3D (solid line) cell-based assays. Hek293 cells were incubated for 4 h at 37°C with the indicated concentrations of TNF $\alpha$ , using PLG2 as a reporter under the control of NF $\kappa$ B-response element. BL measurements were obtained after the addition of 1 mM D- luciferin.

## 6.4 CONCLUSIONS

A high-throughput bioluminescence assay based on micro-patterned multi-well plates is reported. The feasibility of the assay was tested using the well-known transcriptional regulation of the nuclear factor k beta (NF $\kappa$ B) response element in human embryonic kidney Hek293 cells. We obtained concentration-response curves and compared them with those obtained using conventional 2D cell cultures. One of the main advantages of this approach is the non-lysing nature of the assay, which allows for repetitive measurements on the same sample. The assay can be implemented in any laboratory equipped with basic cell culture facilities and paves the way to the development of new 3D assays in fields ranging from drug screening to drug delivery.

## **ACKNOWLEDGMENTS**

This work has been supported in part by Grant OPP1040394 from the Global Health Program of the Bill & Melinda Gates Foundation and the Air Force Office of Scientific Research (FA9550-14-1-0100, BRB) and the National Science Foundation (MCB 1410390, BRB).

## REFERENCES

- [1] Korn, K. and E. Krausz (2007) Cell-based high-content screening of small-molecule libraries. *Curr. Opin. Chem. Biol.* 11, 503-510.
- [2] Roda, A., P. Pasini, M. Mirasoli, E. Michelini and M. Guardigli (2004) Biotechnological applications of bioluminescence and chemiluminescence. *Trends Biotechnol.* 22, 295-303.
- [3] Nakajima, Y. and Y. Ohmiya (2010) Bioluminescence assays: multicolor luciferase assay, secreted luciferase assay and imaging luciferase assay. *Expert. Opin. Drug. Discov.* 5, 835-849.
- [4] Didiot, M.C., S. Serafini, M.J. Pfeifer, F.J. King and C.N. Parker (2011) Multiplexed reporter gene assays: monitoring the cell viability and the compound kinetics on luciferase activity. *J. Biomol. Screen.* 16, 786-793.
- [5] Haugwitz, M., O. Nourzaie, T. Garachtchenko, L. Hu, S. Gandlur, C. Olsen, A. Farmer, G. Chaga and H. Sagawa (2008) Multiplexing bioluminescent and fluorescent reporters to monitor live cells. *Curr. Chem. Genomics.* 25, 11-9.
- [6] Maguire, C.A., M.S. Bovenberg, M.H. Crommentuijn, J.M. Niers, M. Kerami, J. Teng, M. Sena-Esteves, C.E. Badr and B.A. Tannous (2013) Triple bioluminescence imaging for in vivo monitoring of cellular processes. *Mol. Ther. Nucleic Acids.* 18; 2:e99.
- [7] Branchini, B.R., T.L. Southworth, J.P. DeAngelis, A. Roda and E. Michelini (2006) Luciferase from the Italian firefly *Luciola italica*: molecular cloning and expression. *Comp. Biochem. Physiol. B. Biochem. Mol. Biol.* 145, 159-167.
- [8] Ohmiya, Y. (2015) Simultaneous multicolor luciferase reporter assays for monitoring of multiple genes expressions. *Comb. Chem. High Throughput Screen.* 18, 937-945.

- [9] Amaral, D.T., G. Oliveira, J.R. Silva and V.R. Viviani (2016) A new orange emitting luciferase from the Southern-Amazon *Pyrophorus angustus* (Coleoptera: Elateridae) click-beetle: structure and bioluminescence color relationship, evolutionary and ecological considerations. *Photochem. Photobiol. Sci.* 15, 1148-1154.
- [10] Branchini, B.R., T.L. Southworth, D.M. Fontaine, D. Kohrt, M. Talukder, E. Michelini, L. Cevenini, A. Roda and M.J. Grossel (2015) An enhanced chimeric firefly luciferase-inspired enzyme for ATP detection and bioluminescence reporter and imaging applications. *Anal. Biochem.* 484, 148-153.
- [11] Thorne, N., M. Shen, W.A. Lea, A. Simeonov, S. Lovell, D.S. Auld and J. Inglese (2012) Firefly luciferase in chemical biology: a compendium of inhibitors, mechanistic evaluation of chemotypes, and suggested use as a reporter. *Chem Biol.* 19, 1060-1072.
- [12] Auld, D.S., N. Thorne, D.T. Nguyen and J. Inglese (2008) A specific mechanism for nonspecific activation in reporter-gene assays. *ACS Chem. Biol.* 3, 463-470.
- [13] Beken, S., P. Kasper and J.W. van der Laan (2016) Regulatory Acceptance of Alternative Methods in the Development and Approval of Pharmaceuticals. *Adv. Exp. Med. Biol.* 856, 33-64.
- [14] Michelini, E., L. Cevenini, M.M. Calabretta, D. Calabria and A. Roda (2014) Exploiting in vitro and in vivo bioluminescence for the implementation of the three Rs principle (replacement, reduction, and refinement) in drug discovery. *Anal. Bioanal. Chem.* 406, 5531-5539.
- [15] Michelini, E., L. Cevenini, L. Mezzanotte, A. Coppa and A. Roda (2010) Cell-based assays: fuelling drug discovery. *Anal. Bioanal. Chem.* 398, 227-238.

- [16] Horvath, P., N. Aulner, M. Bickle, A.M. Davies, E.D. Nery, D. Ebner, M.C. Montoya, P. Östling, V. Pietiäinen, L.S. Price, S.L. Shorte, G. Turcatti, C. von Schantz and N.O. Carragher (2016) Screening out irrelevant cell-based models of disease. *Nat. Rev. Drug Discov.* In press doi: 10.1038/nrd.2016.175
- [17] Antoni, D., H. Burckel, E. Josset and G. Noel (2015) Three-dimensional cell culture: a breakthrough in vivo. *Int. J. Mol. Sci.* 16, 5517-5527.
- [18] Laschke, M.W. and M.D. Menger (2016) Life is 3D: Boosting Spheroid Function for Tissue Engineering. *Trends. Biotechnol.* In press doi:10.1016/j.tibtech.2016.08.004.
- [19] Nath, S. and G.R. Devi. (2016) Three-dimensional culture systems in cancer research: Focus on tumor spheroid model. *Pharmacol Ther.*163, 94-108.
- [20] Verma, R., R.R. Adhikary and R. Banerjee (2016) Smart material platforms for miniaturized devices: implications in disease models and diagnostics. *Lab Chip.* 16, 1978-1992.
- [21] Konstantinov, S.M., M.M. Mindova, P.T. Gospodinov and P.I. Genova (2004) Three-dimensional bioreactor cultures: a useful dynamic model for the study of cellular interactions. *Ann. N.Y. Acad. Sci.* 1030, 103-115.
- [22] Das, V., T. Fürst, S. Gurská, P. Džubák and M. Hajdúch (2016) Reproducibility of Uniform Spheroid Formation in 384-Well Plates: The Effect of Medium Evaporation. *Biomol. Screen.* 21, 923-930.
- [23] Bäcker, A., O. Erhardt, L. Wietbrock, N. Schel, B. Göppert, P. Abaffy, T. Sollich, A. Cecilia and F.J. Gruhl (2016) Silk scaffolds connected with different naturally occurring biomaterials for prostate cancer cell cultivation in 3D. *Biopolymers.* In press doi: 10.1002/bip.22993

- [24] Ivanov, D.P., T.L. Parker, D.A. Walker, C. Alexander, M.B. Ashford, P.R. Gellert and M.C. Garnett (2014) Multiplexing spheroid volume, resazurin and acid phosphatase viability assays for high-throughput screening of tumour spheroids and stem cell neurospheres. *PLoS One*. 2014 9:e103817.
- [25] Sirenko, O., T. Mitlo, J. Hesley, S. Luke, W. Owens and E.F. Cromwell (2015) High-content assays for characterizing the viability and morphology of 3D cancer spheroid cultures. *Assay Drug. Dev. Technol.* 13, 402-414.
- [26] Kelm, J.M., N.E. Timmins, C.J. Brown, M. Fussenegger and L.K. Nielsen (2003) Method for generation of homogeneous multicellular tumor spheroids applicable to a wide variety of cell types. *Biotechnol. Bioeng.* 83, 173-180.
- [27] Michelini, E., L. Cevenini, L. Mezzanotte, P. Leskinen, M. Virta, M. Karp and A. Roda (2008) A sensitive recombinant cell-based bioluminescent assay for detection of androgen-like compounds. *Nat. Protoc.* 3, 1895-1902.
- [28] Cevenini, L., G. Camarda, E. Michelini, G. Siciliano, M.M. Calabretta, R. Bona, T.R. Kumar, A. Cara, B.R. Branchini, D.A. Fidock, A. Roda and P. Alano (2014) Multicolor bioluminescence boosts malaria research: quantitative dual-color assay and single-cell imaging in *Plasmodium falciparum* parasites. *Anal. Chem.* 86, 8814-8821.
- [29] Anada, T., J. Fukuda, Y. Sai and O. Suzuki (2012) An oxygen-permeable spheroid culture system for the prevention of central hypoxia and necrosis of spheroids. *Biomaterials.* 33, 8430-8441.
- [30] Langan, L.M., N.J. Dodd, S.F. Owen, W.M. Purcell, S.K. Jackson and A.N. Jha (2016) Direct Measurements of Oxygen Gradients in Spheroid Culture System Using Electron Parametric Resonance Oximetry. *PLoS. One.* 11, e0149492.

[31] Jack, G.D., J.F. Garst, M.C. Cabrera, A.M. DeSantis, S.M. Slaughter, J. Jervis, A.I. Brooks, M. Potts and R.F. Helm (2006) Long term metabolic arrest and recovery of HEK293 spheroids involves NF-kappaB signaling and sustained JNK activation. *J. Cell Physiol.* 206, 526-536.

## CHAPTER 6

---

### **Future Directions**

---

From an analytical point of view, living cells provide an excellent tool to obtain precise functional information, which is hard to obtain with conventional analytical techniques. This information is highly valuable in several fields including drug screening, food safety and quality assessment, and environmental monitoring.

Whole-cell bioluminescent (BL) biosensors for multianalyte detection have been developed and implemented into smartphone-based devices for point-of-care and point-of-need applications. Cell biosensors offer the peculiar feature of providing quantitative information about the actual biological activity of analytes present in a sample. For achieving more valuable information, e.g., in terms of reliability of data, in particular in relation to toxicity and bioactivity, many 3D cell models will be developed providing an environment that faithfully mimics the *in vivo* physiological conditions.

Conscious that one of the major limitation of the proposed smartphone-based assays is connected to the use of living mammalian cells, two main challenges will be addressed: the identification of innovative strategies for cell immobilization to keep biosensors alive and responsive for long periods of time, and the improvement of light emitted by the cells to enable detection with portable light detectors, while keeping adequate sensitivity, comparable with that obtained with benchtop detectors. In particular, the feasibility of immobilizing the 3D “sentinel cells” will be evaluated to obtain ready-to-use cartridges that can be stored for long periods of time, without losing their responsiveness, until needed. For this reason, future work will be directed to optimize the shelf-life of cell cartridges i.e. direct growth of cell-biosensor on 3D-scaffolds inside the 3D-printed cartridges and the immobilization of cells into suitable biocompatible matrices to improve cell viability during cell storage and reduce the time-to response signal. Moreover, the use of alternative eukaryotic cell lines will be also explored. In particular more robust cell lines (e.g. fish cell lines),

that are less demanding in terms of culturing condition and can be maintained at atmospheric CO<sub>2</sub> will be explored.

3D BL cell biosensors for multianalyte detection will be developed in order to evaluate the toxicity and presence of pollutants in water, food and the environment. To this end, a multicolor bioluminescent assay will be developed in a smartphone-biosensing platform with improved analytical performance in terms of increased shelf-life and predictivity of results. To increase robustness of the biosensor we will include an internal viability control exploiting two red-green emitting luciferases requiring the same substrate, whose feasibility has been previously demonstrated in conventional 2D cell cultures. In this perspective, the proposed biosensing platform would aim to become a useful tool for a first level on-site screening of potentially harmful compounds or toxic substances, prioritizing samples for a more accurate chemical analysis.

## **Acknowledgments**

The present works have been performed in the Laboratory of Analytical and Bioanalytical Chemistry headed by Prof. Aldo Roda. I thank him and his co-workers, especially my supervisor Prof. Elisa Michelini, Dr. Luca Cevenini and PhD student Antonia Lopreside.